

**Effects of Sevoflurane and Amyloid β Isoforms on Dendritic Spine Density
and Astrocyte-Mediated Synaptic Engulfment: An Ex Vivo Study on
Hippocampal Brain Slices**

Qinfang Shi

Complete reprint of the dissertation approved by the TUM School of Medicine and Health
of the Technical University of Munich for the award of the

Doktorin der Medizin (Dr. med.)

Chair: Prof. Kathrin Schumann

Examiners:

1. apl Prof. Dr. Gerhard Rammes
2. Priv.-Doz. Dr. Andrea Welling

The dissertation was submitted to the Technical University of Munich on 24 August 2023 and
accepted by the TUM School of Medicine and Health on 4 January 2024.

Abstract

Background: With an ever-increasing life expectancy and improvement in surgical safety, more and more patients with Alzheimer's disease (AD) need anesthesia care. The toxicity of amyloid β ($A\beta$) peptides is a major cause of AD. However, the interaction of $A\beta$ with general anesthetics remains unclear. Consequently, understanding this interaction is important for performing anesthesia in AD patients.

Sevoflurane is one of the most commonly used inhalation anesthetics for elderly patients, but new evidence suggests that it may have neurotoxic effects on the AD brain. Therefore, in the present study, we aimed to investigate the interaction of sevoflurane with $A\beta$ -dependent pathophysiology.

Methods: To mimic AD patients receiving inhalation anesthesia, sevoflurane (0.4 minimal alveolar concentration (MAC) or 1.2 MAC) was applied to acute hippocampal brain slices pre-incubated with $A\beta$ isoforms- $A\beta_{1-40}$, $A\beta_{1-42}$, $A\beta_{pE3}$ and 3NTyr $A\beta$. Dendritic spines of the pyramidal neurons in the CA1 region were quantified, astrocyte-mediated synaptic engulfment was assessed, and phagocytosis receptor multiple epidermal growth factor-like domains 10 (MEGF10), astrocyte marker-gial fibrillary acidic protein (GFAP), and GFAP breakdown products (GFAP-BDPs) were evaluated.

Results: 1) Among the four $A\beta$ isoforms, $A\beta_{1-40}$, $A\beta_{1-42}$, and 3NTyr $A\beta$ decreased DSD, with 3NTyr $A\beta$ having the highest efficacy, and only 3NTyr $A\beta$ decreased the expression of GFAP- α ; 2) in the absence of $A\beta$, 1.2 MAC sevoflurane had a greater effect on decreasing DSD than 0.4 MAC sevoflurane; 3) when present together, 0.4 MAC sevoflurane led to a reversible enhancement downregulation of DSD induced by all four $A\beta$ isoforms, whereas 1.2 MAC occurred only for $A\beta_{1-40}$ and $A\beta_{1-42}$. For $A\beta_{pE3}$ and 3NTyr $A\beta$, 1.2 MAC sevoflurane didn't enhance the decrease of DSD. Additionally, an increase in the stubby spine for $A\beta_{pE3}$ and an increase in thin spines for 3NTyr $A\beta$ were observed after sevoflurane removal; 4) 1.2 MAC

sevoflurane applied with either A β pE3 or 3NTyrA β together resulted in a decrease of astrocyte-mediated synaptic engulfment, while neither A β nor sevoflurane alone had a significant effect; 5) when A β (A β ₁₋₄₀, A β ₁₋₄₂, A β pE3 or 3NTyrA β) was present, 0.4 MAC sevoflurane increased the expression of GFAP- α and decreased the expression of GFAP-BDPs. In contrast, only when 3NTyrA β was present, 1.2 MAC sevoflurane increased the expression of GFAP-BDPs and tended to decrease the expression of GFAP- α .

Conclusion: These findings indicate that: 1) Among the four A β isomers, 3NTyrA β exerted the greatest impact on spine dynamics and astrocyte structure; 2) 0.4 MAC sevoflurane did not protect against or enhance dendritic spine toxicity of A β isoforms; 3) 1.2 MAC sevoflurane interfered with A β -induced dendritic spine toxicity. However, further studies are needed to determine whether this effect is detrimental or not; 4) astrocytes are sensitive targets of sevoflurane, and in the presence of 3NTyrA β , sevoflurane may have a dual effect on astrocyte structure depending on concentration.

Zusammenfassung

Hintergrund: Mit der ständig steigenden Lebenserwartung und der Verbesserung der chirurgischen Sicherheit benötigen immer mehr Patienten mit der Alzheimer-Krankheit (AD) eine anästhesiologische Versorgung. Die Toxizität von Amyloid β ($A\beta$)-Peptiden ist eine der Hauptursachen für Alzheimer. Die Wechselwirkung von $A\beta$ mit Allgemeinanästhetika bleibt jedoch unklar. Folglich ist das Verständnis dieser Wechselwirkung wichtig für die Durchführung einer Allgemeinanästhesie bei Alzheimer-Patienten.

Sevofluran ist eines der am häufigsten verwendeten Inhalationsanästhetika für ältere Patienten, aber neue Erkenntnisse deuten darauf hin, dass es neurotoxische Wirkungen auf das AD-Gehirn haben könnte. In der vorliegenden Studie wollten wir daher die Wechselwirkung von Sevofluran mit der $A\beta$ -abhängigen Pathophysiologie untersuchen.

Methoden: Um die Pathologie eines Gehirns von AD-Patienten die eine Inhalationsanästhesie erhalten, zu imitieren, wurde Sevofluran (0,4 minimale alveolare Konzentration (MAC) oder 1,2 MAC) auf akute Hippocampus-Gehirnschnitte aufgetragen, die mit den $A\beta$ -Isoformen $A\beta_{1-40}$, $A\beta_{1-42}$, $A\beta_{pE3}$ und $3NTyrA\beta$ vorinkubiert wurden. Folgende Parameter wurden dann quantifiziert: die Dichte der dendritischen Dornfortsätze (DSD) der Pyramidenneuronen in der CA1-Region, deren von Astrozyten vermittelte synaptische Eliminierung, die Expression des Phagozytoserezeptor Multiple Epidermal Growth Factor-like Domains 10 (MEGF10), die Expression des Astrozytenmarker Glial Fibrillary Acidic Protein (GFAP) und die GFAP-Abbauprodukte (GFAP-BDPs).

Ergebnisse: 1) Von den vier $A\beta$ -Isoformen verringerten $A\beta_{1-40}$, $A\beta_{1-42}$, und $3NTyrA\beta$ die DSD, wobei $3NTyrA\beta$ die höchste Wirksamkeit hatte, und nur $3NTyrA\beta$ verringerte die Expression von GFAP- α ; 2) in Abwesenheit von $A\beta$ hatten 1,2 MAC Sevofluran eine größere Wirkung auf die Verringerung der DSD als 0.4 MAC Sevofluran; 3) bei gleichzeitiger Gabe von 0,4 MAC Sevofluran kam es zu einer reversiblen Verstärkung der durch alle vier $A\beta$ -Isoformen

induzierten Downregulation der DSD, während 1,2 MAC nur für $A\beta_{1-40}$ und $A\beta_{1-42}$ auftraten. Für $A\beta_{pE3}$ und 3NTyr $A\beta$ verstärkten 1,2 MAC Sevofluran die Abnahme der DSD nicht. Darüber hinaus wurde nach der Entfernung von Sevofluran eine Zunahme der stumpfen Dornfortsätze (*stubby spines*) für $A\beta_{pE3}$ und eine Zunahme der dünnen Stacheln für 3NTyr $A\beta$ beobachtet; 4) 1,2 MAC Sevofluran, das zusammen entweder mit $A\beta_{pE3}$ oder 3NTyr $A\beta$ verabreicht wurde, führte zu einer Abnahme des Astrozyten-vermittelten synaptischen Phagozytose, während weder $A\beta$ noch Sevofluran allein einen signifikanten Effekt hatten; 5) Wenn $A\beta$ ($A\beta_{1-40}$, $A\beta_{1-42}$, $A\beta_{pE3}$ oder 3NTyr $A\beta$) vorhanden war, erhöhte 0,4 MAC Sevofluran die Expression von GFAP- α und verringerte die Expression von GFAP-BDPs. Im Gegensatz dazu erhöhte 1,2 MAC Sevofluran nur bei Anwesenheit von 3NTyr $A\beta$ die Expression von GFAP-BDPs und verringerte tendenziell die Expression von GFAP- α .

Schlussfolgerung: Diese Ergebnisse zeigen: 1) Von den 4 $A\beta$ -Isomeren hatte 3NTyr $A\beta$ den größten Einfluss auf die Dynamik der Dornfortsätze und die Astrozytenanatomie; 2) 0,4 MAC Sevofluran schützte nicht vor der toxischen Wirkung der $A\beta$ -Isoformen auf die DSD und verstärkte sie auch nicht; 3) 1,2 MAC Sevofluran beeinflusste die $A\beta$ -induzierte Wirkung auf die DSD. Es sind jedoch weitere Studien erforderlich, um festzustellen, ob dieser Effekt nachteilig ist oder nicht; 4) Astrozyten stellen sensitive Ziele für Sevofluran dar, und in Gegenwart von 3NTyr $A\beta$ kann Sevofluran konzentrationsabhängig die Wirkung auf die Astrozytenanatomie verstärken.

List of Contents

1. Introduction	8
1.1 Postoperative delirium	8
1.2 Alzheimer's disease and Aβ hypothesis	9
1.3 Anesthesia, AD, and POD	12
1.4 Sevoflurane	14
1.5 Synapses and dendritic spines	17
1.6 Astrocytes	20
1.7 Objectives	24
2. Materials and Methods	24
2.1 Animals	24
2.2 Key resources tables	24
2.3 Acute hippocampal brain slices preparation	26
2.4 Aβ isoforms (Aβ₁₋₄₀, Aβ₁₋₄₂, AβpE3, 3NTyrAβ) preparation and incubation	28
2.5 Sevoflurane application	28
2.6 Experiment schedule and groups	29
2.7 Analysis of dendritic spines	31
2.8 Immunofluorescence and colocalization analysis	32
2.9 Western blot	36
2.10 Statistical analysis	41
3. Results	41
3.1 The effect of Aβ and sevoflurane on DSD	41
3.2 The effects of astrocyte-mediated synaptic engulfment	53
3.3 The effects of Aβ and sevoflurane on the expression of MEGF10, GFAP and GFAP-BDPs	59
4. Discussion	66

4.1 The effect of Aβ and sevoflurane on DSD	66
4.2 The effect of Aβ and sevoflurane on MEGF10-mediated synaptic engulfment of astrocytes.....	71
4.3 The effect of Aβ and sevoflurane on the expression of GFAP and GFAP-BDPs	73
5. Summary and Conclusions.....	76
6. Acknowledgements.....	77
7. Reference.....	79

1. Introduction

1.1 Postoperative delirium

Postoperative delirium (POD) is one of the most common neurocognitive disorders in the elderly following surgery and anesthesia, occurring within a week after surgery and characterized by acute and fluctuating changes in mental status, attention, and level of consciousness[1-3]. The incidence of POD has been reported to range from 6% to 54%, with wide variations depending on patient condition, surgical procedure, assessment tools, and frequency of assessment[4, 5]. POD is associated with various adverse outcomes, including prolonged hospitalization, increased mortality, long-term cognitive dysfunction, and increased healthcare costs, imposing a serious burden on patients and society[6-9]. Due to the lack of effective treatments for diagnosed POD currently, prevention of POD is extremely important to improve the quality of life after surgery.

Despite the high morbidity of POD, much is unclear about its etiology and pathophysiology. It is currently considered that POD is an acute brain dysfunction induced by exogenous stressors in the susceptible brain[10]. Risk factors accounting for POD include advanced age, pre-existing cognitive impairment, history of delirium, medications (sedative-hypnotics), sleep deprivation, and a history of alcohol or drug abuse, with advanced age and preoperative baseline cognitive impairment being the most relevant risk factors for the development of POD[11, 12]. In addition, the intraoperative depth of anesthesia and the choice of general anesthetics have also been suggested to be associated with the incidence of POD in high-risk patients[13-15].

Regarding the pathophysiology of POD, currently, several complementary mechanisms synergistically contribute to cognitive and behavioral changes of delirium. The leading theories include, neuroinflammation[16], blood-brain barrier (BBB) disruption[17], neuronal aging[18], neurotransmitter imbalance[19], and neural network connectivity alterations[20].

In addition to neurons, there is growing evidence suggesting that astrocyte and microglia malfunction are also involved in postoperative neurocognitive deficits[19, 21, 22].

1.2 Alzheimer's disease and A β hypothesis

Alzheimer's disease (AD) is an insidious progressive neurodegenerative disorder, which accounts for the most common form of dementia and is one of the greatest public health problems worldwide[23]. It is an age-related neurodegenerative disease characterized by progressive and global cognitive decline. With the progress of society and the increasing life expectancy, more and more people are suffering from AD. It is estimated that approximately 50 million people worldwide are suffering from AD currently[24, 25].

Significant progress has been made in understanding AD since it was first described by German neuropathologist Alois Alzheimer in 1907. However, the exact pathophysiology of AD is not yet clear. Several hypotheses have been proposed, one of the most famous of which is the amyloid cascade hypothesis[26]. The cornerstone of the hypothesis is that A β peptide deposition is the causative factor of AD, which initiates pathological cascade responses leading to cognitive impairment and dementia[27, 28] (Figure 1). Although the amyloid cascade hypothesis has been debating by scientists over the past decades, emerging evidence from labs and clinics supports the concept that the accumulation of A β peptides is an early and initiating factor in AD[29, 30]. Moreover, it is increasingly accepted that soluble A β oligomers, maybe the more neurotoxic species than large, insoluble A β fibrillary deposits, adversely affect synaptic structure and plasticity[31, 32].

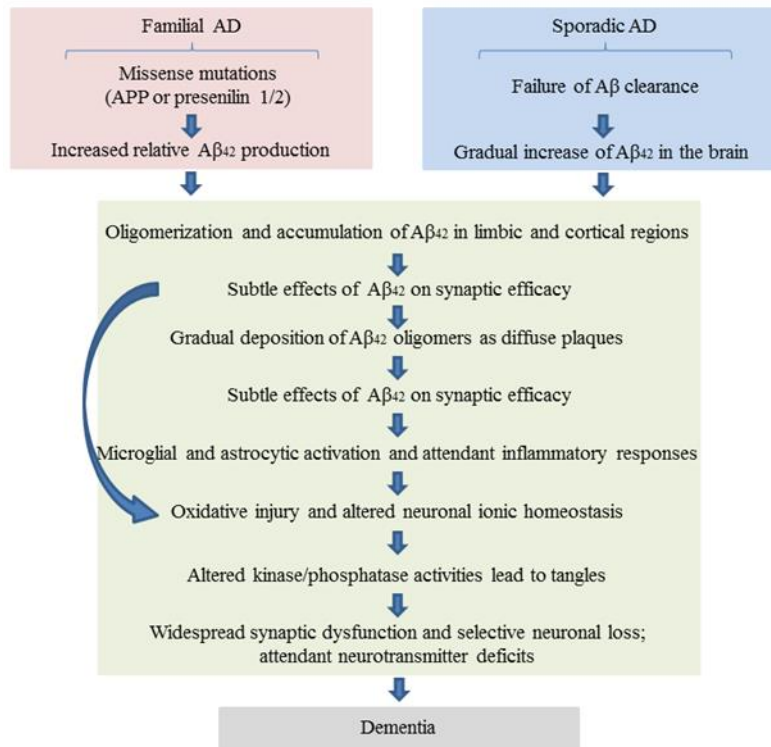


Figure 1. The amyloid cascade hypothesis in familial and sporadic AD[28, 33].

Aβ is a 37 to 43 amino acids peptide that is produced from amyloid precursor protein (APP) by proteolytic cleavage with β-secretases and γ-secretases via the amyloidogenic pathway to generate Aβ monomers. Aβ monomer is usually nontoxic, but it forms toxic oligomers and amyloid fibers [34]. Due to the imprecise cleavage, Aβ peptides exist in multiple isoforms with different N and C termini. In addition to size differences, post-translational modifications of Aβ (such as oxidation, phosphorylation, nitration, and pyroglutamylation) also generate different Aβ isoforms with different pathological properties[35-37] (Figure 2).

In the cerebral cortex of AD patients, Aβ₁₋₄₀ is the major species of amyloid peptide, while Aβ₁₋₄₂ has a higher propensity to aggregate and is more neurotoxic[38, 39]. Amongst the post-translationally modified species, pyroglutamate modified Aβ (AβpE3) and nitrated Aβ (3NTyrAβ) peptides have received much attention as potential participants in AD pathology due to their abundance in the AD brain, high aggregation tendency, stability, cytotoxicity, and the ability to cause severe neuronal loss in transgenic mice[35, 40, 41]

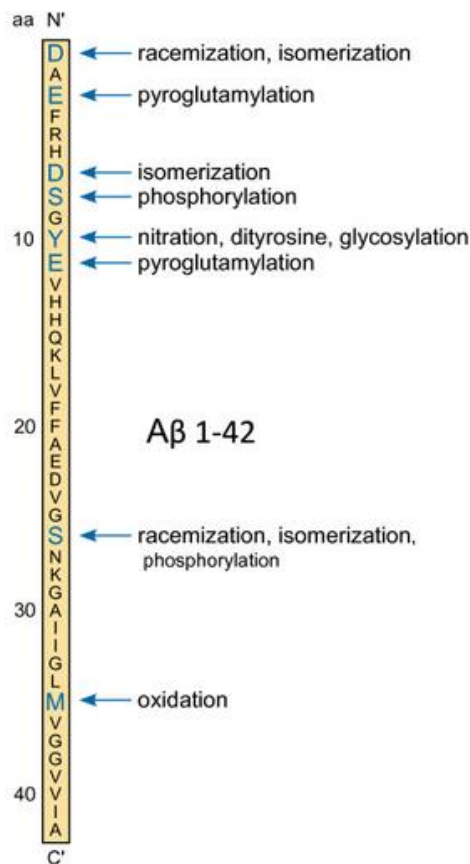


Figure 2. Locations of post-translational modifications in Aβ₁₋₄₂. Post-translational modified amino acid residues are labeled with blue letters[35].

The formation of AβpE3 requires the removal of the first two amino acids from Aβ₁₋₄₂. Then, aspartate 11 is modified by pyroglutamic acid (11pE-Aβ). In the subsequent dehydration reaction, the terminal glutamate is transformed into pyroglutamate[42, 43]. It has shown that pyroglutamate formation at the N-terminus can resist cleavage by most aminopeptidases, increase the peptides' toxicity, and promote the formation of Aβ aggregates[40, 41]. And intracerebroventricular injections of AβpE3 or Aβ₁₋₄₂ confirmed that the toxicity of AβpE3 to neurons is similar to that of Aβ₁₋₄₂[44].

In addition to aspartate 11, which serves as a post-translational modification site of Aβ₁₋₄₂, the tyrosine at position 10 of Aβ₁₋₄₂ is a molecular target of peroxynitrite. Peroxynitrite is an intermediate product for generating 3NTyrAβ from NO[35]. It was shown that 3NTyrAβ plays

a key role in initiating plaque formation in AD transgenic mice[45]. In addition, 3NTyrA β increased the tendency of A β to aggregate and has been identified in the core of the amyloid plaques[45].

A recent study from our laboratory showed that when A β ₁₋₄₀, A β ₁₋₄₂, A β pE3 and 3NTyrA β were applied to mouse hippocampal brain slices for 90 min, all isoforms concentration-dependently reduced the ability to induce long-term potentiation (LTP) in the hippocampus after tetanic stimulation of the Schaffer collaterals with IC₅₀s of 9 nM, 2 nM, 35 nM and 2 nM, respectively[46], which further confirmed that besides A β ₁₋₄₂, other forms of A β peptides also exert potent synaptotoxicity.

1.3 Anesthesia, AD, and POD

With an ever-increasing life expectancy and improvement in surgical safety, the number of elderly undergoing surgery is steadily growing, and correspondingly, the number of old patients with AD requiring anesthesia care is booming. Although general anesthesia was initially thought to induce a reversible state of unconsciousness, in recent decades, a hypothesis has been proposed that exposure to general anesthetics, especially in young children and the elderly, may trigger long-term morphological and functional alterations in the brain, thereby accelerate the neuropathologic change of AD and lead to the subsequent cognitive decline[47-51]. As a result, there is growing concern about whether commonly used anesthetics deteriorate this devastating disease or lead to postoperative neurocognitive deficits and persistent cognitive dysfunction in the elderly[52].

Although the relationship between neurocognitive impairments and general anesthesia exposure remains to be determined, it is well established that patients with compromised cognitive ability preoperatively (e.g., dementia) are at higher risk of postoperative neurocognitive impairments, and even mild impairment of cognitive functions can predict the development of POD[12, 53, 54]. Recently, a systematic review and meta-analysis of 16 clinical studies including 62,179 patients, has confirmed that preoperative cognitive

impairment is associated with up to an 8-fold increased risk of POD in elderly patients undergoing cardiac surgery[55]. Besides, A randomized control trial (the BALANCED study) involving a total of 6,644 patients at 8 medical centers in 3 countries showed that for patients undergoing major surgery, electroencephalogram (EEG)-guided light anesthesia (bispectral index (BIS) =50) had a significantly lower incidence of POD compared to deep anesthesia (BIS=35) (19% vs 28%)[14]. Despite the controversy, it is now considered that deep anesthesia may increase the occurrence of POD, especially in patients with high risk[56]. Accordingly, it is imperative for perioperative physicians, especially anesthesiologists, to understand how anesthetics modulate the anesthetic state of the brains in patients with AD and whether general anesthetics worsen the cognitive function of AD patients.

Although various studies have demonstrated the toxic effects of general anesthetics on the vulnerable brain, preclinical studies have shown that anesthetics are also neuroprotective[57, 58]. Zhao et al. showed that exposure to a low concentration of isoflurane (0.6%) promoted the proliferation and differentiation of human neural progenitor cells without causing cell damage[57]. And short-term exposure to 0.7% isoflurane reduced CA1 cell death and morphology damage in rat hippocampal slices under oxygen-glucose deprivation[59]. Various molecular mechanisms have been proposed for the neuroprotective effects of anesthetics, including upregulation of nitric oxide synthase[60], moderate increases in cytosolic calcium concentration[58], activation of ATP-dependent potassium channels, and reduction of excitotoxic stressors and cerebral metabolic rate[61].

It seems that, at high concentrations for a prolonged duration, general anesthetics become lethal stress factors and induce neurotoxicity, while at low concentrations for a short duration, general anesthetics are sublethal stress factors and induce endogenous neuroprotective mechanisms thereby providing neuroprotection[58].

For the clinical effects of anesthetics, low concentrations induce amnesia, analgesia, and hypnosis, while high concentrations cause deep sedation, muscle relaxation, and diminished

motor and autonomic responses to noxious stimuli. Minimum alveolar concentration (MAC), first proposed by Dr. Edmund Eger in 1965, is now the standard measurement of potency for all inhalation anesthetics[62]. MAC refers to the end-tidal concentration (in standardized pressure units) of an inhalation anesthetic that prevents motor response to surgical incision in 50% of subjects, and MAC values vary among species. The MAC for humans was calculated from healthy humans aged approximately 40 years[62].

MAC-awake, which assesses perceptive awareness rather than memory, is the concentration at which the response to verbal command is suppressed in 50% of the patients. It is usually one-third of the MAC for commonly used inhalation agents, such as desflurane and sevoflurane [63].

1.4 Sevoflurane

Since its first use, anesthesia has evolved tremendously and has become indispensable in modern surgery. As one of the most commonly used inhalation anesthetics in clinical practice at present, sevoflurane ($C_4H_7F_7O$) first synthesized in 1968 and approved for clinical use in the early 1990s, has been used in clinics for more than 30 years[64, 65]. Over the years of clinical application, the safety and efficacy of sevoflurane have been well established across all populations, while its exact anesthetic mechanism is still unclear. Various molecular targets have been identified for the anesthetic actions of sevoflurane. Among them, ligand-gated ionotropic receptors, such as γ -aminobutyric acid (GABA) A receptors, glutamate receptors, and acetylcholine receptors, are the most important. It has been demonstrated that sevoflurane potentiates the activity of GABA A receptors, and inhibits the activity of nicotinic acetylcholine receptors and glutamate receptors[66-68].

Sevoflurane is an ether compound with a slightly different structure from that of isoflurane. The two alkyl groups of sevoflurane are fluoromethyl and 1,1,1,3,3,3-hexafluoroisopropyl[68] (Figure 3). The structure of sevoflurane affects its physicochemical properties, which in turn influences the induction of and recovery from anesthesia, anesthetic potency and clinical

effect dose. The blood–gas partition coefficient of sevoflurane is 0.69, which is only half that of isoflurane[69]. The low blood-gas partition coefficient provides sevoflurane with the properties of rapid induction of, and fast recovery from anesthesia. In addition, due to minimal effects on the cardiovascular system and virtually no organ toxicity, sevoflurane is one of the most popular anesthetics in clinical anesthesia for elderly patients. According to publications, the MAC for humans of sevoflurane was reported to be between 1.71% to 2.05%[70]. And like other anesthetics, the MAC of sevoflurane for humans is lower in the elderly, at about 1.48% (mean age 71.4 years old)[71].

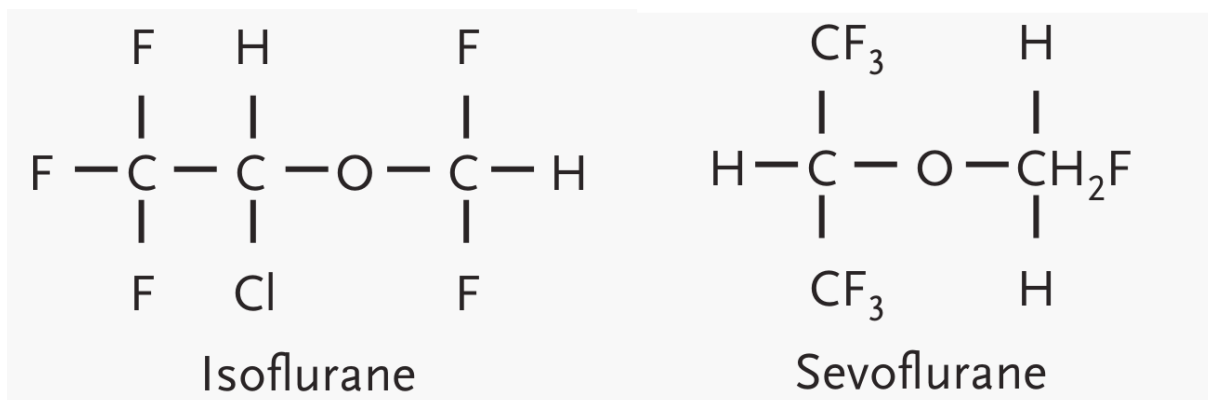


Figure 3. The structure of isoflurane and sevoflurane. The figure is modified from the publication “Mechanisms of Actions of Inhaled Anesthetics” [68].

Although the safety and efficacy of sevoflurane have been well confirmed, recently a series of lab and clinical studies have shown that sevoflurane exposure may have potentially harmful neurobehavioral effects such as aggravating AD neuropathogenesis and inducing postoperative neurocognitive disorders, especially in vulnerable brains, such as those of AD patients[72-74]. In Human H4 neuroglioma cells and 5-9 months C57/BL6 mice, sevoflurane-induced apoptosis and upregulated amyloid precursor protein cleaving enzyme and A β levels, which suggest that sevoflurane may promote AD neuropathogenesis[73]. And in the AD transgenic mice brain, sevoflurane exposure elevated tumor necrosis factor- α expression levels [72]. In terms of clinical trials, a double-blind prospective clinical study showed that, compared to propofol, sevoflurane anesthesia in elderly patients is associated with a higher

incidence of POD[13]. Similarly, in elderly patients with pre-existing cognitive impairments, compared to propofol, sevoflurane produced a greater effect on cognitive function at 7 days postoperatively[75]. Several hypotheses, such as neuroinflammation, mitochondrial oxidative stress, and A β aggregation, have been proposed to be associated with sevoflurane-induced neurobehavioral disorders, but the exact mechanisms remain unclear[76].

Although various studies have indicated sevoflurane's toxic effects, some studies show that sevoflurane has neuroprotective effects[77, 78]. In a model of focal cerebral ischemia in Sprague-Dawley (SD) rats, sevoflurane preconditioning improved neurologic scores and reduced infarct size after reperfusion[79]. In children undergoing magnetic resonance examinations under general anesthesia, low doses of sevoflurane downregulated S100 β protein levels in serum, which may indicate that sevoflurane has a neuroprotective effect on the CNS[78].

Consequently, current findings on the effects of sevoflurane on the brain are inconsistent. Therefore, to improve clinical anesthesia, further investigation should focus on sevoflurane's impact on patients with pathological situations. In addition, due to the widespread clinical application of sevoflurane, there is an urgent need to uncover the mechanisms of toxicity to reduce the adverse effects of sevoflurane.

In the clinic, inhalation anesthetics are administered in the gas phase. When performing in vitro experiments in the lab at room temperature, it is important to be clear that the concentrations of inhalation anesthetics correlate with the clinical effect. Meanwhile, it is necessary to emphasize that MAC calculated in the aqueous phase is the proper choice for clinically relevant concentrations. Franks et al. demonstrated that the aqueous phase potency of inhalation anesthetics is relatively stable in the temperature range of 20–37 °C[80]. Calculating from the partial pressure value and the saline/gas partition coefficient and subsequently applying temperature corrections, the corresponding MAC value of sevoflurane

in the aqueous phase (saline) of rodents in vitro experiments was approximately 0.38 mM[69, 80, 81].

1.5 Synapses and dendritic spines

1.5.1 Synapses and memory

Synapses are functional units of the central nervous system (CNS) that connect neurons to form the brain's circuits. As such, the brain can be viewed as a vast collection of highly diverse and dynamic synapses[82]. It is estimated that there are more than 100 trillion synapses in the human neocortex[83].

Synapses can be divided into two categories: chemical and electrical synapses. In the vertebrate CNS, most are chemical synapses. A chemical synapse comprises a presynaptic neuron terminal containing synaptic vesicles, a widened intercellular space (synaptic cleft), and a postsynaptic structure. The postsynaptic density (PSD) is an electron-dense region localized at the postsynaptic sites of excitatory synapses, characterized by a high concentration of receptors, scaffold proteins, signaling enzymes, and cytoskeletal proteins.

Synaptic transmission is the information processing between neurons in the CNS. In chemical synapses, depolarizing the action potential reaching the presynaptic terminal releases neurotransmitters from the synaptic vesicles. Then, the neurotransmitters diffuse across the synaptic cleft and bind to specific receptors on the postsynaptic membrane, leading to the opening (or closing) of ion channels and subsequently changing the membrane conductance and potential of the postsynaptic neuron.

Over the past few decades, tremendous progress has been made in understanding synaptic structure, molecular composition, and physiological functions. It is widely recognized that synapses play a central role in memory storage. Synaptic plasticity, the activity-dependent changes in the efficiency and strength of synaptic connections, is the fundamental component of memory and learning[84]. LTP and long-term depression (LTD) are two forms of synaptic plasticity. LTP is the long-term strengthening of the synaptic connection following brief, high-

frequency stimulation, whereas LTD is the weakening of synaptic strength[85]. LTP and LTD indicate that the strength of synaptic connections can be changed by learning, which are the elementary components of memory storage.

Because the hippocampus is a key brain region for learning and memory and has a unique trisynaptic pathway, numerous studies on synaptic plasticity (LTP/LTD) are carried out in the hippocampus. Information from the cortex is communicated via the perforating pathway connecting the entorhinal cortex (EC) with the dentate gyrus (DG), which in turn communicates with Cornu Ammonis (CA) 3 through mossy fiber. Then CA3 connects to CA1 through the Schaffer collateral pathway. Finally, CA1 projects back to the EC[86].

Memory deficits and cognitive impairments are the main symptoms of AD, so it is not surprising that synaptic dysfunction (e.g., synaptic loss and synaptic structural impairments) is a common feature of AD[87]. Studies have shown that synaptic dysfunction is the main neurobiological basis for cognitive impairment in AD patients, and significant synaptic dysfunction, especially synaptic loss, occurs long before the appearance of cognitive decline[88]. Therefore, understanding the potential mechanisms of synaptic dysfunction in AD in the early stages can help us understand and treat this devastating disease.

1.5.2 Dendritic spines and plasticity

Dendritic spines are tiny membranous protrusions on the dendritic shaft, serving as the anatomical sites of most excitatory synapses and playing a key role in learning and memory[89]. Typically, a dendritic spine consists of a rounded “head” and a thinner “neck”, while the morphology of dendritic spines exhibits extensive diversity and can change rapidly in size and shape. Filopodia, the smallest protrusions, are highly dynamic and can form or eliminate very quickly, while the mushroom type, the largest spines, are more likely to remain stable for months[89, 90].

The cytoskeleton of the spine consists of actin networks, the change of which mediates lasting alterations in spine plasticity[89] (Figure 4). Usually, synaptic strengthening and LTP are associated with an increase in spine number and/or an enlargement of the spine head, while synaptic weakening and LTD lead to spine retraction and/or shrinkage[91]. The structural plasticity of dendritic spines is closely related to learning, memory, and other cognitive processes.

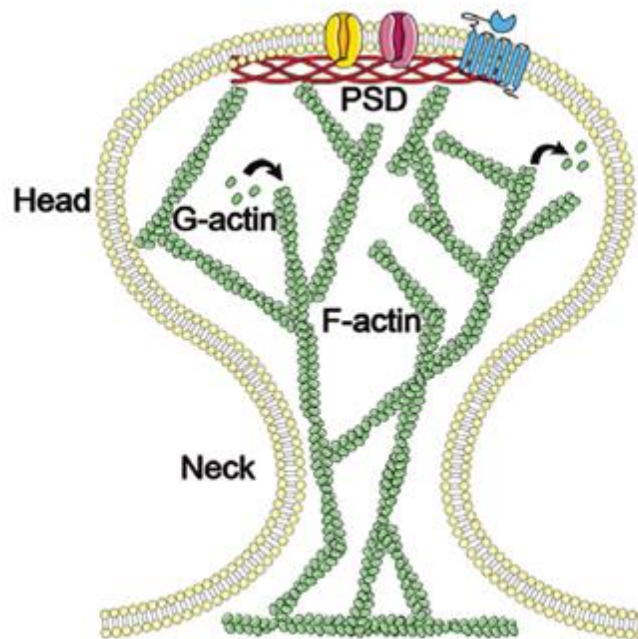


Figure 4. Illustration of the structure of a dendritic spine[89]. Typically, the structure of a dendritic spine is built primarily on the actin cytoskeleton, with a thin neck connected to the dendrite and a protruding, rounded head.

1.5.3 Dendritic spines classification

The classification of spines into predefined morphological groups is a standard method to study the relationship between dendritic spine shape and function. Based on different morphologies, dendritic spines are usually categorized into mushroom, thin, and stubby spines[92].

Mushroom spines are defined by large bulbous heads and narrow necks, with the diameter of the head being much larger than that of the neck. Thin spines are smaller and longer than the

diameter of the neck, and the head and neck are similar in diameter. Stubby spines are short, flat spines that lack distinctive head and neck configurations and are similar in length and width (Figure 5). In some studies, filopodia and cup-shaped spines are also accepted as dendritic spines[93]. Filopodia are the smallest protrusions on dendrites, often described as elongated hair-like structures, and are often considered the precursors of dendritic spines.

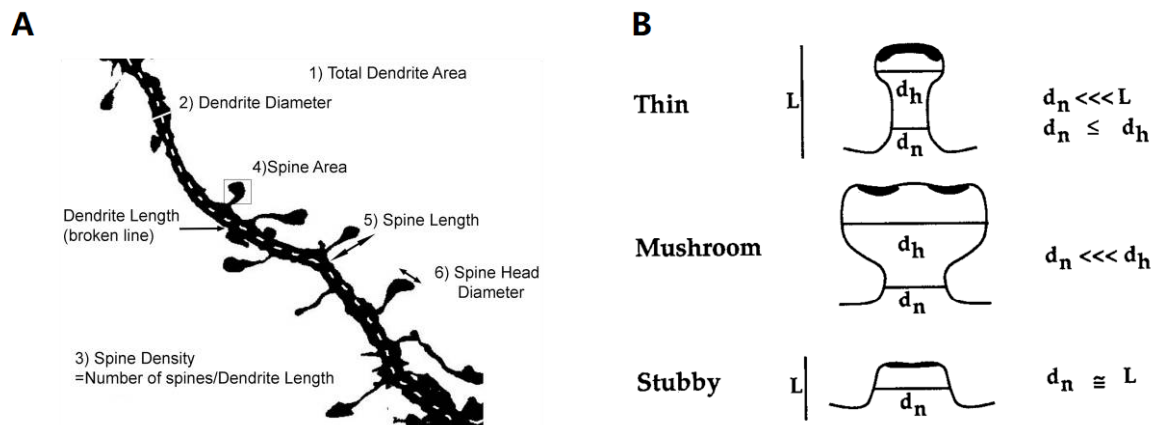


Figure 5. (A) A typical dendrite segment from a pyramidal neuron and the quantification parameters are shown[94]. (B) Criteria for classification of dendritic spines[92].

Mushroom spines have large head areas which contain large PSDs. In addition, large spines have perisynaptic astrocytic processes that can provide synaptic stability. Thus, mushroom spines are thought to be stable spines for memory storage. In comparison, thin spines have smaller PSDs with a greater potential for enlargement, and form or disappear rapidly in response to synaptic activity. Therefore, thin spines are considered immature synapses and can be used to indicate plasticity capacity in neural circuits [95].

1.6 Astrocytes

1.6.1 Physiology of Astrocytes

Astrocytes, also named astroglia, are the mammalian brain's most abundant glial cell types. For a long time, they were considered as the “glue” in the brain, only providing the structural and metabolic environment for neurons. In the last two decades, dramatic progress has been

made in the knowledge of astrocytes. Now it is generally accepted that astrocytes are highly heterogeneous in morphology and function[96]. Due to the complex morphology, astrocytes interact with various cells, including neurons, microglia, and endothelial cells, to keep the homeostasis of the CNS and thus actively participate in various physiological and pathological processes of the CNS.

The physiological functions of astrocytes mainly include 1) regulation of neuronal activity and synaptic homeostasis; 2) supporting and the formation of the blood-brain barrier; 3) supplying trophic factors and nutrients to neurons; 4) maintenance of ionic and water balance in the CNS; 5) and repairment after traumatic brain injury[96-98].

1.6.2 Astrocyte-mediated synaptic phagocytosis

In the CNS, a single astrocyte extends thousands of fine membranous processes that closely interact with pre- and post-synaptic structures to form “tripartite synapses” [99]. Based on this, astrocytes interact with neurons in both directions for information processing and are closely involved in synaptic activities, including formation, maturation, and elimination of the synapses, thus maintaining the homeostasis of synapses and regulation of synaptic transmission[100, 101].

In the adult hippocampus, synapses are constantly undergoing rapid formation and elimination. Activity-dependent learning prunes silence synapses to make space for the formation of new synapses, thereby maintaining the homeostasis of neural circuits. Therefore, synapse elimination is a central mechanism of neurological remodeling during learning and memory. Astrocyte-mediated synaptic phagocytosis is one of the mechanisms of synaptic elimination to maintain hippocampal synaptic connectivity and plasticity[102]. Multiple epidermal growth factor-like domains 10 (MEGF10) and myeloid-epithelial-reproductive tyrosine kinase (MERTK) are two phagocytic receptors for astrocytes (Figure 6). The absence of either phagocytic receptor reduces astrocyte's relative phagocytic capacity by 50% [103]. And recent

studies have shown that the dysregulation of astrocyte-mediated synaptic phagocytosis is one of the causes of synaptic degeneration, leading to the development of maladaptive plasticity and cognitive deficits in various CNS disorders such as AD[101, 103].

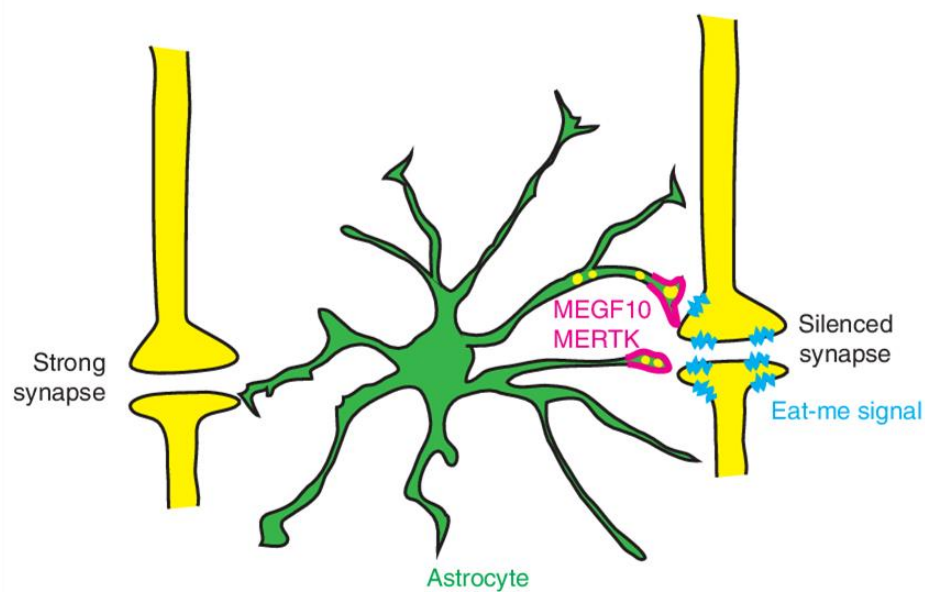


Figure 6. Astrocytes (green) eliminate synapses by recognizing “eat-me signals” presented in the silent synapses (light blue) and engulf them through MEGF10 and MERTK (magenta) phagocytic receptors[101].

1.6.3 Astrocyte morphology and GFAP

Astrocytes are complex stellate-shaped cells with many processes forming well-defined territories. This highly complex morphology makes astrocytes to be in close contact with synapses, blood vessels, and other glial cells through delicate processes. Furthermore, the structure of astrocytes is highly dynamic and activity-dependent. Change or loss of astrocyte morphology is a common feature of many neurological disorders[104].

GFAP, an intermediate filament protein found in mature astrocytes of the CNS, is a highly dynamic part of the cytoskeleton and responsible for maintaining mechanical strength of astrocytes while also supporting surrounding neurons and the blood brain barrier. In addition, GFAP has long been considered as a specific marker of astrocytes[105]. GFAP protein has three structural domains: amino-terminal “head”, central helical “rod”, and carboxy-terminal

“tail”. The rod domain is consistent, while the head and tail domains are variable with different sizes and amino acid sequences[106]. To form intermediate filaments, GFAP proteins undergo a gradual polymerization process of monomer → dimer → tetramer. Only the tetramer can form the filament, which is a symmetric, nonpolar structure (Figure 7). The head domain is important for filament elongation, whereas the tail domain is critical for GFAP oligomerization[106]. Thus, the structural integrity of GFAP proteins is essential for the formation and elongation of astrocytes' intermediate filament.

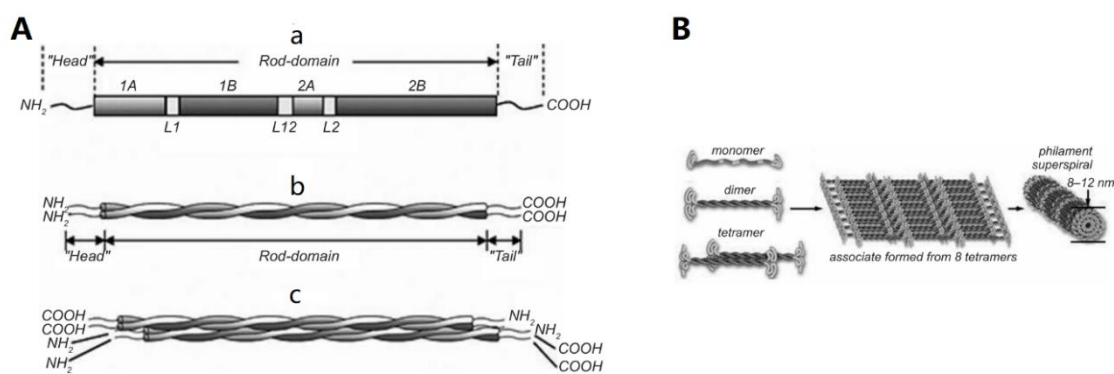


Figure 7. (A) GFAP structure. GFAP monomer, GFAP dimer, and tetramer assembly. a: Monomer, b: parallel dimer, and c: antiparallel tetramer. (B) Hierarchic principle of GFAP oligomerization model and the structure of an intermediate filament[106].

10 different isoforms of GFAP have been identified in astrocytes[107, 108]. GFAP- α is the predominant isoform in the brain with the classic 432 residues. Besides isoforms, GFAP proteins are susceptible to several post-translational modifications. One of the key post-translational modifications of GFAP is proteolysis/fragmentation, which is a calcium-activated protease calpain-mediated truncation at both the C- and N-terminals, resulting in a series of truncated GFAP breakdown products (BDPs) during glial cell challenge[108].

In addition to being a specific marker for astrocytes, GFAP helps to maintain the specific morphology of astrocytes, control the migration, and maintain the stability of astrocyte processes. However, more and more studies suggest that GFAP is also involved in a wide

variety of other processes that are important for synaptic plasticity, such as cellular signaling and neuron-glia interactions[109, 110].

1.7 Objectives

With the increasing life expectancy and improvement of surgical safety, the number of patients with AD needing anesthesia is steadily growing. There is great concern that anesthesia may induce postoperative neurocognitive deficits in patients with AD or even exacerbate the progression of AD. Consequently, it is critical to explore the effects of anesthetics on the pathophysiology of AD.

In this study, we investigated the effects of sevoflurane (0.4 MAC and 1.2 MAC) and different A β isoforms-A β ₁₋₄₀, A β ₁₋₄₂, A β pE3, and 3NTyrA β) on DSD and astrocyte-mediated synaptic engulfment, to explore the interactions between sevoflurane and A β -dependent pathophysiology.

2. Materials and Methods

2.1 Animals

Adult male Thy1-eGFP and C57BL/6 mice (8-12 weeks old; Charles River, Munich, Germany) were used. All mice were kept and fed under standard conditions (12:12 h light/dark cycle, 22 \pm 2°C, 60% humidity) with free access to tap water and standard mouse food. Mice were randomly assigned to each group. All procedures followed a protocol approved by the Technical University Munich and the Government of Upper Bavaria.

2.2 Key resources tables

Table 1: Main reagents for this study

REAGENT or RESOURCE	Manufacturer	CAS Registry Number
A β ₁₋₄₀	Bachem	131438-79-4
A β ₁₋₄₂	Bachem	107761-42-2
A β pE3	Bachem	183449-57-2
Carbogen (95% O ₂ and 5% CO ₂)	Linde	10021938
Color-coded prestained protein marker, 10-250 kDa	Cell Signaling Technology	74124S

D-(+) Glucose-Monohydrate	Sigma-Aldrich	14431-43-7
DMSO	Sigma-Aldrich	67-68-5
Frozen section media	Leica	3801480
Isoflurane	Cp-pharma	
Methanol	Merck, Darmstadt	67-56-1
Normal Goat Serum	Sigma Aldrich	S26
NuPAGE® LDS Sample Buffer (4X)	Thermo Fisher Scientific	
Paraformaldehyde powder	Millipore	30525-89-4
Phenylmethanesulfonyl fluoride (PMSF)	Sigma-Aldrich	329-98-6
Potassium chloride	Sigma-Aldrich	7447-40-7
ProLong™ Glass Antifade Mountant with NucBlue™ Stain	Thermo Fisher	P36985
Sevoflurane	Baxter	CA2L9117
Sodium azide	Sigma-Aldrich	26628-22-8
Sodium bicarbonate	Sigma-Aldrich	144-55-8
Sodium chloride	Sigma-Aldrich	7647-14-5
Sodium phosphate monobasic monohydrate	Sigma-Aldrich	10049-21-5
Triton-X-100	Sigma Aldrich	9036-19-5
3NTyrAβ	Bachem	
10X PBS (Phosphate Buffered Saline)	PanReac AppliChem	A0965,9050

Table 2: Equipments for this study

Equipment	Manufacturer	
Centrifuge	Tuttlingen	EBA 200 Hettich
ChemiDoc XRS System	BIO-RAD	Bio-Rad ChemiDoc XRS System with Universal Hood II
Confocal Microscope	Leica	Leica TCS SP8 X equipped with special pulsed (78 MHz) "super continuum white light laser"
Cryotome	ThermoFisher	CryoStar NX70
Electrophoresis chamber	BIO-RAD	Mini-PROTEAN Tetra Vertical
Gel casting system	BIO-RAD	
Microtome	Leica	Leica VT100S
Vaporisers for sevoflurane	Drägerwerk	
Water bath	Köttermann	3044
Water purification system	Merck, Darmstadt (GER)	Milli-Q®

Table 3: Softwares for this study

Software	Manufacturer	Websites
Image Lab™ 6.0	BIO-RAD, Munich (GER)	Download ImageLab6.0 by Bio-Rad Laboratories (informer.com)

IMARIS 9.7 (or higher) for Neuroscientists	Oxford instrument, Bitplane	https://imaris.oxinst.com/microscopy-imaging-software-free-trial
LAS X (Acquisition software)	Leica microsystems	https://www.leica-microsystems.com/products/microscope-software/p/leica-las-x-ls/
Prism 8	GraphPad Software, San Diego (USA)	

Table 4: Antibodies for this study

Antibodies	Manufacturer	No.
Anti-mouse IgG, HRP-linked Antibody	Cell Signaling Technology	7076
Anti-rabbit IgG, HRP-linked Antibody	Cell Signaling Technology	7074
Goat Anti-Mouse IgG H&L (Alexa Fluor® 647)	Abcam	ab150115
Goat Anti-Rabbit IgG Fc (Alexa Fluor® 488)	Abcam	ab150089
Mouse GFAP	Cell Signalling Technology	3450
Rabbit ALDH1L1	Cell Signalling Technology	85828
Rabbit MEGF10	Sigma-Aldrich	ABC10
Rabbit PSD95	Cell Signalling Technology	3670S

2.3 Acute hippocampal brain slices preparation

2.3.1 Prepare 2 L of preparation ringer solution and 1 L of mess ringer (artificial cerebrospinal fluid (aCSF) solution)

2.3.1.1 Making 2 L of preparation ringer solution

The following reagents were dissolved in approximately 1.5 L of Milli-Q water in the order shown in Table 5 with constant stirring. When the solid reagents were completely dissolved, the volume of the solution was increased to 2 L. The preparation ringer solution can be kept at -80°C for up to 1 month.

Table 5: Composition of the preparation Ringer solution

Preparation Ringer Solution (2 L)
--

Reagents	Final concentration (M)	Amount (g)
NaCl	0.125	14.610
KCl	0.0025	0.373
NaH ₂ PO ₄ -Monohydrate	0.00125	0.345
D- (+) Glucose-Monohydrate	0.025	9.909
NaHCO ₃	0.025	4.201
MgCl ₂ -Hexahydrate	0.006	2.440
CaCl ₂ -Dihydrate	0.00025	0.074

2.3.1.2 Making 1 L of aCSF solution

The following reagents in Table 6 were dissolved in approximately 800 mL of Milli-Q water with constant stirring. When the solid reagents were completely dissolved, the volume of the entire solution was increased to 1 L. The aCSF solution can be stored at 4 °C for up to seven days.

Table 6: Composition of aCSF

Mess Ringer (aCSF) (1L)		
Reagents	Final concentration (M)	Amount (g)
NaCl	0.125	7.305
KCl	0.0025	0.186
NaH ₂ PO ₄ -Monohydrate	0.00125	0.172
D- (+) Glucose-Monohydrate	0.025	4.954
NaHCO ₃	0.025	2.1
MgCl ₂ -Hexahydrate	0.001	0.203
CaCl ₂ -Dihydrate	0.002	0.294
After 15 min of oxygenation with carbogen, the pH value should be 7.30 (7.20 - 7.40).		

2.3.2 Acute hippocampal brain slices preparation

- 1) The microtome and the water bath were turned on before sacrificing the mice. The temperature of the water bath was kept at 35 °C.
- 2) 70 mL of aCSF was poured into a beaker, continuously oxygenated with carbogen, and placed inside the water bath.

- 3) A petri dish with mess ringer solution was prepared and oxygenated with carbogen constantly.
- 4) Ice was put outside of the microtome box to maintain the preparation ringer solution in a slushy state for smooth slicing of the mouse brain. The microtome box was filled with preparation ringer solution with carbogen oxygenating.
- 5) After mice were anesthetized with isoflurane in an anesthesia chamber and decapitated, the brains were quickly taken and immediately placed into an ice-cold preparation ringer solution.
- 6) The sagittal brain slices, including the hippocampus with a thickness of 400 μm , were prepared using the microtome.

2.4 A β isoforms (A β ₁₋₄₀, A β ₁₋₄₂, A β pE3, and 3NTyrA β) preparation and incubation

- 1) 1 mg of A β isoform (either one of A β ₁₋₄₀, A β ₁₋₄₂, A β pE3, and 3NTyrA β) was dissolved in hexafluoro-2-propanol (HFIP) (400 μL), then the mixture was incubated at room temperature (21°C to 24°C) until it became a clear solution.
- 2) The solution was dispensed into 20 \times 2 mL microcentrifuge tubes.
- 3) The tubes were placed in a lyophilizer until white pellets formed at the bottom of the tubes, usually taking up to 2 h. Thereafter the tubes were placed at -80°C.
- 4) When ready to use, 100 μM of A β was made by adding 111 μL freshly dissolved in dimethyl sulfoxide (DMSO) to one tube and then was sonicated on an ultrasonic bath for 15 min to make the A β dissolve completely.
- 5) After the acute hippocampal brain slices recovered at room temperature for 1 h, the four A β isoforms were added accordingly to the beakers with aCSF. And the final concentration of every A β isoform was diluted to 50 nM.

2.5 Sevoflurane application

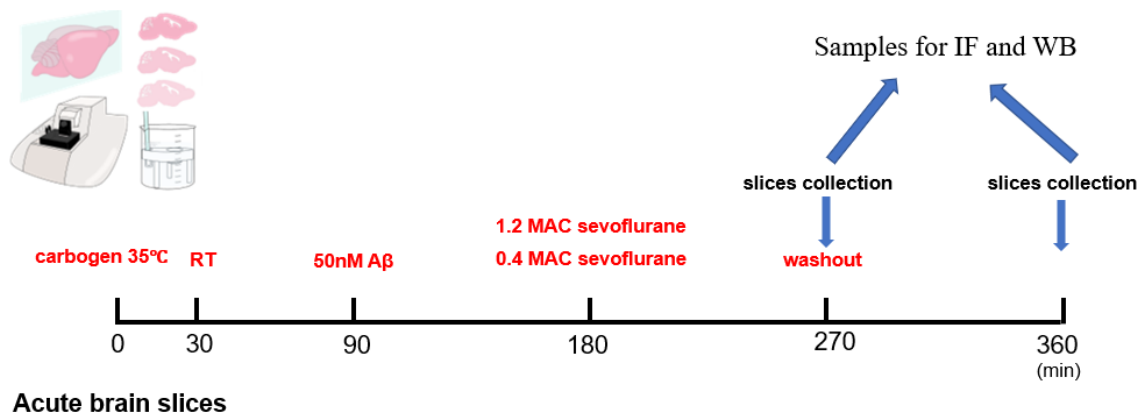
In addition to the anesthetic effect, sevoflurane is an effective sedative with rapid onset, fast recovery, and little organ toxicity. In addition, sevoflurane has bronchodilatory and pulmonary

protective effects[111]. Therefore, sevoflurane is recommended for the sedation of critically ill patients in the intensive care unit (ICU). The recommended sevoflurane concentration for these patients is approximately MAC-awake, which is the concentration required to suppress 50% of patients' responses to verbal commands. MAC-awake is about one-third of the MAC for the commonly used inhalation anesthetics such as desflurane and sevoflurane[63, 112].

It is widely known that MAC estimates the median concentration of an inhalation anesthetic. Only half of the subjects are anesthetized at this dose while the other half are not. Obviously, a minimum anesthetic concentration would be more useful for anesthesiologists who must prevent patients from moving during the surgery. However, a minimum concentration applicable to 100% of patients cannot be computed from the anesthetic dose-response assay. Therefore, in clinical practice, the concentration that ensures that 95% of patients do not move under noxious stimulation is recommended, corresponding to 1.2 MAC[112].

Therefore, we chose these two concentrations (0.4 MAC and 1.2 MAC) of sevoflurane in the present study. According to the publication of Cesarovic, N et al., the MAC of sevoflurane in C57BL/6 mice is about 3.25 % [113], thus for our study, the corresponding concentrations of sevoflurane in the gas phase for 0.4 MAC_{rodent} and 1.2 MAC_{rodent} are about 1.4% and 4% in sevoflurane vaporizer settings. Since sevoflurane is administered clinically in the gas phase, samples from the recording chamber were taken and filled into airtight glass containers for gas chromatographic measurements to determine the aqueous concentrations of sevoflurane. In our laboratory, using acute mouse brain slices, Rainer Haseneder et al. found that the aqueous MAC concentration of sevoflurane at room temperature is 0.38 mM [81]. Therefore, the corresponding aqueous concentrations of sevoflurane in our study are 0.15 mM (1.4%/0.4 MAC_{rodent}) and 0.46 mM (4%/1.2 MAC_{rodent}), respectively.

2.6 Experiment schedule and groups



Acute brain slices

Figure 8. Schedule of Aβ isoforms incubation and sevoflurane exposure in ex vivo hippocampal brain slices. Mice were decapitated after being anesthetized with isoflurane. Brains were removed quickly, and 400 μm sagittal slices were sectioned in ice-cold, carbogen-saturated preparation Ringer solution. The acute hippocampal brain slices were incubated in the carbogen-saturated aCSF at 35°C for 30 min, followed by another 60 min at room temperature. Acute hippocampal brain slices were then incubated with different Aβ isoforms-Aβ₁₋₄₀, Aβ₁₋₄₂, Aβ_{pE3} and 3NTyrAβ with a final concentration of 50 nM for 90 min. Next, sevoflurane at 0.4 MAC or 1.2 MAC was applied to the acute hippocampal brain slices for 90 min, followed by another 90 min sevoflurane washout with carbogen. The acute hippocampal brain slices were always aerated with carbogen. The control groups were gassed only with carbogen throughout the experiment. RT, room temperature; IF, immunofluorescence; WB, Western Blot.

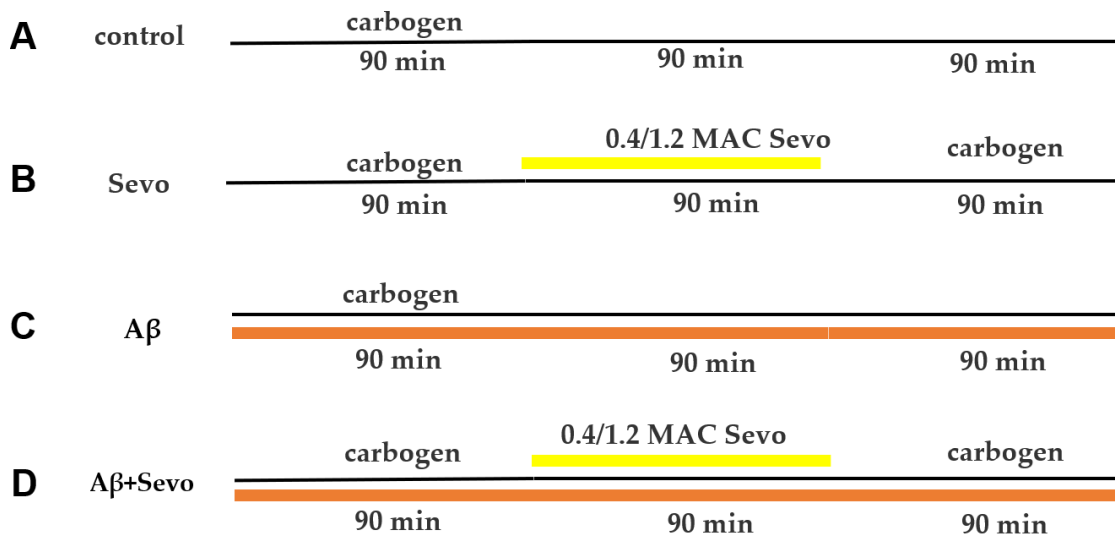


Figure 9. The timeline and workflow of Amyloid Beta incubation and sevoflurane exposure. (A) Control, the black line represents carbogen gassing. (B) Sevoflurane (Sevo) exposure and washing out. The black line represents carbogen gassing, and the yellow line represents Sevo gassing. (C) Aβ incubation. The black line represents carbogen gassing, and the brownish line represents Aβ incubation.

(D) A β pre-incubation and sevoflurane exposure. The black line represents carbogen gassing, the yellow line represents Sevo gassing, and the brownish line represents A β incubation.

2.7 Analysis of dendritic spines

- 1) 8-12 weeks old male Thy1-eGFP mice were used to analyze dendritic spines. After different treatments, the acute brain slices were fixed with 4% paraformaldehyde (Merck, Germany) over two nights, then were cryoprotected with 30% sucrose for another 3 days.
- 2) Sections of 50 μ m thickness were prepared using a cryotome. Only selected slices with intact hippocampus. After 3 washes with 1 x PBS for 5 min, the sections were transferred to slides and the cover slipped.
- 3) Images of CA1 pyramidal neuron dendritic spines were acquired by confocal microscope at 0.3 μ m interval z-stacks with a 63x/1.40 NA oil-immersion objective. Only second-order apical dendritic segments were considered, 100-200 μ m from the pyramidal soma (Figure 10).

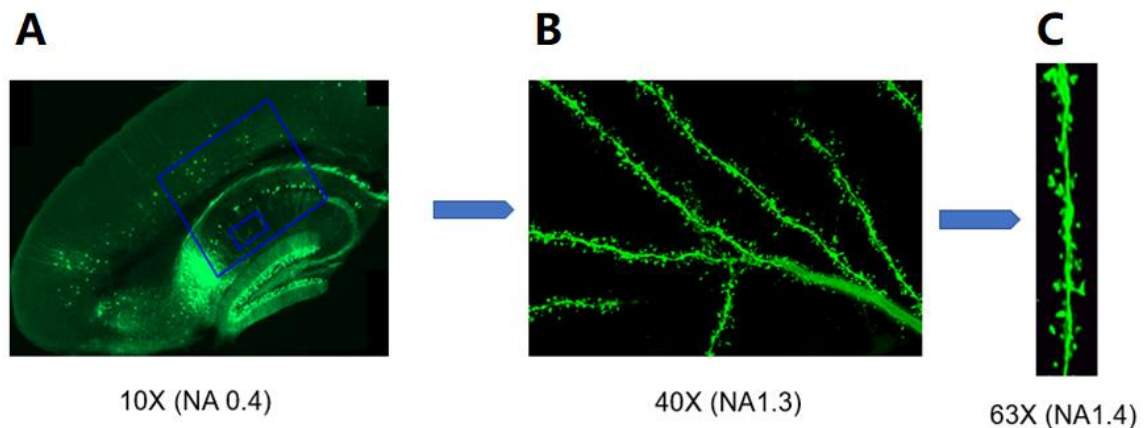


Figure 10. Overviewing the process of dendritic spine acquisition. (A) Sagittal image of the hippocampus of a Thy1-eGFP mouse. Using a 10x objective to locate the CA1 region of the hippocampus. (B) Apical dendrites of a pyramidal neuron. Switching to a 40x oil objective, select one dendrite and place it in the middle of the field. Only second-order apical dendritic segments, situated at a distance between 100 to 200 μ m from the pyramidal soma were considered. (C) Maximum intensity projection of a segment of dendrite. Images were acquired with a confocal microscope at 0.3

μm interval z-stacks with a 63x oil-immersion objective. All the images were taken with Leica TCS SP8 X equipped with a "super continuum white light laser" Confocal Microscope.

- 4) The acquired dendritic images were enlarged and analyzed with Leica Application Suite (LAS) X software, 20-50 μm in length, and 6-8 dendrites were analyzed per mouse.
- 5) As mentioned above, dendritic spines were categorized as thin, mushroom, and stubby subtypes based on established criteria[92]. It is difficult to distinguish filopodia from long, thin spines, in our study, filopodia was classified as thin spines. Dendritic spines were classified as thin if the length diameter was greater than the neck, and the diameters of the head and neck were similar. Dendritic spines were classified as mushrooms if the diameter of the head was much greater than the neck. Dendritic spines were classified as stubby if the diameter of the neck was similar to the length of the spine. Dendritic spine density was expressed as the number of spines per 10 μm of dendrite.
- 6) The double-check analysis of the dendritic spines was performed by a PhD in our lab who is very experienced in this field.

2.8 Immunofluorescence and colocalization analysis

Regarding methodology on this part, I have published a protocol as a co-first author with a PhD in our lab. In that paper, we provided a detailed protocol for colocalization analysis of postsynaptic marker PSD95 within individual high-resolution astrocytes in the CA1 region of the hippocampus in an *ex vivo* model. Therefore, I cited most of the details from the protocol with permission from the other co-authors[114].

2.8.1 Immunofluorescence staining

- 1) After treatments, the acute hippocampal brain slices from the 8-12 weeks old C57BL/6 mice were collected and fixed with 4% PFA over two nights.
- 2) The slices were then cryoprotected with 30% sucrose for 3 days.

- 3) 30 μm thickness sections were cut with a cryotome for immunofluorescence staining.
- 4) Then the 30 μm sections were washed with 1 x PBS for 3 x 10 min and blocked with blocking solution (1 x PBS + 10% normal goat serum + 0.3% Triton-X-100) for 2 h at room temperature.
- 5) Thereafter, primary antibodies (rabbit anti-PSD95 (1:400); mouse anti-GFAP (1:800)) were applied, and then sections were put on a shaker at 4°C over two nights.
- 6) Sections were rinsed with 1 x PBS for 3 x 10 min and incubated with secondary antibodies (Alexa Fluor 488/647-conjugated goat anti-mouse/rabbit (1:500)) at room temperature for 2 h in dark.
- 7) After 3 x 10 min wash with 1 x PBS, sections were mounted, and coverslipped with DAPI mounting medium.

2.8.2 Image Acquisition

High-resolution astrocytes from the stratum radiatum layer of the CA1 region of the hippocampus were selected in our study. We took 4-8 sections of images per animal with the Leica TCS SP8 confocal microscope.

- 1) Firstly CA1 region of the hippocampus was located. Start from a low magnification (10/0.40 NA) and (20/0.75 NA). Nuclear staining helps to identify the CA1 region (Figure 11).
- 2) Switch to 63x/1.40 NA oil immersion objective for single astrocyte acquisition. The z-stack was set according to the volume of the astrocyte.
- 3) Deconvolution: the lightning function of the Leica Confocal SP8 was applied to deconvolve the images to improve resolution, then exported the deconvolved images to Imaris software for the colocalization analysis.

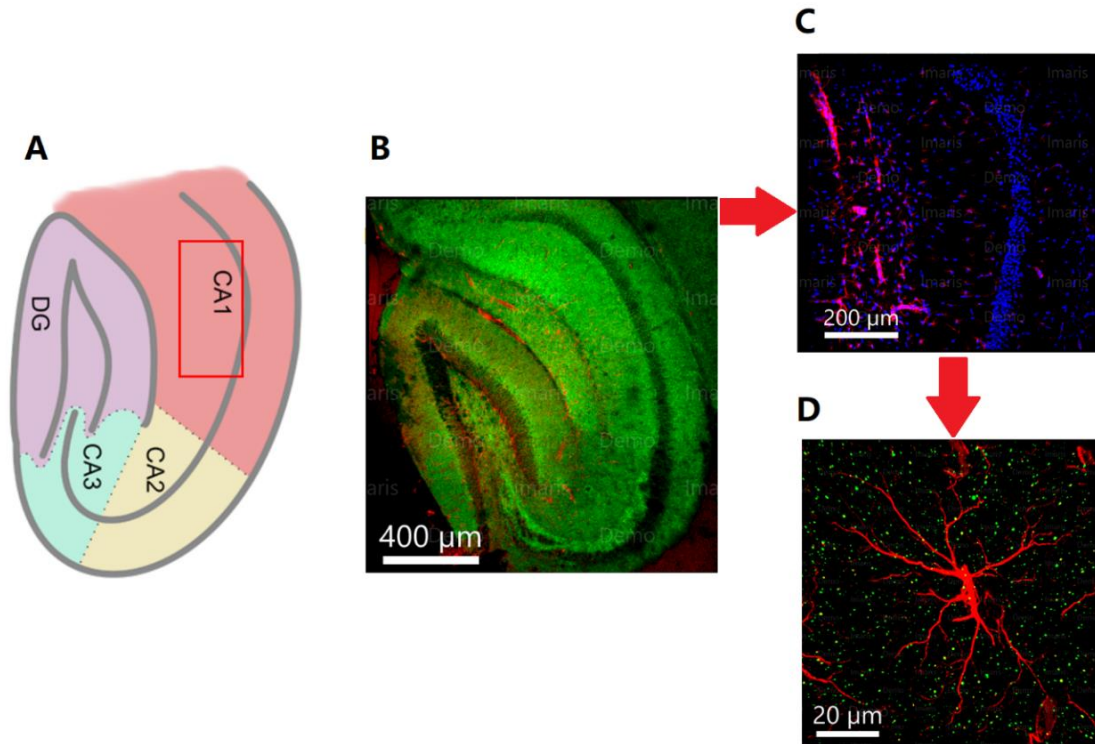


Figure 11. Overview of the PSD95-GFAP interaction in the CA1 region of the hippocampus[114]. (A) Schematic representation of different regions of the hippocampus. The stratum radiatum is marked with a red box. (B) 10/0.40 magnification of a sagittal hippocampal section stained with PSD95 (green) and GFAP (red). Scale Bar = 400 μm . (C) 20/0.75 magnification focusing on the CA1 region stained with NucBlueTM (cyan) and astrocyte (red). Just below the densely stained area (pyramidal layer) is the stratum radiatum layer. Scale Bar = 200 μm . (D) 63/1.40 magnification of a high-resolution individual astrocyte (red) stained alongside PSD95 (green). Scale Bar = 20 μm .

2.8.3 Quantitative analysis of astrocyte-mediated synaptic engulfment

The images were analyzed with Imaris software to calculate the colocalization of PSD95 and GFAP (Figure 12).

- 1) Create the surface of a single astrocyte. “Segment only a region of interest” was selected under the “Algorithm Settings” box. A guide to surface construction was opened, and then the surface of the astrocyte was rendered by adjusting the signal threshold corresponding to the GFAP channel.

- 2) Processing the rendered astrocyte. After surface reconstruction of the astrocyte, the unwanted signals from other nearby astrocytes must be filtered out before proceeding to the next step.
- 3) Masking the surface of the astrocyte. Clicked the “Edit” tab under a newly built surface. Set voxels outside the surface to 0 to eliminate any signals outside the rendered surface.
- 4) Set the threshold intensity for the PSD95 (channel A). Manually set the threshold for the PSD95 channel by randomly selecting 10 unambiguous green dots and averaging the intensity to set the threshold for channel A.
- 5) Select the masked GFAP in Channel B and set the intensity threshold. Since we had eliminated the background signals by threshold masking of the original GFAP channel, therefore, the threshold intensity of Channel B can be directly set at 1.
- 6) Select the “Region of Interest”. What we were interested in is the colocalization of PSD95 within a single astrocyte. Thus, the masked GFAP channel was chosen as the region of interest.
- 7) Build Coloc Channel. Clicked “Build Coloc Channel” tab, and a new tab with the analyzed parameters opened. % of ROI colocalized gave us an estimation of the amount of PSD95 present in the whole volume of the astrocyte, therefore, it is what we are interested in in our study.

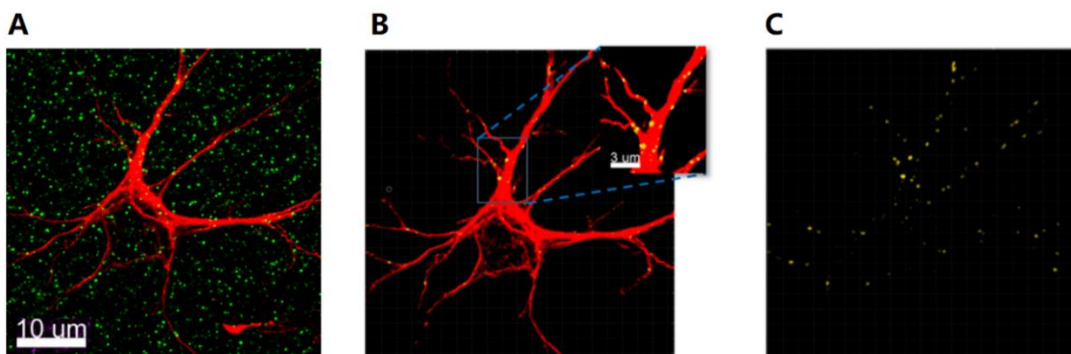


Figure 12. Representative images of astrocyte-mediated synaptic phagocytosis of postsynaptic marker PSD95[114]. (A) A high-resolution astrocyte (shown in red) and post-synaptic marker PSD95

(shown in green). (B) Rendered astrocyte with Imaris software. The colocalization points inside the astrocyte are shown in yellow. (C) The colocalized PSD95 within astrocytes in maximal projection view.

2.9 Western blot

2.9.1 Protein extraction and sample preparation

- 1) After different treatments, the hippocampi of the acute brain slices were dissected in ice-cold aCSF quickly.
- 2) Dissected hippocampi were placed with ice-cold lysis buffer (shown in Table 8), grinded the hippocampi with a pestle into homogenate, then incubated the homogenate for 30 min on ice.

Table 8: Components of lysis buffer

Lysis buffer	
Reagents	Amount (uL)
RIPA	970
100 PMSF	20
50 Complete	10
Peptains	1
200 μ L lysis buffer for 3-4 slices hippocampus	

- 3) The homogenate was centrifuged at 12000 rpm for 30 min at 4°C. The supernatant was collected.
- 4) The supernatant with ice-cold lysis buffer was diluted into 1:5 and 1:10. Milli-Q water, pre-diluted protein standard assay, and diluted protein samples were piped into a 96-well plate accordingly, 3 repetitions per sample.

- 5) Then the RC DC (reducing agent and detergent compatible) protein assay reagents A and B were added; after that, the plate was placed on a horizontal shaker for 30 min at room temperature in the dark.
- 6) Protein concentrations in the supernatant of hippocampal tissues were determined by BIO-RAD's DC protein assay.
- 7) The total protein concentration of each sample was adjusted to 2 $\mu\text{g}/\mu\text{L}$ by mixing with 4x sample buffer and lysis buffer.
- 8) The prepared samples were heated at 95°C for 5 min and then stored at -20°C or -80°C until use.

2.9.2 The preparation of sodium dodecyl sulfate-polyacrylamide gel electrophoresis (SDS-PAGE)

- 1) First, the glass plates were cleaned for making gels. The plates were washed with detergent, rinsed several times with Milli-Q water, then wiped with ethanol, and let the plates air dry.
- 2) The lower edges of the two glass plates were ensured to be horizontal and free of cuttings, then the glass plates (long inside and short outside) were installed to ensure the gel rack was horizontal.
- 3) Separation gels preparation (Table 9). N, N, N', N'-Tetramethyl ethylene diamine (TEMED), and ammonium persulfate (APS) were finally added to the solution. The solution was mixed thoroughly and then poured into the space between the plates. Then, the separating gels were sealed with Milli-Q water carefully, followed by 40 min polymerization at room temperature.

Table 9: Components of separation gels

Polyacrylamide separation gel	Amount (8%SDS-PAGE)	Amount (10%SDS-PAGE)
Reagents	Amount	Amount
dH ₂ O	4.6 mL	4.1 mL
Acrylamide/bis (30% 37.5:1; Bio-Rad)	2.8 mL	3.3 mL
Tris-HCl (1.5 M, pH 8.8)	2.5 mL	2.5 mL
10 % SDS in dH ₂ O	100 uL	100 uL
Ammonium persulfate (APS), 10%	50 uL	50 uL
N, N, N', N'-tetramethyl ethylene-diamine (TEMED)	10 uL	10 uL

- 4) After the polymerization of the separation gels, prepare the stacking gels (Table 10) (caution: PH of Tris-HCL for the preparation of stacking gels is different from that of separation gels). After the stacking gel solution was added on the separation gels, combs with 15 wells were placed into the stacking gel solution (make sure no air bubbles between the comb wells and gel). Then the solution was polymerized for 30 min at room temperature.

Table 10: Components of stacking gels (5% SDS-PAGE)

Polyacrylamide stacking gels	
Reagents	Amount
dH ₂ O	6.1 mL
Acrylamide/bis (30% 37.5:1; Bio-Rad)	1.3 mL
Tris-HCl (1.5 M, pH 6.8)	2.5 mL
10 % SDS in dH ₂ O	100 µL
Ammonium persulfate (APS), 10%	100 µL
N,N,N',N'-tetramethyl ethylene-diamine (TEMED)	10 µL

- 5) In the end, the gels were carefully removed from the rack, and completely immersed in Milli-Q water at placed at 4°C (freshly prepared SDS-PAGE is preferred).

2.9.3 Electrophoresis and transferring

- 1) Running buffer (25 mM Tris, 190 mM glycine, and 0.1% SDS) was poured into the electrophoresis rack, the combs inserted in the stacking gel were carefully removed, and the wells were rinsed out with running buffer to ensure no gel debris in the wells.
- 2) Loading the marker and samples. A 10 µl broad range (10-250 kDa) color-coded pre-stained protein marker (Cell Signaling Technology) was applied to the first well and 20 µl of each sample to the rest wells (do not add air bubbles with the sample).
- 3) Electrophoresis. The electrophoresis tank lids were installed (make sure red to red, black to black). The vertical electrophoresis setup was run at a constant voltage of 80 V for 30 min, then switched to 120 V until the blue sample buffer ran out of SDS-PAGE.
- 4) Polyvinylidene fluoride (PVDF) membrane activation. The PVDF membrane was incubated within methanol for 30 s to 60 s to ensure that the membrane became transparent, and then the membrane was washed with Milli-Q water 3 times.
- 5) After the electrophoresis was completed, gels were taken out from the gels rack. The stacking gels were removed, and the separation gels were carefully transferred to the transferring buffer (25 mM Tris and 192 mM glycine).
- 6) Thereafter, the blot sandwiches were prepared in the following order: black board (bottom layer) → first layer of sponge pad → two layers of filter paper → SDS-PAGE → PVDF membrane → two layers of filter paper → second layer of sponge pad → red board. Ensure no air bubbles exist between the layers, especially between the SDS-PAGE and PVDF membrane.

- 7) The blot sandwiches were installed in the gel tank (make sure black to black, red to red) with transferring buffer and an ice pad. The level of the transferring buffer should be above the PVDF membrane.
- 8) The membrane was transferred at a constant voltage of 80 V for 1 h.

2.9.4 Blocking and antibodies incubation

- 1) Imaging the PVDF membranes. The membranes were washed with Tris-buffered saline with Tween (TBST, 20 mM Tris, 150 mM NaCl, and 0.1% Tween-20, pH=7.7) for 5 min and imaged with ChemiDoc XRS + System and Image-lab software. The images of the membranes were saved.
- 2) Blocking the PVDF membranes. Then the membranes with 10% Roti-Block (Roth, Karlsruhe, Germany) were blocked on a 3D shaker at room temperature for 1 h.
- 3) Primary antibodies incubation. Membranes were incubated with primary antibodies on a shaker at 4°C overnight. (Mouse anti-GFAP, # 3450, Cell Signaling Technology, USA 1:1000; rabbit anti-MEGF10, Millipore, USA, 1:500; rabbit anti-GAPDH, Cell Signaling Technology, USA, 1:5000).
- 4) Secondary antibodies incubation. On the second day, the membranes were washed with TBST for 3 x 10 min. Horseradish peroxidase-conjugated secondary antibodies (1:10000, anti-rabbit or mouse IgG; Cell Signaling Technology, USA) were applied and incubated at room temperature for 1h. After that, the membranes were rinsed with TBST for 3 x 10 min.
- 5) Imaging the membranes. The membranes were put in the Enhanced Chemiluminescence (ECL) detection reagent in a dark box with 30 s shaking on a horizontal shaker. The membranes were placed in the ECL solution in a dark box with 30 s shaking on a horizontal shaker. Images were taken with ChemiDoc XRS + System (Bio-Rad, Germany) and Image-lab software. Components of ECL detection reagent (2 mL 1M Tris (pH=8.5), 6.1 µL 30% H₂O₂, 89 µL p-Coumaric acid solution (44.29

mg in 1 mL DMSO), 200 μ L Luminol solution (44.29 mg in 1 mL DMSO) and 18 mL Milli-Q water).

- 6) Reuse the membranes. After imaging one protein in the sample, the membranes were washed with TBST for 3 x 5 min, then stripped with Western Blot Stripping Buffer for 30 min and rinsed with TBST for 3 x 5 min. After that, the membranes can be used to detect another protein in the sample.

2.9.5 Analysis of Western Blot

The ImageLab™ was used for analyzing Western blot results by measuring the intensity of each band in increment images. The intensity was normalized with the stain-free blot image of the membranes taken under ultraviolet light. The band intensity of each lane was normalized to the total amount of protein in that lane, and all results were compared to the standard protein samples.

2.10 Statistical analysis

Statistical analysis was performed under GraphPad Prism 8 software. For the comparisons of dendritic spine density (DSD, the average number of spines in a segment of 10 μ m length dendrite), Western blot, and astrocyte-mediated synaptic engulfment among three or more groups, one-way analysis of variance (ANOVA) followed by Dunnett's multiple comparisons test was performed. An unpaired t-test was performed to compare the two groups. Data were reported as mean \pm standard error of the mean (SEM). The statistical significance was defined at $p < 0.05$.

3. Results

3.1 The effects of A β and sevoflurane on DSD

The extracellular accumulation of A β in the brain is one of the major factors for dendritic spine loss in AD. To mimic AD patients receiving anesthesia, 0.4 MAC and 1.2 MAC sevoflurane were applied to A β pre-incubated acute hippocampal brain slices. The interaction

of different A β isoforms (A β ₁₋₄₀, A β ₁₋₄₂, A β pE3 and 3NTyrA β) with sevoflurane (0.4 MAC and 1.2 MAC) on DSD in CA1 pyramidal neurons was investigated.

3.1.1 3NTyrA β had the greatest effect on the dendritic spines among the 4 A β isoforms

A β species, A β ₁₋₄₀, A β ₁₋₄₂, A β pE3 and 3NTyrA β , concentration-dependently inhibited CA1-LTP in acute hippocampal slices after 90 min incubation[46]. And induction of LTP in excitatory neurons is accompanied by an increase in spine density and enlargement of spines[115]. Here we checked the effects of low nanomolar concentration (50 nM) of A β ₁₋₄₀, A β ₁₋₄₂, A β pE3 and 3NTyrA β on DSD of CA1 pyramidal neurons.

After 180 min incubation with 50 nM concentration, A β ₁₋₄₀, A β ₁₋₄₂, and 3NTyrA β decreased DSD significantly, and 3NTyrA β had the greatest effect on the reduction of DSD among the four A β isoforms (Figure 13B-C). In addition, it seems that only thin spines were affected (Figure 13B, D), and the density of stubby and mushroom spines remained unchanged (Figure 13B, E-F).

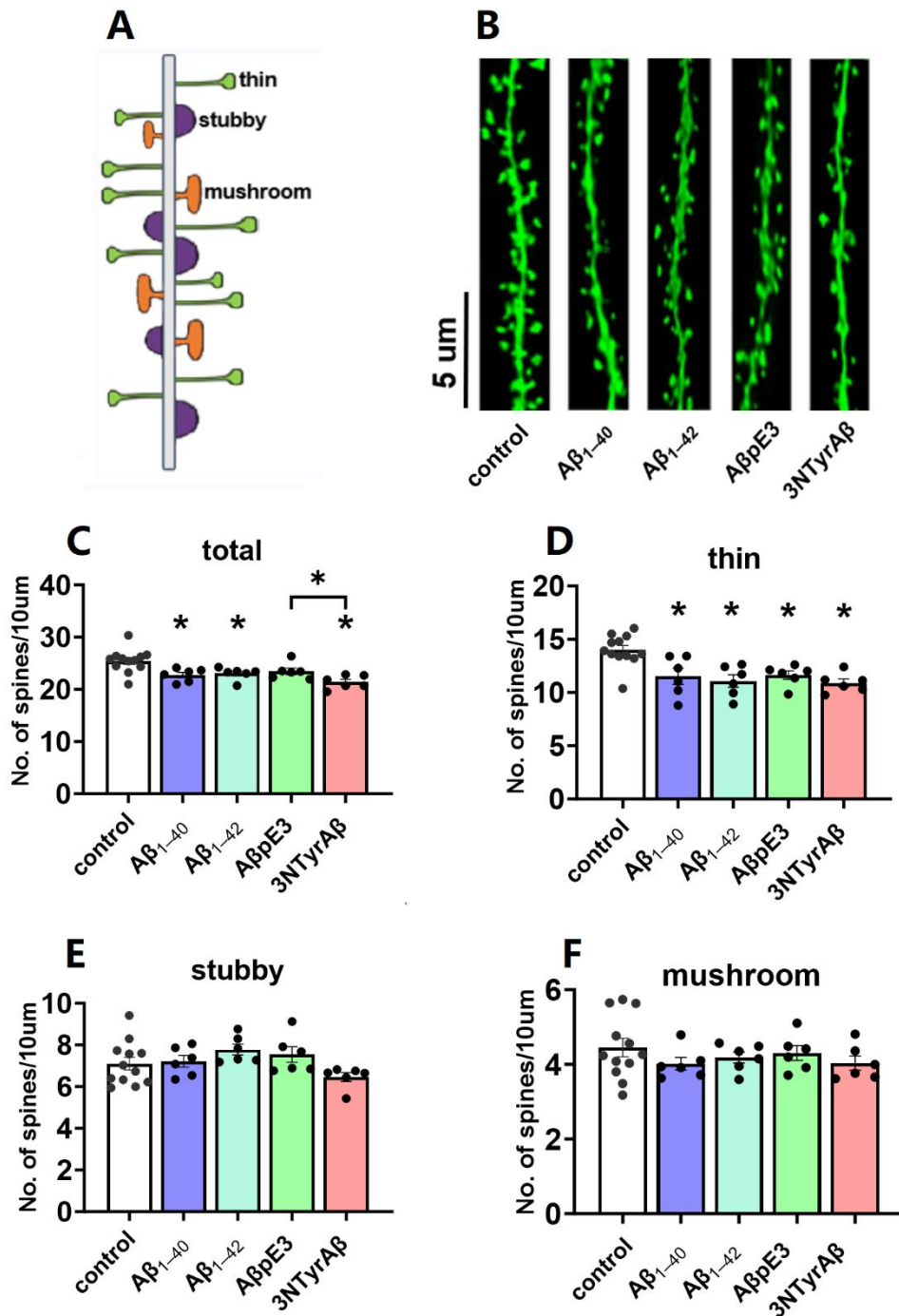


Figure 13. Aβ₁₋₄₀, Aβ₁₋₄₂, and 3NTyrAβ decreased the DSD, 3NTyrAβ had the greatest effect. (A) Schematic graph of different types of spines. (B) Representative apical dendritic segments of CA1 pyramidal neurons from the control, Aβ₁₋₄₀, Aβ₁₋₄₂, AβpE3, 3NTyrAβ incubation groups. Scale bar = 5 μm. (C) Columnar chart diagram overviewed the total DSD for respective groups. Except for AβpE3, all three Aβ isoforms decreased total DSD after 180 min incubation. Control [25.44 ± 0.64], Aβ₁₋₄₀ [22.75 ± 0.52], Aβ₁₋₄₂ [23.04 ± 0.49], AβpE3 [23.47 ± 0.63], 3NTyrAβ [21.39 ± 0.53]; control vs. Aβ₁₋₄₀: n = 12/6, p = 0.0132; control vs. Aβ₁₋₄₂: n = 12/6, p = 0.0305; control vs. AβpE3: n = 12/6, p = 0.1093; control vs. 3NTyrAβ: n = 12/6, p = 0.0002, one-way ANOVA followed by Dunnett's multiple comparisons test. Moreover, total DSD was lower in the 3NTyrAβ in comparison with the AβpE3.

A β pE3 [23.47 \pm 0.63] vs. 3NTyrA β [21.39 \pm 0.53]: n = 6/6, p = 0.0303, unpaired t-test. (D) The density of thin spines was decreased for all four A β isoforms. Control [13.99 \pm 0.43], A β ₁₋₄₀ [11.52 \pm 0.76], A β ₁₋₄₂180 [11.08 \pm 0.60], A β pE3 [11.63 \pm 0.39], 3NTyrA β [10.89 \pm 0.37]; control vs. A β ₁₋₄₀: n = 12/6, p = 0.005; control vs. A β ₁₋₄₂: n = 12/6, p = 0.009; control vs. A β pE3: n = 12/6, p = 0.0074; control vs. 3NTyrA β : n = 12/6, p = 0.0004; one-way ANOVA followed by Dunnett's multiple comparisons test. (E-F) Neither the stubby nor mushroom density changed significantly. Data are shown as mean \pm SEM. The number of points in B-E represents the number of animals. Every data point in the columnar chart diagram represents the mean DSD from 6-8 dendrites per animal. *P < 0.05.

3.1.2 1.2 MAC sevoflurane exerted a lasting effect on decreasing DSD

The effect of sevoflurane on spine dynamics seems dependent on developmental stage, exposure concentration, exposure duration, and brain regions [116, 117]. 3% sevoflurane 6h exposure to postnatal day 7 (PND) rats reduced apical DSD of CA1 pyramidal neurons at PND 21 [116]. However, 2h 2.5% sevoflurane application increased the DSD of pyramidal neurons in the prefrontal cortex over 6 h in juvenile rats[117].

From our observations, 0.4 MAC sevoflurane had the tendency to decrease DSD, and 1.2 MAC sevoflurane decreased DSD in CA1 pyramidal neurons during the exposure (Figure 14A, C). For the effects on specific subtypes, the thin spines were reduced concentration-dependent under 0.4 MAC and 1.2 MAC sevoflurane (Figure 14A, D). Moreover, 1.2 MAC sevoflurane decreased the density of stubby spines (Figure 14A, E). Neither 0.4 nor 1.2 MAC sevoflurane decreased the density of mushroom spines (Figure 14A, F). It seems that the mushroom spine was more resistant to sevoflurane exposure than the other two subtypes.

After the removal of sevoflurane for 90 min, the effect of 0.4 MAC sevoflurane on DSD was reversed, whereas, for 1.2 MAC sevoflurane, there was a residual effect on total DSD (Figure 14B, G-J). This is likely manifested by the persistent reduction of thin spines after 90 min washout (Figure 14B, H).

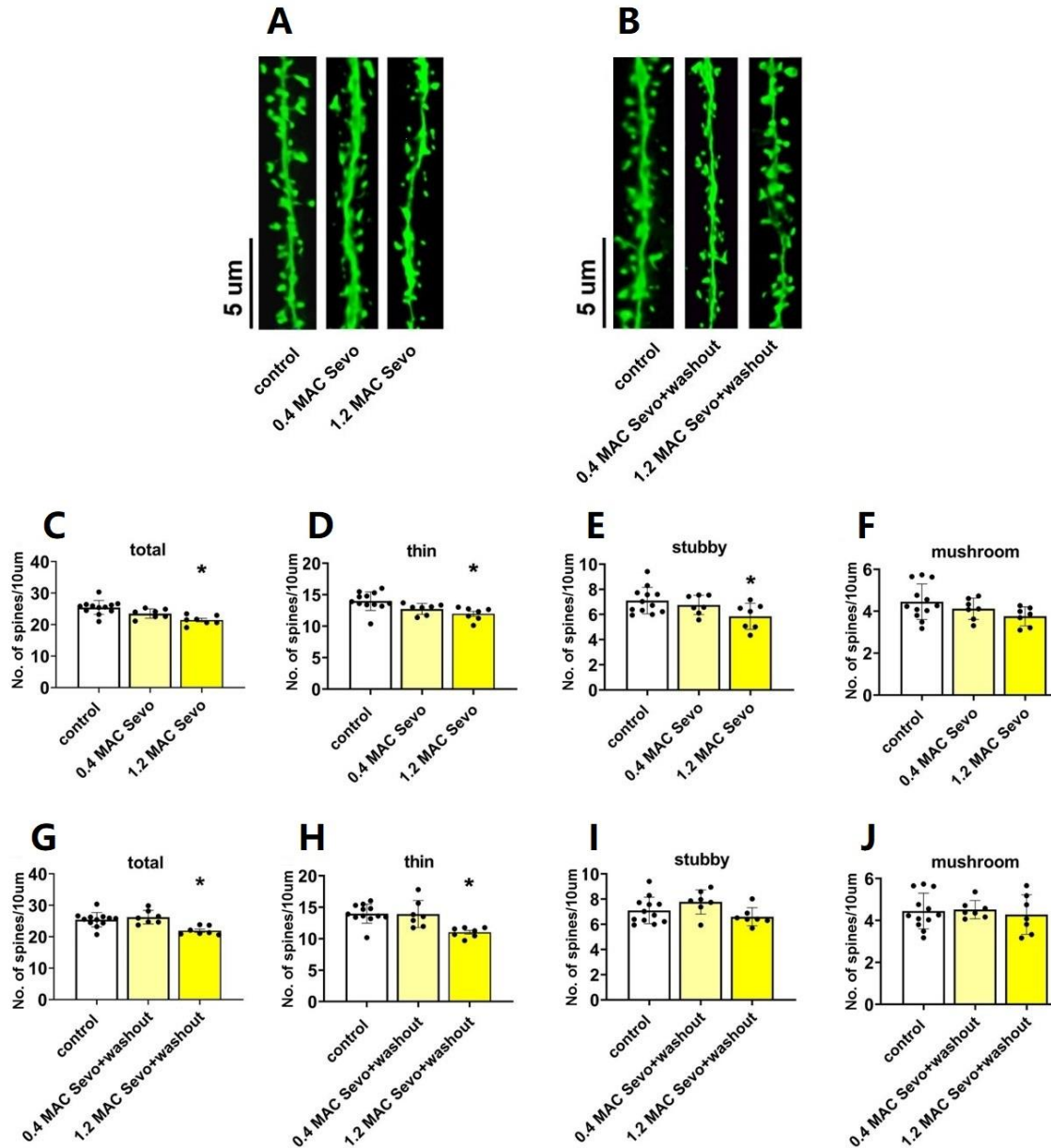


Figure 14. 1.2 MAC sevoflurane exerted a lasting effect on decreasing DSD. (A-B) Representative apical dendritic segments of CA1 pyramidal neurons from the control, 0.4 MAC and 1.2 MAC sevoflurane groups, during treatments and after 90 min removal respectively. Scale bars = 5 μ m. (C) 0.4 MAC sevoflurane had the tendency to reduce DSD, and 1.2 MAC sevoflurane significantly reduced DSD. Control [25.44 \pm 0.64], 0.4 MAC sevoflurane (Sevo) [23.50 \pm 0.56], 1.2 MAC Sevo [21.41 \pm 0.56]; control vs. 0.4 MAC Sevo: n = 12/7, p = 0.0809; control vs. 1.2 MAC Sevo: n = 12/7, p = 0.0003, one-way ANOVA followed by Dunnett's multiple comparisons test. (D) The thin spines were reduced concentration-dependent under 0.4 and 1.2 MAC sevoflurane. Control: [13.99 \pm 0.42] vs. 0.4 MAC Sevo: [12.75 \pm 0.33], n = 12/7, p = 0.0884; control: [13.99 \pm 0.42] vs. 1.2 MAC Sevo: [11.97 \pm 0.38], n = 12/7, p = 0.0042, one-way ANOVA followed by Dunnett's multiple comparisons test. (E) 1.2 MAC sevoflurane decreased the density of stubby spines. control: [7.10 \pm 0.30] vs. 0.4 MAC Sevo: [6.76 \pm 0.29], n = 12/7, p = 0.9349; control: [7.10 \pm 0.30] vs. 1.2 MAC Sevo: [5.85 \pm 0.39], n=12/7, p =

0.0270, one-way ANOVA followed by Dunnett's multiple comparisons test. (F) Neither 0.4 nor 1.2MAC sevoflurane decreased the density of mushroom spines. control: $[4.45 \pm 0.25]$ vs. 0.4 MAC Sevo: $[4.16 \pm 0.20]$, $n = 12/7$, $p = 0.5840$; control: $[4.45 \pm 0.25]$ vs. 1.2 MAC Sevo: $[3.76 \pm 0.17]$, $n = 12/7$, $p = 0.0800$, one-way ANOVA followed by Dunnett's multiple comparisons test. (F-G) After the removal of sevoflurane, the reduction of DSD produced by 0.4 MAC sevoflurane was reversed, while for 1.2 MAC sevoflurane, there was a residual effect. Control $[25.41 \pm 0.66]$, 0.4 MAC Sevo + washout $[26.21 \pm 0.82]$, 1.2 MAC Sevo + washout $[21.91 \pm 0.50]$; control vs. 0.4 MAC Sevo + washout, $n = 12/7$, $p = 0.8362$; control vs. 1.2 MAC Sevo + washout, $n = 12/7$, $p = 0.0029$, one-way ANOVA followed by Dunnett's multiple comparisons test. (H) The residual effect of 1.2 MAC sevoflurane is manifested as a reduction in the thin spines. Control $[13.97 \pm 0.48]$, 0.4 MAC Sevo + washout $[13.92 \pm 0.82]$, 1.2 MAC Sevo + washout $[11.02 \pm 0.29]$; control vs. 0.4 MAC Sevo + washout, $n = 12/7$, $p > 0.9999$; control vs. 1.2 MAC Sevo + washout, $n = 12/7$, $p = 0.0013$, one-way ANOVA followed by Dunnett's multiple comparisons test. (I-J) After sevoflurane removal, neither 0.4 nor 1.2 MAC sevoflurane affected the dynamics of stubby and mushroom spines. Sevo, sevoflurane. Data are shown as mean \pm SEM. The number of points in B-E represents the number of animals. Every data point in the columnar chart diagram represents the average DSD from 6-8 dendrites per animal. * $P < 0.05$.

3.1.3 The interaction of sevoflurane and A β on CA1 dendritic spines dynamics

3NTyrA β exerted the greatest effect on the spine remodeling among the four isomers; here, the interaction of 3NTyrA β with 0.4 MAC/1.2 MAC sevoflurane is presented in graphs. The effects of the other three A β isoforms are summarized and presented in tables thereafter.

Here, we observed that 0.4 MAC sevoflurane enhanced the decrease of DSD induced by 3NTyrA β (Figure 15A-B). Surprisingly, 1.2 MAC sevoflurane didn't further decrease DSD led by 3NTyrA β (Figure 15A-B) but increased the thin spine's density (Figure 15A, C). It appears that the increase in the thin spines compensated for the reduction in the stubby and the effect on the mushroom spines, resulting in a smaller overall impact on the total spines (Figure 15A, D-E).

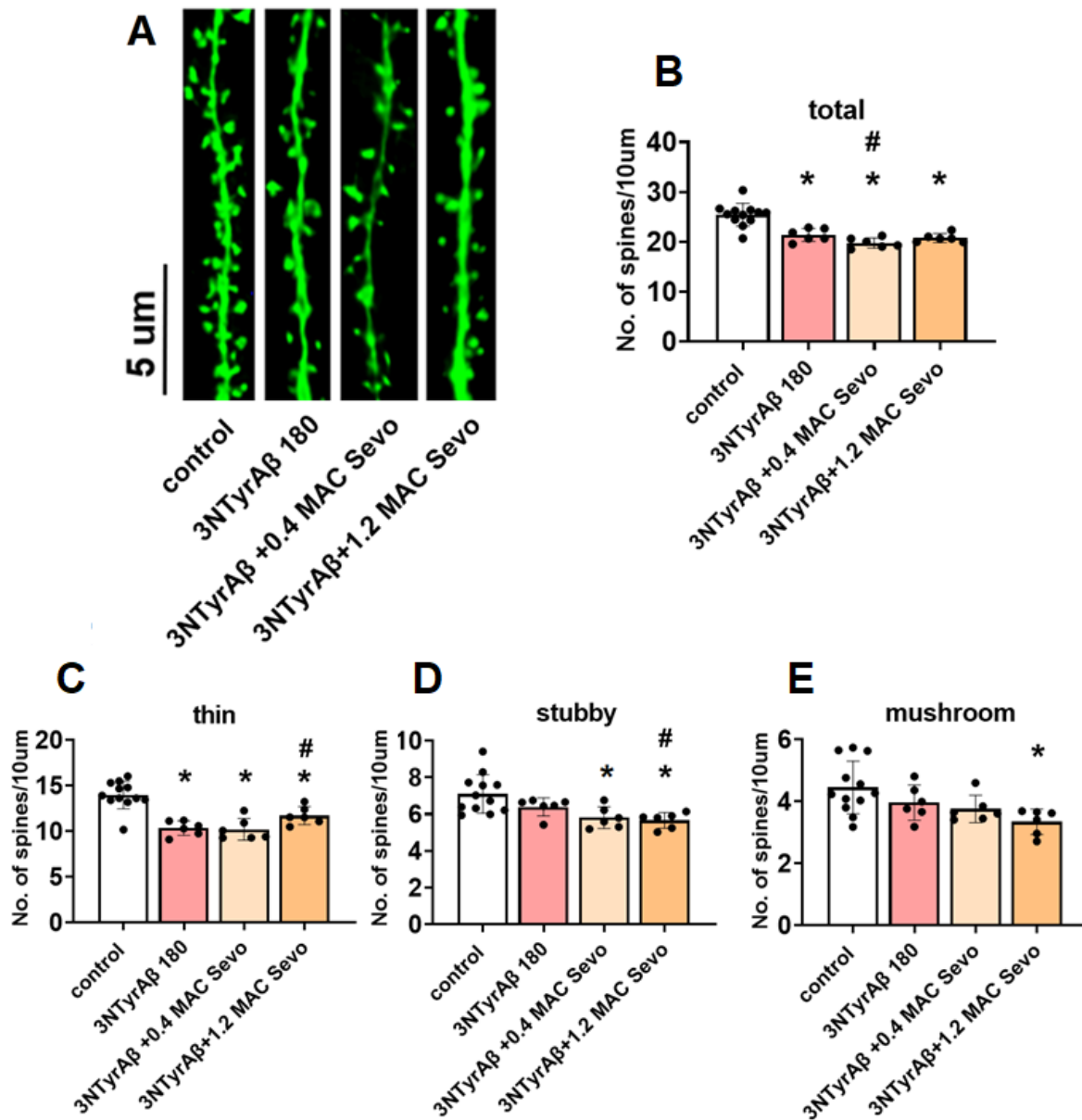


Figure 15. In the presence of 3NTyrA β , 0.4 MAC sevoflurane further decreased DSD. (A) Representative apical dendritic segments of CA1 pyramidal neurons from the control, 3NTyrA β , 3NTyrA β +0.4 MAC, and 3NTyrA β +1.2 MAC sevoflurane groups, respectively. Scale bar = 5 μ m. (B) In the presence of 3NTyrA β , 0.4 MAC sevoflurane further reduced DSD, while 1.2 MAC sevoflurane didn't enhance the DSD reduction induced by 3NTyrA β . Control [25.44 \pm 0.64], 3NTyrA β [21.39 \pm 0.53], 3NTyrA β + 0.4 MAC Sevo [19.78 \pm 0.42], 3NTyrA β + 1.2 MAC Sevo [20.77 \pm 0.36]; 3NTyrA β vs. 3NTyrA β + 0.4 MAC Sevo, n = 6/6, p = 0.0378; 3NTyrA β vs. 3NTyrA β + 1.2 MAC Sevo, n = 6/6, p = 0.5199, one-way ANOVA followed with Dunnett's multiple comparisons test. (C) In the presence of 3NTyrA β , 1.2 MAC sevoflurane increased the density of thin spines. Control [13.97 \pm 0.44], 3NTyrA β [10.35 \pm 0.33], 3NTyrA β + 0.4 MAC Sevo [10.20 \pm 0.49], 3NTyrA β + 1.2 MAC Sevo [11.93 \pm 0.44]; 3NTyrA β vs. 3NTyrA β + 0.4 MAC Sevo: n = 6/6, p = 0.9578; 3NTyrA β vs. 3NTyrA β + 1.2 MAC Sevo: n = 6/6, p = 0.0331, one-way ANOVA followed with Dunnett's multiple comparisons test. (D) 1.2 MAC sevoflurane reduced the density of stubby spines. Control [7.10 \pm 0.30], 3NTyrA β













[6.4 ± 0.20], 3NTyrAβ + 0.4 MAC Sevo [5.81 ± 0.24], 3NTyrAβ + 1.2 MAC Sevo; 3NTyrAβ vs. 3NTyrAβ + 0.4 MAC Sevo: n = 6/6, p = 0.1148; 3NTyrAβ vs. 3NTyrAβ + 1.2 MAC Sevo: n = 6/6, p = 0.0436, one-way ANOVA followed with Dunnett's multiple comparisons test. (E) And neither 0.4 MAC nor 1.2 MAC sevoflurane decreased the density of mushroom spines, co-applying 1.2 MAC sevoflurane with 3NTyrAβ reduced the density of mushroom spines. Control [4.45 ± 0.25], 3NTyrAβ [3.96 ± 0.23], 3NTyrAβ + 0.4 MAC Sevo [3.76 ± 0.18], 3NTyrAβ + 1.2 MAC Sevo [3.36 ± 0.16]; 3NTyrAβ vs. 3NTyrAβ + 0.4 MAC Sevo: n = 6/6, p = 0.6854; 3NTyrAβ vs. 3NTyrAβ + 1.2 MAC Sevo: n = 6/6, p = 0.0741, one-way ANOVA followed with Dunnett's multiple comparisons test; control vs. 3NTyrAβ + 1.2 MAC Sevo: n = 12/6, p = 0.0091, unpaired t-test). Sevo, sevoflurane. 3NTyrAβ 180, 3NTyrAβ incubation for 180 min. Data are shown as mean ± SEM. The number of points in B-E represents the number of animals. Every data point in the columnar chart diagram represents the mean DSD from 6-8 dendrites per animal. P < 0.05. *: significant difference from control; #: significant difference from 3NTyrAβ.

Table 11. The effects of 0.4 MAC/1.2 MAC sevoflurane on total DSD in Aβ pre-incubated acute hippocampal slices

DSD	Aβ ₁₋₄₀	Aβ ₁₋₄₂	AβpE3	3NTyrAβ	compared to
0.4 MAC Sevo	* ↓	* ↓	* ↓	* ↓	control
	# ↓	# ↓	-	# ↓	Aβ 180
1.2 MAC Sevo	* ↓	* ↓	* ↓	* ↓	control
	# ↓	# ↓	-	-	Aβ 180

Applying 0.4 MAC sevoflurane promoted the decrease of DSD induced by Aβ (except for AβpE3). For 1.2 MAC sevoflurane, an enhancement effect was also observed except for AβpE3 and 3NTyrAβ. For comparison with the control, an unpaired t-test was performed, and for comparison with Aβ, one-way ANOVA followed by Dunnett's multiple comparisons test was performed. P < 0.05. *: significant difference from control; #: significant difference from corresponding Aβ isoforms; -: not significantly different from the control or corresponding Aβ isoforms.

Table 12. Effects of 0.4 MAC/1.2 MAC sevoflurane on subtypes of the spines in Aβ pre-incubated acute hippocampal slices



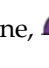
DSD	A β ₁₋₄₀			A β ₁₋₄₂			A β pE3			3NTyrA β			compared to?
													
0.4MAC Sevo	↓*	↓*	—	↓*	↓*	—	↓*	—	—	↓*	↓*	—	control
	—	↓#	—	—	↓#	—	—	↓#	—	—	—	—	A β 180min
1.2MAC Sevo	↓*	↓*	↓*	↓*	↓*	↓*	↓*	—	—	↓*	↓*	↓*	control
	—	↓#	↓#	—	↓#	—	—	↓#	—	↑#	↓#	—	A β 180min

We further analyzed the subtypes of the spines.

The thin spines were decreased among all groups of A β +Sevo compared with the control group. Compared with A β 180 min groups, an increase of thin spines was found only in the 3NTyrA β +1.2MAC Sevo group, indicating a partial recovery of thin spines after the application of sevoflurane into 3NTyrA β pretreated slices.

A more complex result was drawn for stubby spines. A β ₁₋₄₀/A β ₁₋₄₂+Sevo reduced stubby spines compared to either the control or A β group. A reduction was observed when we compared the stubby spines of A β pE3+Sevo with A β pE3, suggesting a combination of effects of A β pE3 and sevoflurane on stubby spines. The combination effect was also observed in the 3NTyrA β +1.2MAC group, as a further downregulation was detected compared with the 3NTyrA β group.

For mushroom spines, all four A β isoforms+1.2 but not 0.4MAC sevoflurane decreased the density in comparison with either control or the corresponding A β , suggesting a pronounced decrease of mushroom by a higher concentration of sevoflurane exposure.

: thin spine, : stubby spine, : mushroom spine. For comparison with the control, an unpaired t-test was performed, and for comparison with A β , one-way ANOVA followed by Dunnett's multiple comparisons test was performed. P < 0.05. *: significant difference from control; #: significant difference from corresponding A β isoforms; -: not significantly different from the control or corresponding A β isoforms.

3.1.4 The effects of sevoflurane removal on total DSD in A β pre-incubated acute hippocampal slices

As mentioned previously, AD Patients are particularly susceptible to POD[54]. Therefore, in these patients, the neurological changes after the withdrawal of anesthetics are a major concern for the anesthesiologists. Previously, Hofmann et al. found that neuronal activity in the CA1 region of acute hippocampal brain slices was not affected by A β incubation alone,

whereas 2% sevoflurane reduced neuronal activity which recovered after washout. However, when slices were pre-incubated with A β , the following application of 2% sevoflurane reduced neuronal signaling and persisted even after 60 min withdrawal of the anesthetic [118].

Here, in the presence of 3NTyrA β , the withdrawal of 0.4 MAC sevoflurane produced a reversible effect on spine dynamics, whereas the removal of 1.2 MAC sevoflurane produced a persistent effect on dendritic spine remodeling (Figure 16A-B). We saw an increase in thin spines after the removal of 1.2 MAC sevoflurane for 90 min, which could be caused by an increase in thin spine formation and/or a decrease in the elimination (Figure 16A, C). For stubby and mushroom spines, compared to 3NTyrA β incubation, no alternations were detected after sevoflurane washout (Figure 16A, D-E). Moreover, in the presence of 3NTyrA β , the removal of 0.4 MAC sevoflurane did not change the density of the mushroom spine compared to the control group (Figure 16A, E), which may indicate 0.4 MAC sevoflurane partially reversed the inhibition of mushroom spine led by 3NTyrA β incubation.

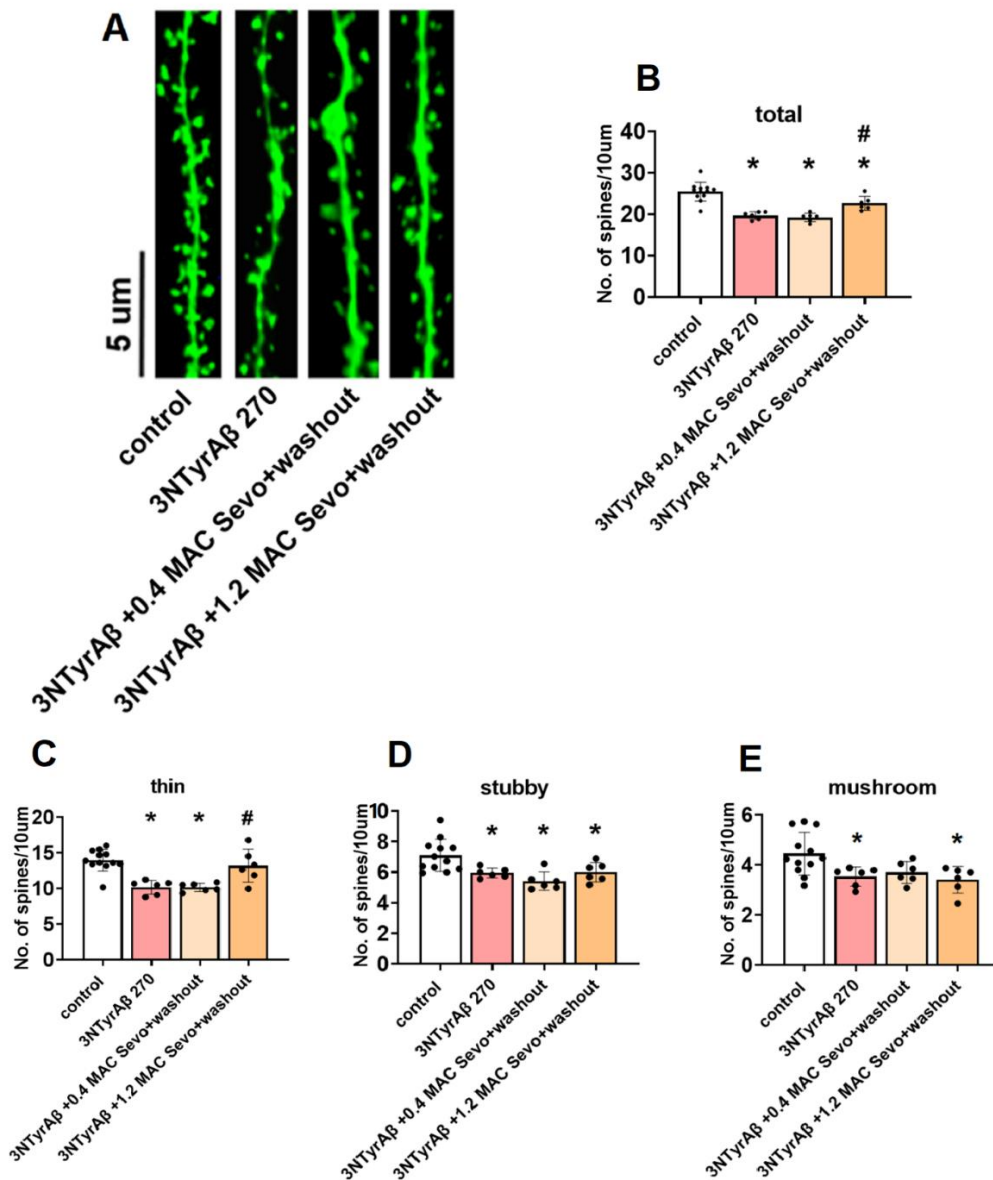


Figure 16. In the presence of 3NTyrA β , 1.2 MAC sevoflurane removal increased DSD. (A) Representative apical dendritic segments of CA1 pyramidal neurons from the control, 3NTyrA β , 3NTyrA β +0.4 MAC+washout, and 3NTyrA β +1.2 MAC sevoflurane+washout groups, respectively. Scale bar = 5 μ m. (B) After 90 min washout, the effect of 0.4 MAC sevoflurane on DSD disappeared, whereas the 1.2 MAC sevoflurane resulted in an increase in DSD. Control [25.41 \pm 0.66], 3NTyrA β 270 [19.67 \pm 0.38], 3NTyrA β + 0.4 MAC Sevo + washout [19.22 \pm 0.42], 3NTyrA β + 1.2 MAC Sevo + washout; 3NTyrA β 270 vs. 3NTyrA β + 0.4 MAC Sevo + washout: n = 6/6, p = 0.7729, 3NTyrA β 270 vs. 3NTyrA β + 1.2 MAC Sevo + washout: n = 6/6, p = 0.0021, one-way ANOVA followed with Dunnett's multiple comparisons. (C) After 90 min washout, for specific types of spines, 1.2 MAC sevoflurane increased the density of thin spines. Control [13.97 \pm 0.48], 3NTyrA β 270 [10.17 \pm 0.40], 3NTyrA β + 0.4 MAC Sevo + washout [10.16 \pm 0.23], 3NTyrA β + 1.2 MAC Sevo + washout [13.19 \pm 0.95]; 3NTyrA β 270 vs. 3NTyrA β + 0.4 MAC Sevo + washout: n = 6/6, p = 0.9999; 3NTyrA β 270













vs. 3NTyrA β + 1.2 MAC Sevo + washout: n = 6/6, p = 0.0065, one-way ANOVA followed with Dunnett's multiple comparisons. (D-E) After 90 min washout, the effects of both 0.4 MAC and 1.2 MAC sevoflurane on stubby and mushroom spine density disappeared. "Sevo", sevoflurane. 3NTyrA β 270, 3NTyrA β incubation for 270min. Data are shown as mean \pm SEM. The number of points in B-E represents the number of animals. Every data point in the scatter plots represents the mean DSD from 6-8 dendrites per animal. P < 0.05. *: significant difference from control; #: significant difference from 3NTyrA β .

Table 13. the effects of sevoflurane removal on total DSD in A β pre-incubated acute hippocampal slices

DSD	A β ₁₋₄₀	A β ₁₋₄₂	A β pE3	3NTyrA β	compared to
0.4 MAC Sevo + washout	* ↓	* ↓	* ↓	* ↓	control
	-	-	-	-	A β 270 min
1.2 MAC Sevo + washout	* ↓	* ↓	* ↓	* ↓	control
	-	-	-	# ↑	A β 270 min

After sevoflurane removal, the enhancement decreasing effect induced by sevoflurane on A β disappeared except for 3NTyrA β incubated hippocampal brain slices. A β 270: A β incubation for 270 min. For comparison with the control, an unpaired t-test was performed, and for comparison with A β , one-way ANOVA followed by Dunnett's multiple comparisons test was performed. P < 0.05. *: significant difference from control; #: significant difference from corresponding A β isoforms; -: not significantly different from the control or corresponding A β isoforms.

Table 14. Effects of sevoflurane removal on subtypes of spine in A β pre-incubated acute hippocampal slices



DSD	A β ₁₋₄₀			A β ₁₋₄₂			A β pE3			3NTyrA β			compared to?
													
0.4MAC Sevo + washout	↓*	↓*	—	↓*	↓*	—	↓*	↓*	—	↓*	↓*	—	control
	—	—	—	—	—	—	—	—	—	—	—	—	A β 270min
1.2MAC Sevo + washout	↓*	↓*	—	↓*	↓*	—	↓*	—	↓*	—	↓*	↓*	control
	—	—	—	—	—	—	—	↑ #	—	↑ #	—	—	A β 270min

We further quantified the subtypes of spines after sevoflurane removal.

The thin spine density in all conditions was reduced, except 3NTyrA β + 1.2 MAC Sevo + washout group, at which a reversible effect of thin spines was observed.

The stubby spine density in all conditions was reduced, except in A β pE3 + 1.2 MAC Sevo + washout, at which a reversible effect of stubby spines was observed.

For mushroom spines, compared to the control, a reduction was only detected in groups of A β pE3/3NTyrA β + 1.2 MAC Sevo + washout.

↑: thin spine, : stubby spine, : mushroom spine. For comparison with the control, an unpaired t-test was performed, and for comparison with A β , one-way ANOVA followed by Dunnett's multiple comparisons test was performed. P < 0.05. *: significant difference from control; #: significant difference from corresponding A β isoforms; -: not significantly different from the control or corresponding A β isoforms.

3.2 The effects of A β and sevoflurane on astrocyte-mediated synaptic engulfment

Dysregulation of astrocyte-mediated synaptic phagocytosis induced by A β accumulation is a key factor in synaptic degeneration and impairment in AD [101, 103]. Furthermore, evidence suggests that impaired glial phagocytosis is associated with postoperative cognitive dysfunction [119]. Therefore, we asked whether astrocytic phagocytosis was involved in A β and sevoflurane-induced alteration of DSD in CA1 pyramidal neurons. Thus, we assessed astrocyte-mediated synaptic phagocytosis by measuring phagocytic index (PI), which is the parameter % of ROI colocalized from the colocalization analysis of Imaris. The relative phagocytosis ability was evaluated by normalizing the PI of the treatment group to that of the control group [103].

3.2.1 None of the four A β isoforms had a significant effect on astrocyte-mediated synaptic engulfment

Here in acute hippocampal brain slice, we checked the acute effect of low nanomolar concentration A β on astrocyte-mediated synaptic engulfment. After 180 min incubation, none of the four A β isoforms significantly affected astrocyte-mediated synaptic engulfment.

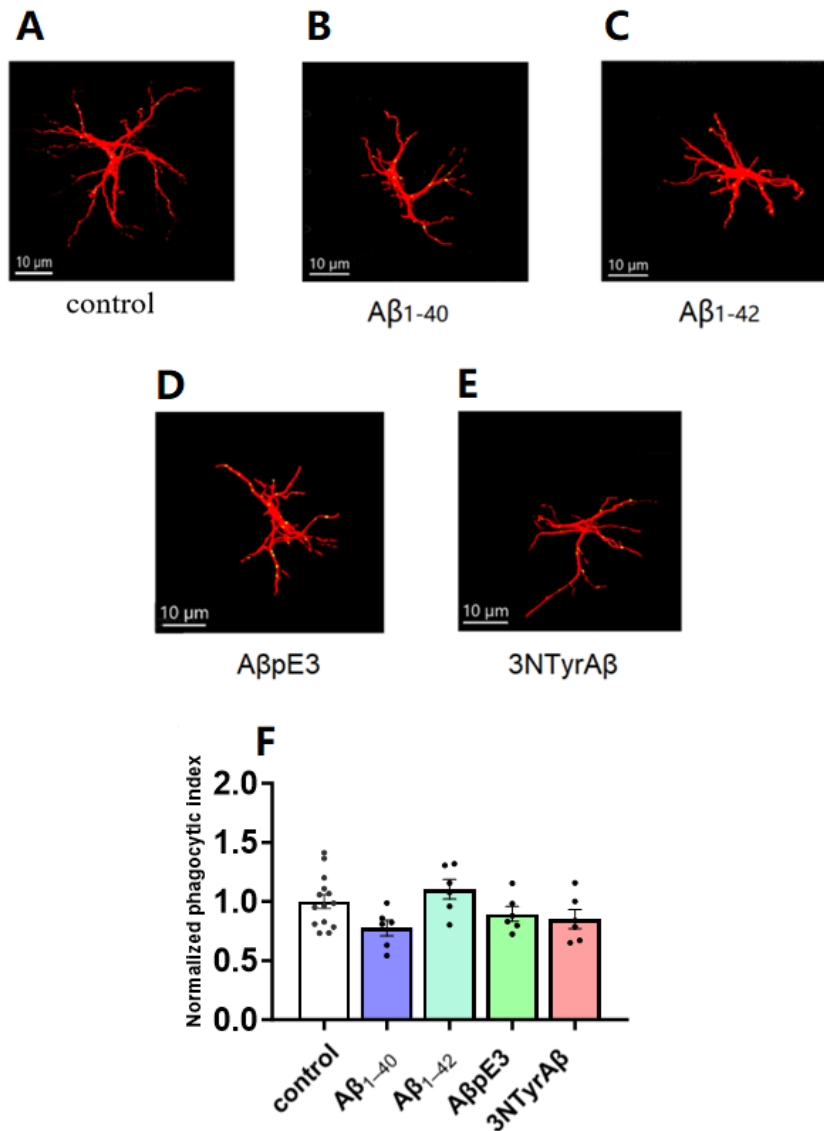


Figure 17. None of the four A β isoforms significantly affected astrocyte-mediated synaptic engulfment. (A-E) Representative maximal projection images showing engulfed PSD95 (shown in yellow) within GFAP stained astrocytes (shown in red) in the control, A β ₁₋₄₀, A β ₁₋₄₂, A β pE3 and 3NTyrA β groups, respectively. The co-localization of PSD95 within the astrocytes is shown in yellow. (F) Compared to the control, none of the four A β isoforms significantly affected astrocyte-mediated synaptic engulfment. Control [100.00 \pm 5.84], A β ₁₋₄₀ [77.50 \pm 6.60], A β ₁₋₄₂ [110.30 \pm 8.22], A β pE3 [89.50 \pm 6.27], 3NTyrA β [85.08 \pm 8.02]; control vs. A β ₁₋₄₀: n=14/6, p= 0.0985; control vs. A β ₁₋₄₂: n=14/6, p >0.9999; control vs. A β pE3: n=14/6, p >0.9999; control vs. 3NTyrA β : n=14/6, p= 0.5121. Data are shown as mean \pm SEM. The number of points in F represents the number of animals. One-way ANOVA followed with Dunnett's multiple comparisons test was performed. *P < 0.05.

2.2.2 Neither 0.4 MAC nor 1.2 MAC had a significant effect on astrocyte-mediated synaptic engulfment

Despite evidence that astrocytes express many anesthetic target proteins, they have been largely overlooked as potential targets for anesthesia. Here we checked the synaptic phagocytosis under sevoflurane exposure and found neither 0.4 MAC nor 1.2 MAC had a significant effect on astrocyte-mediated synaptic engulfment.

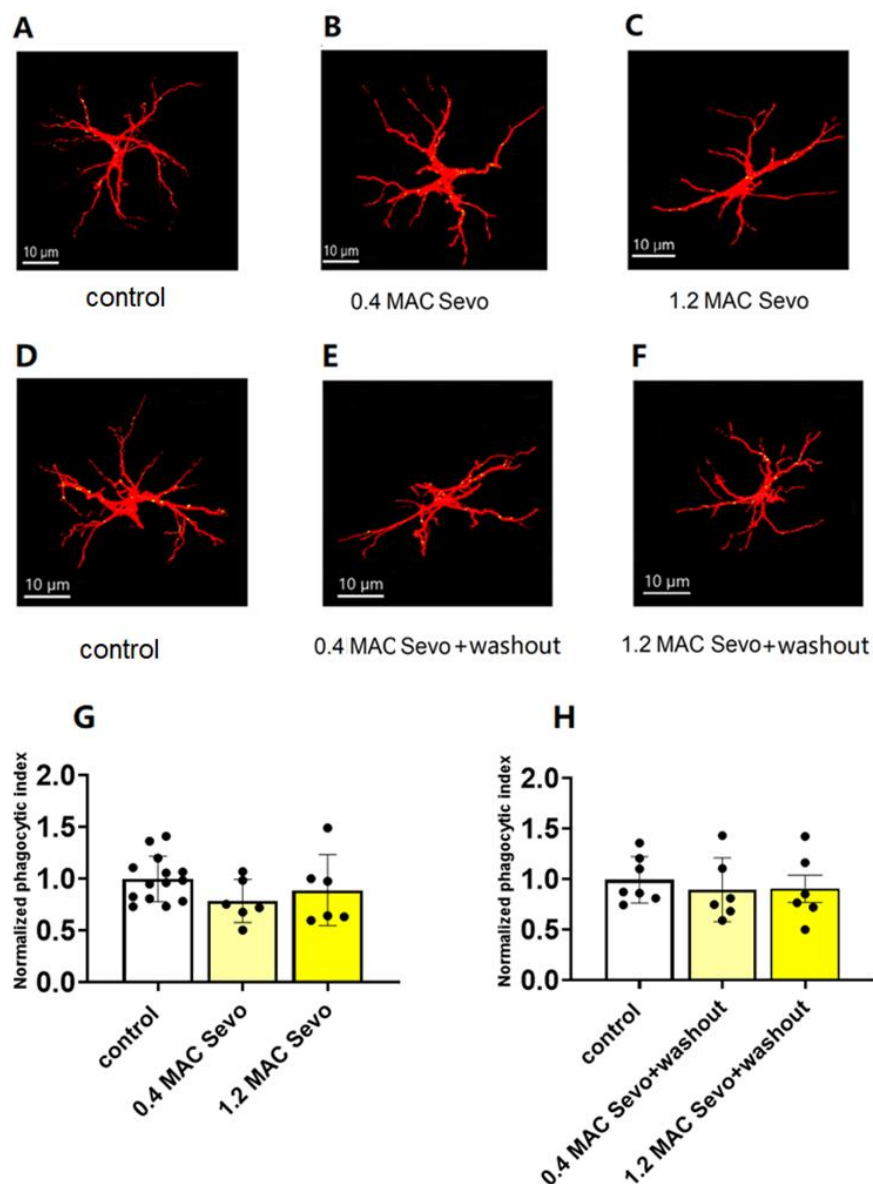


Figure 18. Neither 0.4 MAC nor 1.2 MAC significantly affected astrocyte-mediated synaptic engulfment. (A-F) Representative maximal projection images showing engulfed PSD95 (shown in yellow) within GFAP stained astrocytes (shown in red) in the control, 0.4 MAC sevoflurane, 1.2 MAC sevoflurane, 0.4 MAC sevoflurane+washout and 1.2 MAC sevoflurane + washout groups, respectively.

Individual astrocytes were rendered by Imaris. The co-localization of PSD95 is shown in yellow within the astrocytes. (G) Compared to the control, neither 0.4 MAC nor 1.2 MAC significantly affects astrocyte-mediated synaptic engulfment. Control [100.00 ± 5.84], 0.4 MAC Sevo [78.67 ± 8.48], 1.2 MAC Sevo [89.15 ± 14.08]; control vs. 0.4 MAC Sevo: $n = 14/6$, $p = 0.1706$; control vs. 1.2 MAC Sevo: $n = 14/6$, $p = 0.6028$, one-way ANOVA followed with Dunnett's multiple comparisons. (H) The removal of sevoflurane didn't affect astrocyte-mediated synaptic engulfment either. Control [100.00 ± 8.67], 0.4 MAC Sevo + washout [89.62 ± 12.87], 1.2 MAC Sevo + washout [90.57 ± 13.56]; control vs. 0.4 MAC Sevo + washout: $n = 7/6$, $p = 0.7763$; control vs. 1.2 MAC Sevo + washout: $n = 7/6$, $p = 0.8117$, one-way ANOVA followed with Dunnett's multiple comparison. Sevo, sevoflurane. Data are shown as mean \pm SEM. The number of points in G and H represents the number of animals. * $P < 0.05$.

3.2.3 Application of 1.2 MAC sevoflurane with either A β pE3 or 3NTyrA β decreased astrocyte-mediated synaptic engulfment

Dai et al. demonstrated that 1.3–1.4 MACrodent isoflurane alleviated A β _{1–42}-induced elevation of astrocyte-dependent synaptic engulfment in hippocampal slices. Here in the A β incubated acute hippocampal brain slices, 0.4 MAC sevoflurane had no effect, while 1.2 MAC sevoflurane exposure with either A β pE3 or 3NTyrA β decreased astrocyte-mediated synaptic engulfment.

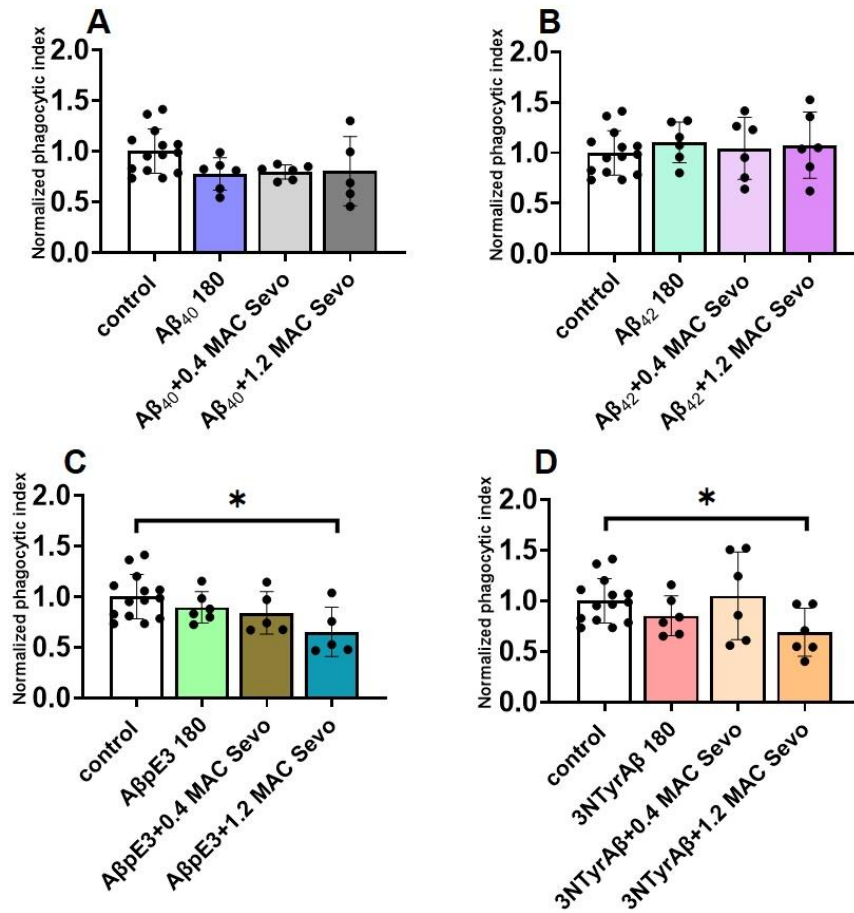


Figure 19. Application of 1.2 MAC sevoflurane with either AβpE3 or 3NTyrAβ decreased astrocyte-mediated synaptic engulfment. (A, B) Aβ_{1-40/1-42}+Sevo (0.4/1.2 MAC) didn't affect the phagocytic index. Control [100.00 ± 5.84], Aβ₁₋₄₀ [77.50 ± 6.60, Aβ₁₋₄₀ + 0.4 MAC Sevo [79.47 ± 2.91], Aβ₁₋₄₀ + 1.2 MAC Sevo [80.31 ± 15.28]; Aβ₁₋₄₀ vs. Aβ₁₋₄₀ + 0.4 MAC Sevo: n = 6/6, p = 0.9813; Aβ₁₋₄₀ vs. Aβ₁₋₄₀ + 1.2 MAC Sevo: n = 6/5, p = 0.9659, one-way ANOVA followed with Dunnett's multiple comparisons; Aβ₁₋₄₂ [101.3 ± 8.22], Aβ₁₋₄₂ + 0.4 MAC Sevo [104.4 ± 12.55], Aβ₁₋₄₂ + 1.2 MAC Sevo [107.6 ± 13.35]; Aβ₁₋₄₂ vs. Aβ₁₋₄₂ + 0.4 MAC Sevo: n = 6/6, p = 0.9105; Aβ₁₋₄₂ vs. Aβ₁₋₄₂ + 1.2 MAC Sevo, n = 6/6, p = 0.9807, one-way ANOVA followed with Dunnett's multiple comparisons. (C, D) Both AβpE3 + 1.2MAC Sevo and 3NTyrAβ + 1.2MAC Sevo decreased the phagocytic index compared with the control. AβpE3 [89.50 ± 6.27], AβpE3 + 0.4 MAC Sevo [83.96 ± 6.27], AβpE3 + 1.2 MAC Sevo [65.32 ± 10.93]; AβpE3 vs. AβpE3 + 0.4 MAC Sevo: n = 6/5, p = 0.8674; AβpE3 vs. AβpE3 + 1.2 MAC Sevo: n = 6/5, p = 0.1243, one-way ANOVA followed with Dunnett's multiple comparisons; control vs. AβpE3 + 1.2 MAC Sevo: n = 14/5, p = 0.0088, unpaired t-test; 3NTyrAβ 180 [85.08 ± 8.02, 3NTyrAβ + 0.4 MAC Sevo [104.9 ± 17.67], 3NTyrAβ + 1.2 MAC Sevo [68.86 ± 9.67]; 3NTyrAβ 180 vs. 3NTyrAβ + 0.4 MAC Sevo, n = 6/6, p = 0.4472; 3NTyrAβ vs. 3NTyrAβ + 1.2 MAC Sevo, n = 6/6, p = 0.5703, one-way ANOVA followed with Dunnett's multiple comparisons, control vs. 3NTyrAβ + 1.2 MAC Sevo, n = 14/6, p = 0.0106, unpaired t-test. Aβ 180, Aβ incubation for 180

min. Sevo, sevoflurane. Data are shown as mean \pm SEM. Points in the scatter plot represent the relative PI of an animal. *P < 0.05.

3.2.4 After the removal of sevoflurane, the inhibition effect of 1.2 MAC sevoflurane with either A β E3 or 3NTyrA β on the astrocyte-mediated synaptic engulfment disappeared

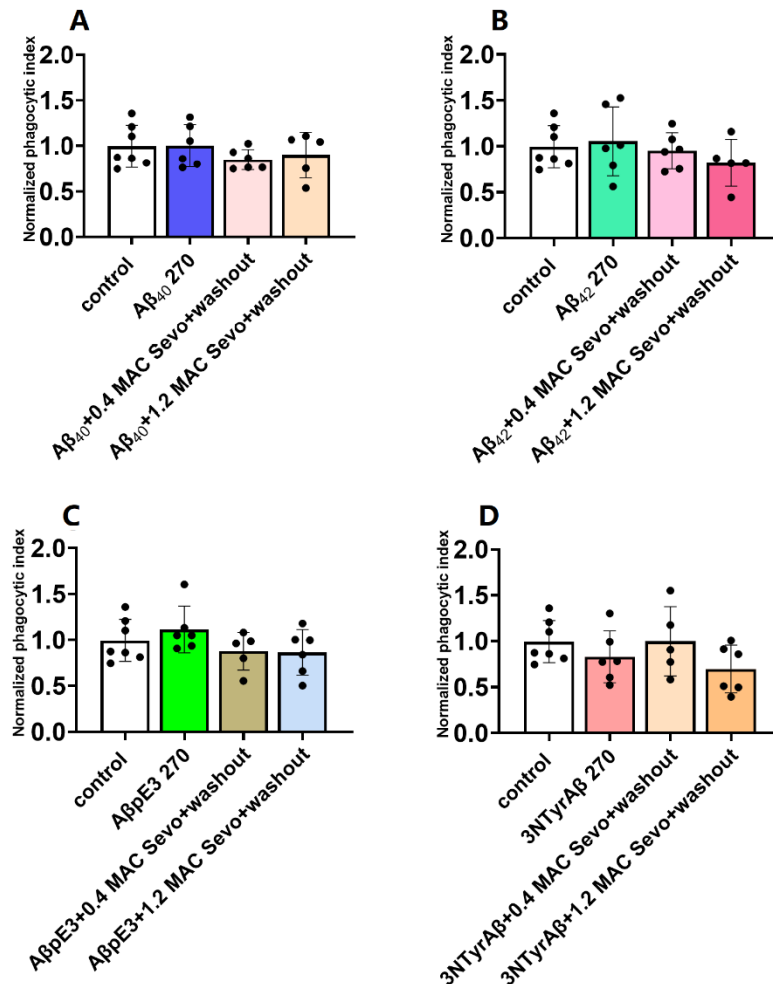


Figure 20. After 90 min washout, co-applicating 1.2 MAC sevoflurane with A β species had no significant effect on astrocyte-mediated synaptic engulfment. (A-D) Removal of sevoflurane in A β -incubated hippocampal slices, only 3NTyrA β + 1.2 MAC sevoflurane + washout had the tendency to decrease astrocyte-mediated synaptic engulfment. Control [100.00 \pm 8.67], 3NTyrA β 270 [83.01 \pm 11.53], 3NTyrA β + 0.4 MAC Sevo + washout [99.84 \pm 16.87], 3NTyrA β + 1.2 MAC Sevo + washout [69.74 \pm 10.59]; 3NTyrA β 270 vs. 3NTyrA β + 0.4 MAC Sevo + washout: n = 6/5, p = 0.5782; 3NTyrA β vs. 3NTyrA β + 1.2 MAC Sevo + washout: n = 6/6, p = 0.6807, one-way ANOVA followed with Dunnett's multiple comparisons; control vs. 3NTyrA β + 1.2 MAC Sevo + washout: n= 7/6, p = 0.0506, unpaired t-test. A β 270, A β incubation for 270 min. Sevo, sevoflurane. Data are shown as mean \pm SEM. Every data point in the scatter plot E represents the relative PI of an animal. *P < 0.05.

3.3 The effects of A β and sevoflurane on the expression of MEGF10, GFAP and GFAP-BDPs

GFAP is not only a specific marker for astrocytes, but also its increased expression has been recognized as a marker for astrocytosis. Astrocytosis is a series of molecular, cellular, and functional changes that occur in astrocytes in response to various CNS traumas and diseases[120]. In this process, astrocytes become reactive and morphologically hypertrophied with changes in gene expression profiles. Reactive astrogliosis might lose the ability to phagocytose synapses and debris by down-regulating phagocytic receptors MERTK and MEGF10[121].

Astrocytosis is a hallmark of AD, which can be triggered by A β oligomers[122]. Therefore, to check if acute application of A β and sevoflurane could induce astrocytosis, we quantify the expression of GFAP. In addition, we also would like to know if MEGF10 is involved in the inhibition of astrocyte-mediated synaptic engulfment observed by the co-application of 1.2 MAC sevoflurane with A β pE3 and 3NTyrA β .

3.3.1 Among the four A β isoforms, only 3NTyrA β downregulated GFAP- α expression

In the rodent brain, only GFAP- α and GFAP- δ are expressed at the protein level. GFAP- α is the most predominant isoform with the best intrinsic capacity to form long filaments[123]. During glial cell challenge, GFAP (especially GFAP- α) is highly vulnerable to calpain-mediated truncation and produces a series of truncated GFAP-BDPs, which can not form filaments due to the lack of C-and N-terminals[106, 124].

Contrary to our expectations, low nanomolar concentration (50 nM) of A β -A β ₁₋₄₀, A β ₁₋₄₂, A β pE3 and 3NTyrA β did not increase GFAP expression, whereas 3NTyrA β decreased GFAP- α expression. The results suggest that acute incubation of A β did not result in astrocytosis, and the downregulation of GFAP- α under 3NTyrA β incubation may indicate astrocyte cytoskeleton atrophy.

Similarly, none of the four A β isoforms have an effect on the expression of phagocytic receptor MEGF10, which is consistent with the previous finding that none of them significantly affect astrocyte-mediated synaptic phagocytosis.

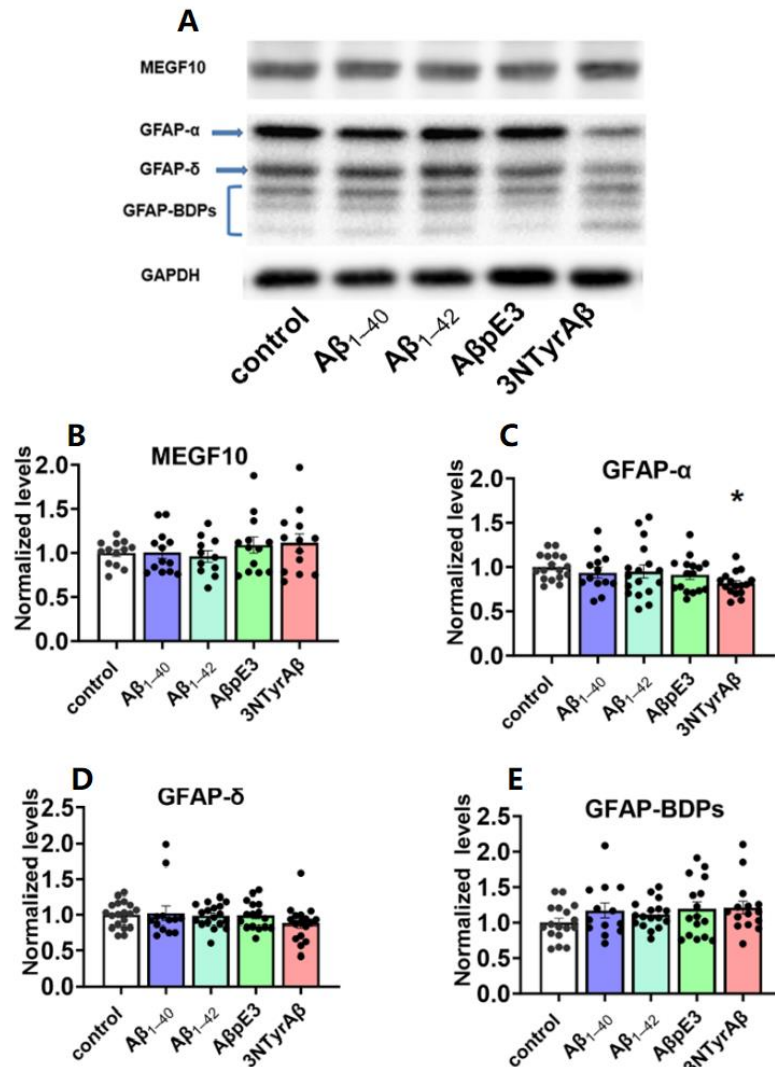


Figure 21. 3NTyrA β downregulated GFAP- α expression in the hippocampus. (A) Representative Western blot bands of MEGF10, GFAP, and GFAP-BDPs in mouse hippocampus. GAPDH served as the loading control. (B) Incubated for 180 min, none of A β isoforms-A β ₁₋₄₀, A β ₁₋₄₂, A β pE3 and 3NTyrA β significantly affected MEGF10 expression. (C) Among the four A β isoforms, only 3NTyrA β decreased the expression of GFAP- α ($p=0.0443$). Control [100 ± 3.52], A β ₁₋₄₀ [93.67 ± 6.11], A β ₁₋₄₂ [94.94 ± 7.42], A β pE [91.00 ± 4.88], 3NTyrA β [81.39 ± 3.30]; control vs. A β ₁₋₄₀: $n = 17/13$, $p=0.8332$; control vs. A β ₁₋₄₂: $n = 17/17$, $p=0.8944$; control vs. A β pE3: $n = 17/17$, $p=0.5555$; control vs. 3NTyrA β : $n = 17/16$, $p = 0.0442$, one-way ANOVA followed by Dunnett's multiple comparisons test. (D-E) None of the A β isoforms produced a significant effect on the expression of GFAP- δ and GFAP-BDPs. Data are shown as mean \pm SEM. The number of points in B-E represents the number of animals. * $P < 0.05$.

3.3.2 Neither 0.4 MAC nor 1.2 MAC sevoflurane produced a significant effect on the expression of MEGF10, GFAP, and GFAP-BDPs

1.4% isoflurane for 4 h decreased the expression of GFAP in rat astrocytes[125]. Here, we applied sevoflurane for 90 min and found that neither 0.4 MAC nor 1.2 MAC sevoflurane produced a significant effect on the expression profile of GFAP.

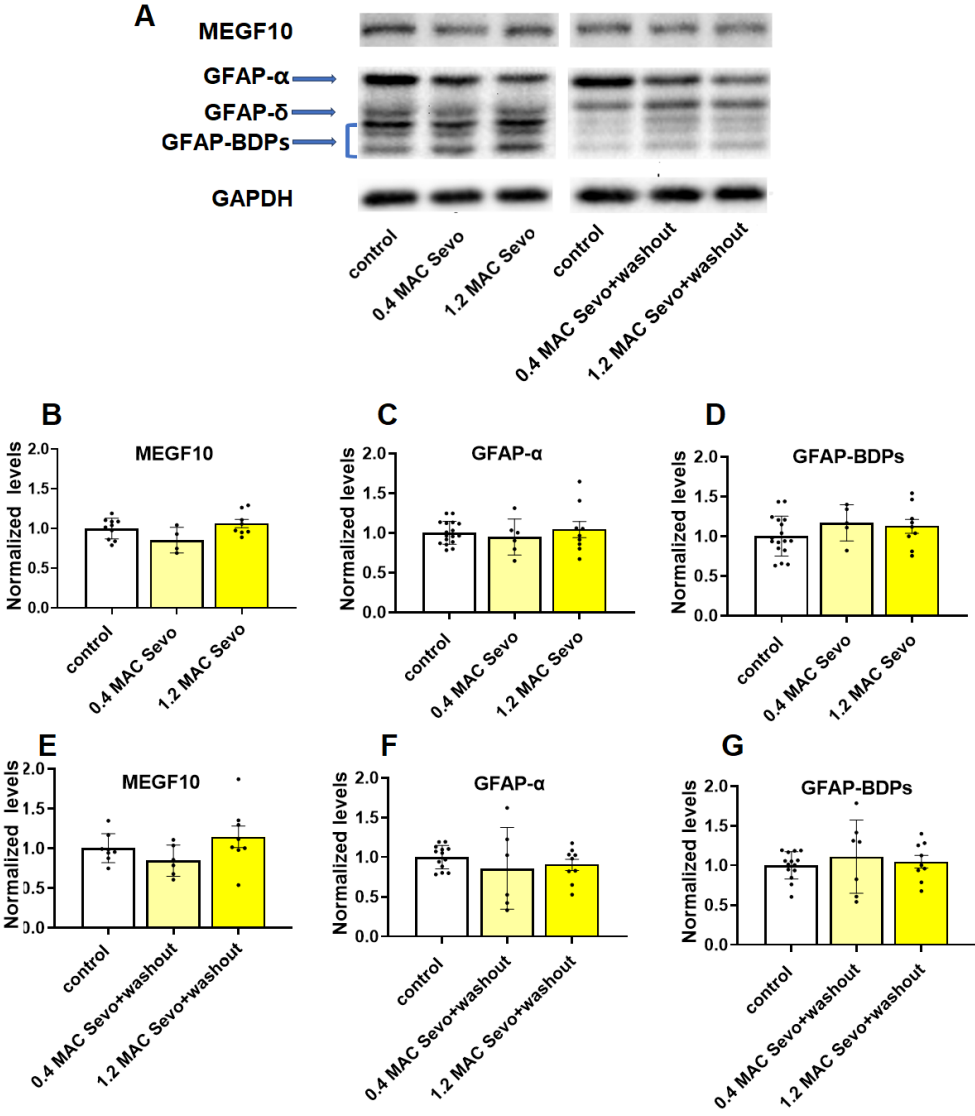


Figure 22. Neither 0.4 MAC nor 1.2 MAC sevoflurane significantly affected the expression of MEGF10, GFAP, and GFAP-BDPs. (A) Representative Western blot bands of MEGF10, GFAP, and GFAP-BDPs. GAPDH served as the loading control. (B-D) During exposure, 0.4 MAC and 1.2 MAC sevoflurane did not significantly affect the expression of MEGF10, GFAP-α and GFAP-BDPs. (E-G) After 90 min washout, 0.4 MAC and 1.2 MAC sevoflurane did not significantly affect the expression of MEGF10, GFAP-α and GFAP-BDPs. “Sevo” in the graph is the abbreviation of sevoflurane. Data

are shown as mean \pm SEM. The number of points in B-G represents the number of animals. One-way ANOVA was performed. *P < 0.05.

3.3.3 Depending on the concentration, a dual effect of sevoflurane on the 3NTyrA β -induced expression of GFAP- α and GFAP-BDPs

Next, we investigated the effects of sevoflurane (0.4 MAC and 1.2 MAC) on the A β -induced expression of GFAP- α and GFAP-BDPs. We found that 0.4 MAC sevoflurane protected against the downregulation of GFAP- α and upregulation of GFAP-BDPs induced by 3NTyrA β . In contrast, 1.2 MAC sevoflurane upregulated the expression of GFAP-BDPs and with the tendency to downregulate GFAP- α expression induced by 3NTyrA β . Sevoflurane appeared to have a dual effect on A β -induced GFAP- α and GFAP-BDPs expression depending on the concentration. Moreover, we found that co-application of 1.2 MAC with 3NTyrA β resulted in the downregulation of astrocyte phagocytic receptor MEGF10 expression in comparison with the control.

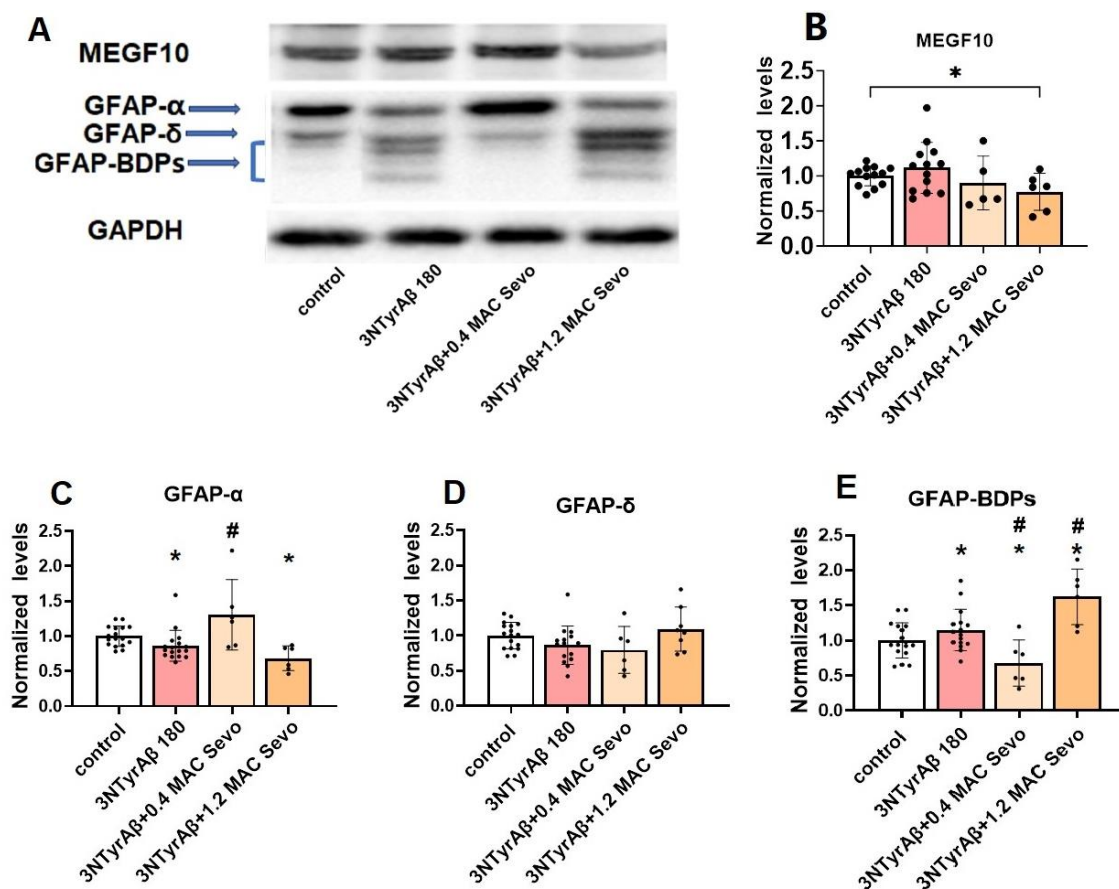


Figure 23. A dual effect of sevoflurane on 3NTyrA β induced expression of GFAP- α and GFAP-BDPs dependent on concentration. (A) Representative Western blot bands of MEGF10, GFAP, and GFAP-BDPs in the control, 3NTyrA β incubation, 3NTyrA β +0.4 MAC, and 3NTyrA β +1.2 MAC sevoflurane groups, respectively. GAPDH served as the loading control. (B) Compared to the control, exposure of 1.2 MAC sevoflurane on acute hippocampal brain slices pretreated with 3NTyrA β significantly downregulated MEGF10 expression. Control [100.00 \pm 3.90], 3NTyrA β [111.60 \pm 10.05], 3NTyrA β + 0.4 MAC Sevo [90.05 \pm 17.20], 3NTyrA β + 1.2 MAC Sevo [64.87 \pm 6.64]; Control vs. 3NTyrA β + 1.2 MAC Sevo: n = 13/6, p = 0.0244, unpaired t-test. (C, E) Application of 0.4 MAC sevoflurane protected against the downregulation of GFAP- α (control [100.00 \pm 3.90], 3NTyrA β [81.39 \pm 3.30], 3NTyrA β + 0.4 MAC Sevo [130.5 \pm 20.54], 3NTyrA β vs. 3NTyrA β + 0.4 MAC Sevo: n = 16/5, p = 0.0072, one-way ANOVA followed with Dunnett's multiple comparisons), and upregulation of GFAP-BDPs induced by 3NTyrA β (control [100.00 \pm 6.07], 3NTyrA β [114.9 \pm 7.41], 3NTyrA β + 0.4 MAC Sevo [67.84 \pm 13.43], 3NTyrA β vs. 3NTyrA β + 0.4 MAC Sevo, n=16/6, p = 0.0112, one-way ANOVA followed with Dunnett's multiple comparisons). Compared to the control, exposure to 0.4 MAC sevoflurane downregulated the expression of GFAP-BDPs (control vs. 3NTyrA β + 0.4 MAC Sevo, n = 17/6, p = 0.0208, unpaired t-test). (D, E) Application of 1.2 MAC sevoflurane upregulated the expression of GFAP-BDPs (3NTyrA β [81.39 \pm 3.30], 3NTyrA β + 1.2 MAC Sevo [68.42 \pm 7.22], NTyrA β vs. 3NTyrA β + 1.2 MAC Sevo: n = 16/6, p = 0.0107, one-way ANOVA followed with Dunnett's multiple comparisons) and with the tendency to downregulated GFAP- α expression induced by 3NTyrA β (3NTyrA β [114.9 \pm 7.41], 3NTyrA β + 1.2 MAC Sevo [162.3 \pm 16.21], NTyrA β vs. 3NTyrA β + 1.2 MAC Sevo: n = 16/6, p = 0.0615 one-way ANOVA followed with Dunnett's multiple comparisons). Compared to the control, exposure of 1.2 MAC sevoflurane downregulated the expression of GFAP- α (control vs. 3NTyrA β + 1.2 MAC Sevo, n=17/6, p<0.001, unpaired t-test) and upregulated the expression of GFAP-BDPs (control vs. 3NTyrA β + 0.4 MAC Sevo: n = 17/6, p = 0.002, unpaired t-test). 3NTyrA β 180, 3NTyrA β incubation for 180 minSevo, sevoflurane. Data are shown as mean \pm SEM. The number of points in B-E represents the number of animals. P < 0.05. *: significant difference from the control; #: significant difference from 3NTyrA β .

Table 15: Application of sevoflurane on the expression of GFAP- α and GFAP-BDPs in A β pre-incubated acute hippocampal brain slices

	A β ₁₋₄₀		A β ₁₋₄₂		A β pE3		3NTyrA β		compared to
	GFAP- α	GFAP-BDPs	GFAP- α	GFAP-BDPs	GFAP- α	GFAP-BDPs	GFAP- α	GFAP-BDPs	
0.4 MAC Sevo	* ↑	* ↓	* ↑	* ↓	* ↑	-	-	* ↓	control
	# ↑	# ↓	# ↑	# ↓	# ↑	# ↓	# ↑	# ↓	A β 180
1.2 MAC Sevo	* ↓	-	* ↓	-	-	* ↑	* ↓	* ↑	control
	-	-	-	-	-	-	-	# ↑	A β 180

Compared to A β , the combination of A β and 0.4 MAC sevoflurane increased the expression of GFAP- α and decreased the expression of GFAP-BDPs. In contrast, 1.2 MAC sevoflurane upregulated the expression of GFAP-BDPs only in the presence of 3NTyrA β . Compared to the control, sevoflurane generally produced dual effects on the expression of GFAP- α and GFAP-BDPs. Specifically, 0.4 MAC sevoflurane upregulated the expression of GFAP- α (except for 3NTyrA β) and decreased the expression of GFAP-BDPs (except for A β pE3); in contrast, 1.2 MAC sevoflurane decreased the expression of GFAP- α (except A β pE3 β) and increased the expression of GFAP-BDPs only in the presence of 3NTyrA β . For comparison with the control, an unpaired t-test was performed, and for comparison with A β , one-way ANOVA followed with Dunnett's multiple comparisons test was performed. P< 0.05. *: significant difference from control; #: significant difference from corresponding A β isoforms; -: not significantly different from the control or corresponding A β isoforms.

3.3.4. Removal of sevoflurane attenuated the effects on A β -induced expression of GFAP and GFAP-BDPs during exposure.

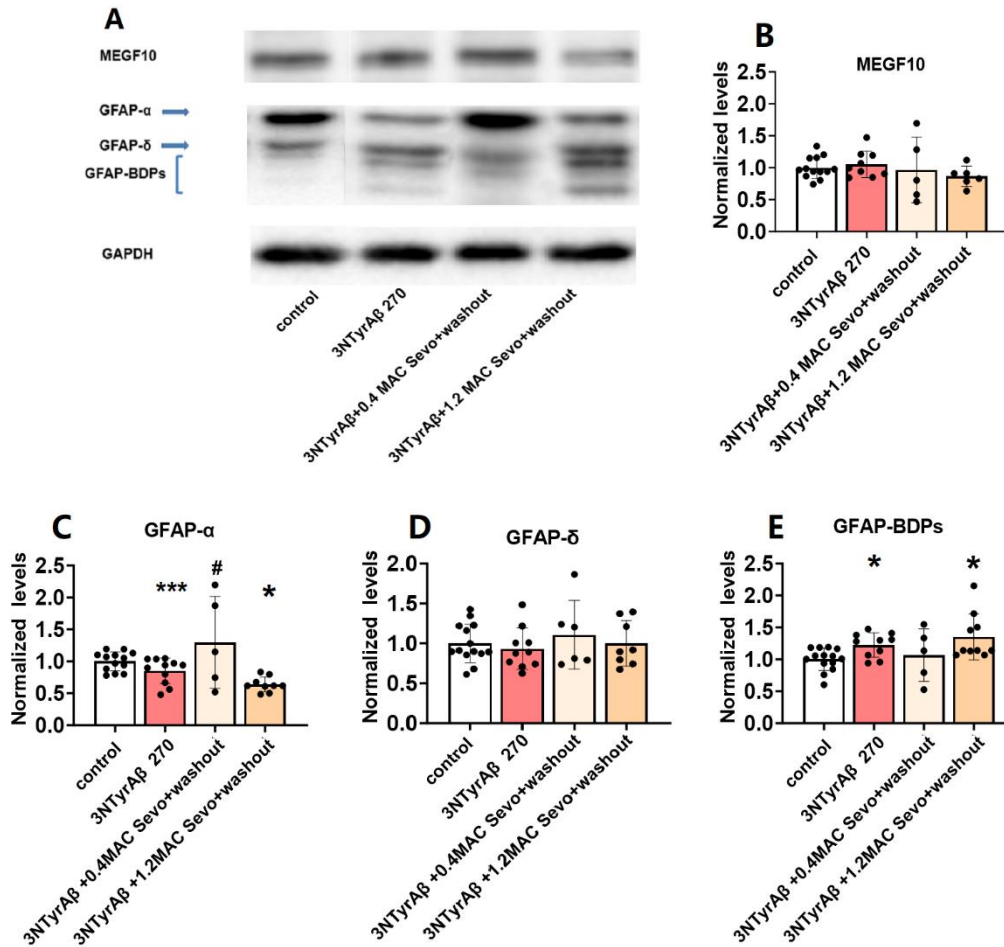


Figure 24. After 90 min washout, the dual effects of sevoflurane on 3NTyrA β -induced expression of GFAP- α and GFAP-BDPs were attenuated. (A) Representative Western blot bands of MEGF10, GFAP, and GFAP-BDPs from the control, 3NTyrA β , 3NTyrA β +0.4 MAC sevoflurane+washout, and 3NTyrA β +1.2 MAC sevoflurane+washout groups, respectively. GAPDH serves as the loading control. After 90 min of sevoflurane washout, (B) the downregulated expression of MEGF10 induced by co-application of 3NTyrA β and 1.2 MAC sevoflurane disappeared. Control [100.00 \pm 4.65], 3NTyrA β 270 [105.20 \pm 6.90], 3NTyrA β + 0.4 MAC Sevo + washout [96.50 \pm 22.99], 3NTyrA β + 1.2 MAC Sevo + washout [86.47 \pm 6.53], control vs. 3NTyrA β + 1.2 MAC Sevo + washout n = 13/6, p = 0.1163, unpaired t test; (C-E) for 0.4 MAC sevoflurane, the upregulation of GFAP- α persisted (control [100.00 \pm 4.11], 3NTyrA β 270 [85.17 \pm 6.02], 3NTyrA β + 0.4 MAC Sevo + washout [129.70 \pm 32.17], 3NTyrA β 270 vs. 3NTyrA β + 0.4 MAC Sevo + washout, n = 9/5, p=0.0465, one-way ANOVA followed with Dunnett's multiple comparisons), while the downregulated expression of GFAP-BDPs was reversed (control [100.00 \pm 4.62], 3NTyrA β 270 [122.50 \pm 5.99], 3NTyrA β + 0.4 MAC Sevo + washout [106.60 \pm 18.36], N TyrA β 270 [122.50 \pm 5.99] vs. 3NTyrA β + 0.4 MAC Sevo + washout: n = 9/5, p = 0.5724, one-way ANOVA followed with Dunnett's multiple comparisons); for 1.2 MAC sevoflurane, the downregulated expression of GFAP- α (3NTyrA β 270 vs. 3NTyrA β + 1.2 MAC Sevo + washout: n = 9/9, p = 0.3108, one-way ANOVA followed with Dunnett's multiple comparisons) and

upregulated expression of GFAP-BDPs were reversed (3NTyrA β 270 vs. 3NTyrA β + 1.2 MAC Sevo + washout: n = 9/ 9, p = 0.5884, one-way ANOVA followed with Dunnett's multiple comparisons). 3NTyrA β 270, 3NTyrA β incubation for 270 min. Sevo, sevoflurane. Data are shown as mean \pm SEM. The number of points in B-E represents the number of animals. P < 0.05. *: significant difference from control; #: significant difference from 3NTyrA β .

Table 16: Removal of sevoflurane on the expression of GFAP- α and GFAP-BDPs in A β pre-incubated acute hippocampal brain slices

	A β ₁₋₄₀		A β ₁₋₄₂		A β pE3		3NTyrA β		compared to
	GFAP- α	GFAP-BDPs	GFAP- α	GFAP-BDPs	GFAP- α	GFAP-BDPs	GFAP- α	GFAP-BDPs	
0.4 MAC Sevo + washout	* \uparrow	-	-	-	-	-	* \uparrow	-	control
	# \uparrow	-	-	-	-	-	# \uparrow	-	A β 270
1.2 MAC Sevo + washout	* \downarrow	* \uparrow	-	-	-	* \uparrow	* \downarrow	* \uparrow	control
	-	-	-	-	-	-	-	-	A β 270

Generally speaking, removing sevoflurane attenuated the effects on the expression of GFAP- α and GFAP-BDPs. Compared to A β and the control, for 0.4 MAC sevoflurane, the upregulation of GFAP- α only existed in A β ₁₋₄₀ and 3NTyrA β , and the effects on c all disappeared. Compared to A β , GFAP-BDPs led by 1.2 MAC sevoflurane in the presence of 3NTyrA β disappeared, and compared to the control, the decreased expression of GFAP- α only existed in A β ₁₋₄₀ and 3NTyrA β , and the increased expression of GFAP-BDPs in all A β except for A β pE3. For comparison with the control, an unpaired t-test was performed, and for comparison with A β , one-way ANOVA followed with Dunnett's multiple comparisons test was performed. *: significant difference from control; #: significant difference from corresponding A β isoforms; -: not significantly different from the control or corresponding A β isoforms.

4. Discussion

4.1 The effect of A β and sevoflurane on DSD

With an increase in life expectancy, an ever-increasing number of AD patients need anesthesia care. POD is one of the most common neurocognitive deficits in AD patients following surgery and anesthesia, whereas its pathophysiology is still unclear currently [11, 12].

Moreover, due to the lack of effective treatments, the prevention of POD is extremely important.

It is now widely considered that general anesthetics at low concentrations for short duration induce neuroprotection, whereas at high concentrations for prolonged duration induce neuronal damage[58]. Moreover, light anesthesia was demonstrated to reduce the incidence of POD and cognitive impairment in elderly patients undergoing major surgery [14]. Therefore, in this part of the study, to mimic AD patients receiving anesthesia, a low and a high concentration (0.4 MAC and 1.2 MAC) of sevoflurane were applied to A β species (A β ₁₋₄₀, A β ₁₋₄₂, A β pE3 and 3NTyrA β) pre-incubated acute hippocampal brain slices, to investigate whether 0.4 MAC sevoflurane could produce protection against the dendritic spine from the interference of A β or 1.2 MAC sevoflurane could enhance A β -induced toxicity on dendritic spine.

The results show that: 1) all the A β isoforms decreased the DSD except for A β pE3 (3NTyrA β had the greatest effect); 2) 0.4 MAC sevoflurane produced a reversible downregulation of DSD in the absence and presence of A β (except A β pE3) pre-incubated hippocampal slices; 3) 1.2 MAC sevoflurane exerted a long-lasting effect on the reduction of the DSD, and 1.2 MAC sevoflurane enhanced the downregulation of DSD induced by A β ₁₋₄₀, A β ₁₋₄₂, and this enhancement was reversed after 90 min of sevoflurane removal; 1.2 MAC sevoflurane didn't enhance the decreasing of DSD induced by A β pE3 and 3NTyrA β , and after sevoflurane removal there were an increase in the stubby spine for A β pE3 and an increase in thin spines for 3NTyrA β .

All the A β isoforms (except A β pE3) downregulation the DSD, a very likely explanation could be that A β interferes with the glutamatergic system via overactivation of N-methyl-D-aspartate (NMDA) receptors, thereby increasing intracellular calcium levels and resulting in excitotoxicity, which leads to synaptic dysfunction and synaptic loss via mitochondrial dysfunction and apoptosis[126-128].

3NTyrA β had the greatest effect, and A β pE3 tended to decrease DSD. Differences in the efficacy of decreasing spine may be due to post-translational modifications changing the aggregation property[45]. A β monomer is usually nontoxic, whereas the A β soluble oligomers aggregated from monomers are thought to be the primary cause of synaptic loss in the early phase of AD[129]. Thus, after post-translational modifications, 3NTyrA β monomers aggregate more readily than other A β isoforms to form soluble oligomers, whereas A β pE3 is the opposite of that. Another possible explanation could be that post-translational modifications change the affinity of A β to the target receptors (e.g., NMDA receptors), resulting in enhanced or attenuated downstream responses (e.g., calcium-influx, synaptic plasticity impairments)[130].

Previous studies have shown that sevoflurane concentration-dependently impaired CA1-LTP in acute hippocampal slices[81], indicating an alternation of synaptic transmission under sevoflurane. Here we observed a concentration-dependent decrease of CA1-dendritic spines under sevoflurane. To mimic the clinical situation and check whether this reduction is persistent, we also analyzed the spines after 90 minutes of sevoflurane removal. The results show that the effect of 0.4 MAC was fully recovered, whereas, for 1.2 MAC of sevoflurane, there is a long-lasting effect on the downregulation of the thin spines.

Regarding the different effects of 0.4 MAC and 1.2 MAC sevoflurane, an important factor is the concentration. 0.4 MAC is the concentration that approximates the MAC-awake, a subanesthetic dose. MAC-awake of inhalation anesthetics usually assesses perceived awareness rather than memory. And 1.2 MAC is a dose that produces clinical anesthesia for surgery. Since dendritic spines are closely associated with memory, it is not difficult to speculate that sevoflurane at 1.2 MAC exerted a greater effect on dendritic spine dynamics than at 0.4 MAC. In addition, it has been demonstrated that inhalation anesthetics dose-dependently destabilize the molecular skeleton of dendritic spines, and the concentration required to inhibit dendritic spine motility is similar to MAC[131]. Similarly, Jimcy et al. also

demonstrated in mature cultured rat hippocampal neurons, that approximate 1.5 MAC_{rodent} isoflurane exposure for 20 min led to rapid non-uniform shrinkage and loss of dendritic spines via actin inhibition[132]. Since the structure of dendritic spines is primarily built on an actin cytoskeleton[89], we can speculate that an actin-based mechanism may account for the greater effects of 1.2 MAC sevoflurane on DSD.

A previous study shows that neuronal activity in the CA1 region of the hippocampus was reduced by 0.6 MAC_{rodent} sevoflurane completely recovered after 60 min of washout[118], which explains the reversible effect of 0.4 MAC sevoflurane on DSD. As for the difference after sevoflurane removal, For the irreversible effects induced by 1.2 MAC of sevoflurane with 90 min washout, it may be because the effect needs a longer time of washout. According to the research by Guang et al., the effect of 1.5% isoflurane vanished after the mice woke up for 8 h in the living mouse cortex[134], we can speculate that with longer washout time, the effects on DSD induced by 1.2 MAC sevoflurane may also be completely reversed.

Notably, we observed that the thin spines were more sensitive than the stubby and mushroom spines under A β species (A β ₁₋₄₀, A β ₁₋₄₂, A β pE3 and 3NTyrA β) incubation and sevoflurane exposure. It is demonstrated that different types of spines have different sensitivities to general anesthetics, and filopodia (in our study was categorized as thin spines) is more sensitive than other subtypes[132, 133]. A possible reason for this could be that thin spines have smaller heads and longer necks with shorter latency to calcium and slower decay kinetics, therefore more susceptible to stimuli than the other two subtypes, which are more stable and mature with a larger head [134]. Mushroom spines have large PSD and are surrounded by perisynaptic astrocytic processes that can help to keep synaptic stability. In contrast, thin spines have smaller PSD with the property of forming or disappearing rapidly depending on activities[95]. This may also account for the more pronounced change in thin spines under A β incubation or sevoflurane exposure.

0.4 / 1.2 MAC sevoflurane was applied to acute hippocampal brain slices pre-incubated with A β to mimic AD patients receiving sevoflurane. Generally speaking, a combination of 0.4 MAC sevoflurane with A β produced a more pronounced CA1 DSD reduction than A β alone. The downregulation was mainly due to stubby spines, since in all A β isoforms + sevoflurane groups, stubby spines were markedly less than A β alone. One possible explanation is that under A β pretreatment, 0.4 MAC sevoflurane produced an additive effect on inhibiting spines. As mentioned above, A β oligomers and sevoflurane inhibit the spine through different mechanisms so that the combination may have an additive effect.

A more complex result regarding the combination of 1.2 MAC sevoflurane with A β was drawn. 1.2 MAC sevoflurane enhanced the downregulation of DSD induced by A β_{1-40} / A β_{1-42} , and the reduction was mainly due to the inhibition of stubby and mushroom spines, which are also called mature spines. Although 1.2 MAC sevoflurane didn't enhance the downregulation of DSD induced by either A β_{pE3} or 3NTyrA β , it did decrease the stubby spine. In the presence of 3NTyrA β , 1.2 MAC Sevo increased the thin spine with the tendency to decrease the mushroom spine. And mushroom spines seem more susceptible to the combination of high concentration of sevoflurane with A β since this type of spine was not changed under A β +0.4MAC sevoflurane but were reduced under all A β isoforms + 1.2 MAC sevoflurane compared to the control.

Those above-mentioned spine dynamics may be due to the interaction of A β with sevoflurane. Previous studies have demonstrated that sevoflurane can accelerate A β_{1-40} and A β_{1-42} production and induce neurotoxicity in the hippocampus[135]. This might be the reason why we observed the combination reduction effects on spines here. Under A β +sevoflurane, different spines take divergent actions due to their own properties and interactions between A β and sevoflurane.

To mimic AD patients recovering from sevoflurane anesthesia, sevoflurane was removed from the A β incubated hippocampal brain slices. After sevoflurane was removed, how did dendritic

spines react? For 0.4 MAC sevoflurane, compared to the $A\beta$, the effect of 0.4 MAC sevoflurane disappeared. While for 1.2 MAC sevoflurane, the effect is a bit more complicated. For $A\beta_{1-40}$ / $A\beta_{1-42}$ / $A\beta_{pE3}$, the effect of 1.2 MAC sevoflurane was completely recovered after 90 min withdrawal. For $A\beta_{pE3}$, although the total DSD did not change, there was an increase in the density of the stubby spines. For 3NTyr $A\beta$, an increase in DSD persisted, accompanied by a lasting increase in thin spines, indicating sevoflurane's residual effect on CA1 spine structure and function after its removal. Dendritic spines contribute to synaptic transmission and plasticity, and abnormal spine structure may induce aberrant synapse connections[89]. In this part, we examined the effects of sevoflurane on the spine dynamics of hippocampal slices preincubated with $A\beta$, which mimics the condition of AD patients receiving sevoflurane. We found that both 0.4 and 1.2 MAC sevoflurane exposure caused significant changes in spine structure in $A\beta$ -incubated slices, with 1.2 MAC sevoflurane having a greater effect. Upon sevoflurane removal, the effects of 0.4 MAC sevoflurane completely disappeared, indicating that it did not protect or enhance the dendritic spine toxicity of $A\beta$. However, residual effects of 1.2 MAC sevoflurane were observed when combined with either $A\beta_{pE3}$ or 3NTyr $A\beta$, which increased the stubby and thin spines respectively. The increase of stubby and thin spines might have implications for the anesthesia of AD patients. However, further study is required to reveal whether this effect is beneficial or not.

4.2 The effect of $A\beta$ and sevoflurane on MEGF10-mediated synaptic engulfment of astrocytes

The activity of astrocytes is one of the crucial mechanisms for synaptic plasticity[136]. Moreover, increasing data suggests that astrocytes are also important targets of $A\beta$, and dysregulation of astrocyte-mediated synaptic phagocytosis can lead to synaptic degeneration, maladaptive synaptic plasticity, and cognitive deficits in AD[101]. Furthermore, research has shown that volatile anesthetics such as isoflurane can affect synapses through astrocyte-mediated phagocytosis [137].

In this part, we aimed to investigate the potential role of astrocytic-mediated synapse elimination in CA1 dendritic spine alterations observed previously. The results indicated that either sevoflurane or A β alone did not significantly affect this process. Furthermore, the combination of 0.4 MAC sevoflurane with A β did not produce a significant effect on astrocyte-mediated synaptic engulfment. However, when we applied 1.2 MAC sevoflurane in combination with either A β pE3 or 3NTyrA β , we observed a reduction in astrocyte-mediated synaptic engulfment, along with downregulation of MEGF10 expression (in 3NTyrA β). Notably, after 90 min 1.2 MAC sevoflurane removal, this effect disappeared.

In the adult hippocampus, MEGF10-mediated astrocytic phagocytosis plays a crucial role in maintaining synaptic homeostasis[103]. Lee, J. H et al. demonstrated that in the CA1 region of the adult hippocampus, astrocytes (not microglia) continuously eliminate excessive and unnecessary adult excitatory synaptic connections in response to neuronal activity. MEGF10-deficient astrocytes reduced excitatory synapse elimination, leading to the accumulation of excessive but functionally impaired excitatory synapses, which in turn leads to an increase in the number of dendritic spines and concomitant impaired cognitive function in mice[138]. Similarly, with the help of an adeno-associated virus, a previous study by Dai et al. in our lab also confirmed that the downregulation of MEGF10 protein level in the hippocampus led to a decrease of presynaptic and postsynaptic markers inside astrocytes[137], which also indicates that MEGF10 plays a critical function in astrocyte-mediated synaptic engulfment.

In this part of the study, we found that the decrease in the expression of MEGF10 was associated with a reduction in astrocyte-mediated synaptic engulfment in the presence of 1.2 MAC sevoflurane and 3NTyrA β . This decrease in synaptic engulfment could lead to less clearance of excitatory synapses, thus partially counteracting the inhibitory effects of 1.2 MAC sevoflurane on dendritic spines. That could be one possible reason why 1.2 MAC sevoflurane did not enhance the decrease of DSD in the 3NTyrA β preincubated hippocampal slices. For A β ₁₋₄₀/ A β ₁₋₄₂, the application of 1.2 MAC sevoflurane did not significantly affect

astrocyte-mediated synaptic engulfment, which is also consistent with the previously observed decrease in DSD induced by 1.2 MAC sevoflurane in A β ₁₋₄₀/A β ₁₋₄₂ preincubated hippocampal slices.

After the removal of sevoflurane, only 3NTyrA β + 1.2 MAC sevoflurane + washout showed a tendency ($p=0.0506$) to decrease astrocyte-mediated synaptic engulfment, which may be associated with the increase of DSD after the removal of 1.2 MAC sevoflurane.

In our study, we don't know whether the decrease in engulfment is beneficial or not, as we are uncertain about the type of synapses involved in this phagocytosis. It appears the decrease in elimination leads to an increase in spine number or even reverses the reduction of DSD. However, if they are silent and malfunction synapses that should be eliminated, then the downregulation of astrocyte-mediated synaptic engulfment will result in an increase in malfunctioning synapses and possibly a more synaptotoxic environment. Thus, it is important to clarify whether the engulfed synapses are active synapses with functionality or silent synapses.

Nevertheless, the effects of sevoflurane and A β on the astrocyte-mediated synaptic engulfment could have potential implications for AD patients receiving anesthesia. However, further studies are necessary to determine which kind of synapses are engulfed and whether this downregulation in phagocytosis is beneficial.

4.3 The effect of A β and sevoflurane on the expression of GFAP and GFAP-BDPs

Astrocytosis is a characteristic feature of Alzheimer's disease (AD), which can be triggered by A β oligomers and associated with synaptic loss. Increased expression of GFAP has been recognized as a marker for astrocytosis[122]. In view of the importance of astrocytosis in AD, in this part, we investigated the effects of sevoflurane (0.4 MAC and 1.2 MAC), as well as A β isoforms (A β ₁₋₄₀, A β ₁₋₄₂, A β pE3 and 3NTyrA β) on the expression of GFAP.

We find that: 1) only 3NTyrA β had a significant downregulating effect on GFAP- α expression among the four A β isoforms; 2) neither 0.4 MAC nor 1.2 MAC sevoflurane had a significant

impact on the expression of GFAP; 3) compared to A β , the combination of A β with 0.4 MAC sevoflurane increased the expression of GFAP- α and decreased the expression of GFAP-BDPs. In contrast, 1.2 MAC sevoflurane upregulated the expression of GFAP-BDPs only in the presence of 3NTyrA β ; 4) generally speaking, after 90 min sevoflurane removal, the effects of sevoflurane on A β -induced expression of GFAP- α and GFAP-BDPs were attenuated.

GFAP is the major component of the astrocyte cytoskeleton, which is essential for the maintenance of astrocytic structure and shape. Among the various isoforms of GFAP, GFAP- α is the predominant isoform with the best capacity to form long filaments, whereas all the other isoforms assemble into relatively compromised networks[123]. Due to this, the levels of GFAP- α levels are closely related to the morphology of astrocytes. The downregulation of GFAP- α may be associated with astrocyte skeleton atrophy [139, 140].

Calcium-activated protease calpain-mediated proteolysis is a common post-translational modification of GFAP, resulting in a series of truncated GFAP-BDPs. They cannot assemble into intermediate filaments due to lack head and tail domains. Studies have shown that the upregulation of GFAP-BDPs is closely associated with astrocyte injury[141, 142]. It can be deduced from this that the downregulation of GFAP-BDPs may be beneficial in maintaining normal astrocyte structure.

Our results showed that 3NTyrA β significantly downregulated GFAP- α expression, which may seem contradictory with the prominent astrogliosis observed in AD[149]. However, it is important to note that this prominent astrogliosis occurs at a very late stage of the disease. During the initial stage of AD, it is hypothesized that astrocytes may experience atrophy[139, 140]. The downregulation of GFAP- α induced by 3NTyrA β in our study may confirm the occurrence of astrocyte atrophy in the onset of AD.

We also observed that in the presence of A β , a subanesthetic concentration (0.4 MAC) of sevoflurane, led to an increase in the expression of GFAP- α and a decrease in the expression of GFAP-BDPs. However, when a higher anesthetic concentration (1.2 MAC) was used in the

presence of 3NTyrA β , the expression of GFAP-BDPs was upregulated. Sevoflurane appears to have a dual effect on the expression of GFAP- α and GFAP-BDPs, depending on the concentration. This effect is particularly evident in the presence of 3NTyrA β , where 0.4 MAC sevoflurane protected against the downregulation of GFAP- α and upregulation of GFAP-BDPs induced by 3NTyrA β . Additionally, 1.2 MAC sevoflurane upregulated the expression of GFAP-BDPs and showed a tendency to downregulate GFAP- α expression induced by 3NTyrA β .

Intracellular calcium homeostasis may be one of the mechanisms related to this dual effect. Brief exposure to subclinical concentrations of inhalation anesthetics induced the release of a small amount of calcium from the endoplasmic reticulum, which is then transferred to the mitochondria, stimulates ATP production, and other mitochondrial functions that provide cytoprotection. However, prolonged exposure to high concentrations of inhalation anesthetics induced excessive calcium release from the endoplasmic reticulum to toxic levels, resulting in overactivated calpains[58, 143]. Since GFAP-BDPs are produced through the proteolysis of GFAP by calpains, the overactivated calpains upregulated the expression of GFAP-BDPs and downregulated GFAP- α expression.

In our study, the more pronounced effect of 0.4 MAC sevoflurane than 1.2 MAC sevoflurane could be due to the fact that the exposure duration in our study was 90 min, which is much shorter than the usual duration for prolonged exposure to high concentrations mentioned above (which usually longer than 4 hours).

After sevoflurane removal, the effects of sevoflurane on A β -induced expression of GFAP- α and GFAP-BDPs were attenuated. This is similar to the effects of sevoflurane removal alleviated astrocyte-mediated synaptic engulfment.

It has been established that GFAP- α and GFAP-BDPs play a crucial role in maintaining the structure and shape of astrocytes. When exposed to 3NTyrA β , sevoflurane seems to have a dual impact on GFAP- α and GFAP-BDPs expression depending on concentration, which

may indicate sevoflurane produced a dual impact on astrocytes structure in the presence of 3NTyrA β . However, it is important to note that we only quantified the expression of GFAP, which can only provide indirect evidence of overall changes in astrocytes' cytoskeleton. Therefore, it is uncertain about the direct effects of A β and sevoflurane on astrocyte morphology. For this reason, future studies should systematically examine parameters that directly relate to astrocyte cytoskeleton and morphology, such as the surface and volume of astrocytes, the complexity of astrocyte processes, and the total length of astrocyte processes.

5. Summary and Conclusions

Understanding the interaction of anesthetics with A β -dependent pathophysiology is important for performing anesthesia and taking precautions against POD in AD patients. In the present study, acute hippocampal slices were pre-incubated with A β isoforms, and sevoflurane was thereafter applied, thus mimicking the clinical condition of an AD patient receiving inhalational anesthesia.

In the first part of this study, the interaction of sevoflurane (0.4 MAC and 1.2 MAC) with A β on DSD was studied. The results showed that both sevoflurane and A β decrease DSD. When present together, 0.4 MAC sevoflurane led to a reversible downregulation of DSD in the presence of A β , while 1.2 MAC sevoflurane produced a reversible enhancement of this downregulation induced by A β ₁₋₄₀ and A β ₁₋₄₂. However, for A β pE3 and 3NTyrA β , 1.2 MAC sevoflurane didn't enhance the decrease of DSD. After removal, residual effects of 1.2 MAC sevoflurane were observed as an increase in stubby and thin spines for A β pE3 and 3NTyrA β , respectively.

In the second part, we investigated the impact of A β and sevoflurane on astrocyte-mediated synaptic phagocytosis. We found that neither sevoflurane nor A β affected astrocyte-mediated synaptic engulfment. However, when either A β pE3 or 3NTyrA β was present, 1.2 MAC sevoflurane downregulated astrocyte-mediated synaptic engulfment. This decrease in synaptic

engulfment partially counteracted the inhibitory effects of 1.2 MAC sevoflurane on DSD in the presence of either A β pE3 or 3NTyrA β , which could be one of the possible reasons that in A β pE3 and 3NTyrA β preincubated slices, 1.2 MAC sevoflurane didn't enhance the decrease of DSD.

In the third part, we focused on the effects of sevoflurane and A β on the expression of GFAP. We discovered that when 3NTyrA β was present, sevoflurane had a dual effect on the expression of GFAP- α and GFAP-BDPs. Specifically, 0.4 MAC sevoflurane increased the expression of GFAP- α and decreased the expression of GFAP-BDPs in the presence of all four A β isoforms. On the other hand, 1.2 MAC sevoflurane caused an increase in the expression of GFAP-BDPs and a tendency to decrease GFAP- α expression when 3NTyrA β was present.

In summary, the results of this study indicate that moderate exposure to 0.4 MAC sevoflurane did not protect against or enhance the dendritic spine toxicity of A β isoforms. Moderate exposure to 1.2 MAC sevoflurane interfered with A β -induced dendritic spine toxicity, whereas future studies are needed to determine whether this effect is deteriorating or not. The clinical concentration of sevoflurane exposed at moderate duration could affect astrocyte structure, which suggests that astrocytes, like neurons, are sensitive targets for anesthetics. Therefore, when studying the effects of anesthetics, we shouldn't overlook astrocytes.

POD is one of the most common neurocognitive disorders in AD patients following surgery and anesthesia, and the potential relationship between POD and AD is gaining attention. Improving the anesthesia method is one of the possible ways to reduce POD in AD patients. The results of this study provide evidence for neural and astrocytes' morphological changes in AD patients receiving sevoflurane, which can serve as a basis for clinical anesthesia choice for AD patients and provide a new thought to reveal the mechanisms underlying POD.

6. Acknowledgements

First of all, I would like to give my heartfelt thanks to my supervisor, Prof. Gerhard Rammes, for giving me this valuable opportunity to study Experimental Anesthesiology at Klinikum Rechts der Isar, Technical University of Munich (TUM). His academic experience and thoughtful ideas have always helped me in the whole process of my doctoral study. And he has always been unfailingly helpful and supportive when I was helpless and frustrated. From the proposal written to the completion of the dissertation, every step was completed under the careful guidance of my supervisor. This study could not have been completed without his precious advice and guidance. So, I must thank Gerhard again.

At the same time, I must express my sincere gratitude to all my colleagues at TUM, who gave me a lot of kind help. Arpit, Xingxing, Nina, Katharina, and all of them. I would like to thank them all sincerely. I can't imagine how I would have gotten through the loneliest time so far without your company and help.

I would also like to thank the China Scholarship Committee for financially supporting my studies and life in Munich.

At last, I would like to thank my family, for their endless love and care for me. Whatever I need and wherever I go, they always support me without any requirement in return.

7. Reference

1. Marcantonio, E.R., *Delirium in Hospitalized Older Adults*. N Engl J Med, 2017. 377(15): p. 1456-1466.
2. Evered L, S.B., Knopman DS, Scott DA, DeKosky ST, Rasmussen LS, Oh ES, Crosby G, Berger M, Eckenhoff RG; Nomenclature Consensus Working Group, *Recommendations for the nomenclature of cognitive change associated with anaesthesia and surgery-2018*. Br J Anaesth, 2018. 121(5): p. 1005-1012.
3. Aldecoa, C., et al., *European Society of Anaesthesiology evidence-based and consensus-based guideline on postoperative delirium*. Eur J Anaesthesiol, 2017. 34(4): p. 192-214.
4. Crocker, E., et al., *Long-Term Effects of Postoperative Delirium in Patients Undergoing Cardiac Operation: A Systematic Review*. Ann Thorac Surg, 2016. 102(4): p. 1391-9.
5. Scholz, A.F., et al., *Systematic review and meta-analysis of risk factors for postoperative delirium among older patients undergoing gastrointestinal surgery*. Br J Surg, 2016. 103(2): p. e21-8.
6. Han, J.H., et al., *Delirium in older emergency department patients is an independent predictor of hospital length of stay*. Acad Emerg Med, 2011. 18(5): p. 451-7.
7. Milbrandt, E.B., et al., *Costs associated with delirium in mechanically ventilated patients**. Critical Care Medicine, 2004. 32(4): p. 955-962.
8. Maniar, H.S., et al., *Delirium after surgical and transcatheter aortic valve replacement is associated with increased mortality*. J Thorac Cardiovasc Surg, 2016. 151(3): p. 815-823.e2.
9. Sprung, J., et al., *Postoperative delirium in elderly patients is associated with subsequent cognitive impairment*. Br J Anaesth, 2017. 119(2): p. 316-323.
10. Pandharipande, P.P., E.L. Whitlock, and C.G. Hughes, *Baseline Vulnerabilities May Play a Larger Role than Depth of Anesthesia or Sedation in Postoperative Delirium*. Anesthesiology, 2021. 135(6): p. 940-942.
11. Bramley, P., et al., *Risk factors for postoperative delirium: An umbrella review of systematic reviews*. Int J Surg, 2021. 93: p. 106063.
12. Jin, Z., J. Hu, and D. Ma, *Postoperative delirium: perioperative assessment, risk reduction, and management*. Br J Anaesth, 2020. 125(4): p. 492-504.
13. Ishii, K., et al., *Total intravenous anesthesia with propofol is associated with a lower rate of postoperative delirium in comparison with sevoflurane anesthesia in elderly patients*. J Clin Anesth, 2016. 33: p. 428-31.
14. Evered, L.A., et al., *Anaesthetic depth and delirium after major surgery: a randomised clinical trial*. Br J Anaesth, 2021. 127(5): p. 704-712.
15. Sumner, M., et al., *Processed electroencephalography-guided general anaesthesia to reduce postoperative delirium: a systematic review and meta-analysis*. Br J Anaesth, 2023. 130(2): p. e243-e253.
16. Alam, A., et al., *Surgery, neuroinflammation and cognitive impairment*. EBioMedicine, 2018. 37: p. 547-556.
17. Taylor, J., et al., *Postoperative delirium and changes in the blood-brain barrier, neuroinflammation, and cerebrospinal fluid lactate: a prospective cohort study*. Br J Anaesth, 2022. 129(2): p. 219-230.
18. Maldonado, J.R., *Neuropathogenesis of delirium: review of current etiologic theories and common pathways*. Am J Geriatr Psychiatry, 2013. 21(12): p. 1190-222.

19. Wang, T., et al., *Malfunction of astrocyte and cholinergic input is involved in postoperative impairment of hippocampal synaptic plasticity and cognitive function*. Neuropharmacology, 2022. 217: p. 109191.
20. Edwin van Dellen, M.D., Ph.D., Arendina W. van der Kooi, Ph.D., Tianne Numan, M.Sc., Huiberdina L. Koek, M.D., Ph.D., Francina A. M. Klijn, M.D., Marc P. Buijsrogge, M.D., Ph.D., Cornelis J. Stam, M.D., Ph.D., Arjen J. C. Slooter, M.D., Ph.D., *Decreased functional connectivity and disturbed directionality of information flow in the electroencephalography of intensive care unit patients with delirium after cardiac surgery*. Anesthesiology, 2014. 121(2): p. 328-35.
21. Liu, Y., et al., *Hippocampal astrocyte dysfunction contributes to etomidate-induced long-lasting synaptic inhibition*. Biochem Biophys Res Commun, 2019. 519(4): p. 803-811.
22. Cao, Y., et al., *The Role of Astrocytes in the Mechanism of Perioperative Neurocognitive Disorders*. Brain Sci, 2022. 12(11).
23. *2018 Alzheimer's disease facts and figures*. Alzheimer's & Dementia, 2018. 14(3): p. 367-429.
24. *World Alzheimer Report 2021*.
25. *2022 Alzheimer's disease facts and figures*. Alzheimers Dement, 2022. 18(4): p. 700-789.
26. J A Hardy, G.A.H., *Alzheimer's Disease: The Amyloid Cascade Hypothesis*. Science 1992. 256(5054): p. 184-5.
27. Karran, E., M. Mercken, and B. De Strooper, *The amyloid cascade hypothesis for Alzheimer's disease: an appraisal for the development of therapeutics*. Nat Rev Drug Discov, 2011. 10(9): p. 698-712.
28. Selkoe, D.J. and J. Hardy, *The amyloid hypothesis of Alzheimer's disease at 25 years*. EMBO Mol Med, 2016. 8(6): p. 595-608.
29. JA Hardy, G.H., *Alzheimer's disease the amyloid cascade hypothesis*. Science, 1992. 256(5054): p. 184-185.
30. Mucke, L. and D.J. Selkoe, *Neurotoxicity of Amyloid β -Protein: Synaptic and Network Dysfunction*. Cold Spring Harbor Perspectives in Medicine, 2012. 2(7): p. a006338-a006338.
31. Haass, C. and D.J. Selkoe, *Soluble protein oligomers in neurodegeneration: lessons from the Alzheimer's amyloid beta-peptide*. Nat Rev Mol Cell Biol, 2007. 8(2): p. 101-12.
32. Ferreira, S.T., et al., *Soluble amyloid-beta oligomers as synaptotoxins leading to cognitive impairment in Alzheimer's disease*. Front Cell Neurosci, 2015. 9: p. 191.
33. Singh, S.K., et al., *Overview of Alzheimer's Disease and Some Therapeutic Approaches Targeting A β by Using Several Synthetic and Herbal Compounds*. Oxid Med Cell Longev, 2016. 2016: p. 7361613.
34. Hardy, J. and D.J. Selkoe, *The amyloid hypothesis of Alzheimer's disease: progress and problems on the road to therapeutics*. Science, 2002. 297(5580): p. 353-6.
35. Heneka, M.P.K.a.M.T., *Truncated and modified amyloid-beta species*. Alzheimer's Research & Therapy, 2014. 6(28).
36. Mori, H., et al., *Mass spectrometry of purified amyloid beta protein in Alzheimer's disease*. Journal of Biological Chemistry, 1992. 267(24): p. 17082-17086.
37. Takaomi C. Saido, T.I., H.S. David M. A. Mann, and S.K. Yasuo Ihara, *Dominant and Differential Deposition of distinct of Distinct β -Amyloid Peptide Species, A1~N3(pE), in Senile Plaques*. Neuron, 1995. 14: p. 457-466.

38. Hamley, I.W., *The amyloid beta peptide: a chemist's perspective. Role in Alzheimer's and fibrillization.* Chem Rev, 2012. 112(10): p. 5147-92.
39. Gal Bitan, M.D.K., Aleksey Lomakin, Sabrina S Vollers, George B Benedek, David B Teplow, *Amyloid β -protein ($A\beta$) assembly $A\beta_{40}$ and $A\beta_{42}$ oligomerize through distinct pathways.* Proc Natl Acad Sci U S A, 2002. 100(1): p. 330-5.
40. Frost, J.L., et al., *Pyroglutamate-3 amyloid-beta deposition in the brains of humans, non-human primates, canines, and Alzheimer disease-like transgenic mouse models.* Am J Pathol, 2013. 183(2): p. 369-81.
41. Jawhar, S., O. Wirths, and T.A. Bayer, *Pyroglutamate Amyloid- β ($A\beta$): A Hatchet Man in Alzheimer Disease.* Journal of Biological Chemistry, 2011. 286(45): p. 38825-38832.
42. Sevalle, J., et al., *Aminopeptidase A contributes to the N-terminal truncation of amyloid beta-peptide.* J Neurochem, 2009. 109(1): p. 248-56.
43. Huse, J.T., et al., *Beta-secretase processing in the trans-Golgi network preferentially generates truncated amyloid species that accumulate in Alzheimer's disease brain.* J Biol Chem, 2002. 277(18): p. 16278-84.
44. Tekirian TL, Y.A., Glabe C, Geddes JW, *Toxicity of pyroglutaminated amyloid beta-peptides 3(pE)-40 and -42 is similar to that of $A\beta_{1-40}$ and -42.* J Neurochem 1999. 73: p. 1584-1589.
45. Kummer, M.P., et al., *Nitration of tyrosine 10 critically enhances amyloid beta aggregation and plaque formation.* Neuron, 2011. 71(5): p. 833-44.
46. Rammes, G., et al., *The NMDA receptor antagonist Radiprodil reverses the synaptotoxic effects of different amyloid-beta ($A\beta$) species on long-term potentiation (LTP).* Neuropharmacology, 2018. 140: p. 184-192.
47. Baranov, D., et al., *Consensus statement: First International Workshop on Anesthetics and Alzheimer's disease.* Anesth Analg, 2009. 108(5): p. 1627-30.
48. Eckel, B., M. Blobner, and G. Rammes, *Anesthetics promoting in vitro $A\beta$ metabolism and amyloid-beta toxicity.* J Alzheimers Dis, 2010. 22 Suppl 3: p. 21-6.
49. Jiang, J. and H. Jiang, *Effect of the inhaled anesthetics isoflurane, sevoflurane and desflurane on the neuropathogenesis of Alzheimer's disease (review).* Mol Med Rep, 2015. 12(1): p. 3-12.
50. Vutskits, L. and Z. Xie, *Lasting impact of general anaesthesia on the brain: mechanisms and relevance.* Nat Rev Neurosci, 2016. 17(11): p. 705-717.
51. Wu, L., et al., *Lasting effects of general anesthetics on the brain in the young and elderly: "mixed picture" of neurotoxicity, neuroprotection and cognitive impairment.* J Anesth, 2019. 33(2): p. 321-335.
52. Jevtovic-Todorovic, V., et al., *Anaesthetic neurotoxicity and neuroplasticity: an expert group report and statement based on the BJA Salzburg Seminar.* Br J Anaesth, 2013. 111(2): p. 143-51.
53. Lowery, D.P., K. Wesnes, and C.G. Ballard, *Subtle attentional deficits in the absence of dementia are associated with an increased risk of post-operative delirium.* Dement Geriatr Cogn Disord, 2007. 23(6): p. 390-4.
54. Weiss, Y., et al., *Preoperative Cognitive Impairment and Postoperative Delirium in Elderly Surgical Patients – a Retrospective Large Cohort Study.* Annals of Surgery, 2022: p. 10.1097/SLA.0000000000005657.
55. Au, E., et al., *Postoperative Outcomes in Elderly Patients Undergoing Cardiac Surgery With Preoperative Cognitive Impairment: A Systematic Review and Meta-Analysis.* Anesth Analg, 2023. 136(6): p. 1016-1028.

56. Carella, M. and V.L. Bonhomme, *Targeting Depth of Anesthesia to Prevent Delirium: Comment*. Anesthesiology, 2022. 136(6): p. 1046-1047.
57. Xuli Zhao, Z.Y., Ge Liang, Zhen Wu, Yi Peng, Donald J Joseph, Saadet Inan, Huafeng Wei, *Dual Effects of Isoflurane on Proliferation, Differentiation, and Survival in Human Neuroprogenitor Cells*. Anesthesiology 2013. 118(3): p. 537-49.
58. Wei, H. and S. Inan, *Dual effects of neuroprotection and neurotoxicity by general anesthetics: role of intracellular calcium homeostasis*. Prog Neuropsychopharmacol Biol Psychiatry, 2013. 47: p. 156-61.
59. Popovic, R., R. Liniger, and Philip E. Bickler, *Anesthetics and Mild Hypothermia Similarly Prevent Hippocampal Neuron Death in an In Vitro Model of Cerebral Ischemia*. Anesthesiology, 2000. 92(5): p. 1343-1349.
60. Kapinya KJ, L.D., Fütterer C, Maurer M, Waschke KF, Isaev NK, Dirnagl U. , *Tolerance against ischemic neuronal injury can be induced by volatile anesthetics and is inducible NO synthase dependent*. Stroke, 2002. 33(7): p. 1889-98.
61. Matchett GA, A.M., Martin RD, Zhang JH. , *Neuroprotective effect of volatile anesthetic agents: molecular mechanisms*. Neurol Res., 2009. 32(1): p. 128-34.
62. Eger, E.I., 2nd, L.J. Saidman, and B. Brandstater, *Minimum alveolar anesthetic concentration: a standard of anesthetic potency*. Anesthesiology, 1965. 26(6): p. 756-63.
63. II, E.I.E., *Age, Minimum Alveolar Anesthetic Concentration, and Minimum Alveolar Anesthetic Concentration-Awake*. Anesth Analg. , 2001. 93(4): p.:947-53.
64. Behne M, W.H., Harder S., *Clinical Pharmacokinetics Of Sevoflurane*. Clin Pharmacokinet, 1999. 36(1): p. 13-26.
65. Smith, I., M. Nathanson, and P.F. White, *Sevoflurane--a long-awaited volatile anaesthetic*. Br J Anaesth, 1996. 76(3): p. 435-45.
66. Franks, N.P., *Molecular targets underlying general anaesthesia*. Br J Pharmacol, 2006. 147 Suppl 1(Suppl 1): p. S72-81.
67. Franks, N.P., *General anaesthesia: from molecular targets to neuronal pathways of sleep and arousal*. Nat Rev Neurosci, 2008. 9(5): p. 370-86.
68. Jason A Campagna, K.W.M., Stuart A Forman, *Mechanisms of Actions of inhaled anesthetics*. N Engl J Med. , 2003 348(21): p. 2110-24.
69. Strum, D.P. and E.I. Eger, 2nd, *Partition coefficients for sevoflurane in human blood, saline, and olive oil*. Anesth Analg, 1987. 66(7): p. 654-6.
70. Katoh, T. and K. Ikeda, *The minimum alveolar concentration (MAC) of sevoflurane in humans*. Anesthesiology, 1987. 66(3): p. 301-3.
71. Nakajima, R., Y. Nakajima, and K. Ikeda, *Minimum alveolar concentration of sevoflurane in elderly patients*. Br J Anaesth, 1993. 70(3): p. 273-5.
72. Lu, Y., et al., *Anesthetic sevoflurane causes neurotoxicity differently in neonatal naive and Alzheimer disease transgenic mice*. Anesthesiology, 2010. 112(6): p. 1404-16.
73. Dong Y, Z.G., Zhang B, Moir RD, Xia W, Marcantonio ER, Culley DJ, Crosby G, Tanzi RE, Xie Z., *The Common Inhalational Anesthetic Sevoflurane Induces Apoptosis and Increases Amyloid Protein Levels*. Arch Neurol. , 2009. 66(5): p. 620-31.
74. Tian, Y., et al., *Sevoflurane Exacerbates Cognitive Impairment Induced by Abeta (1-40) in Rats through Initiating Neurotoxicity, Neuroinflammation, and Neuronal Apoptosis in Rat Hippocampus*. Mediators Inflamm, 2018. 2018: p. 3802324.
75. Tang, N., et al., *Effect of inhalational anaesthetic on postoperative cognitive dysfunction following radical rectal resection in elderly patients with mild cognitive impairment*. J Int Med Res, 2014. 42(6): p. 1252-61.

76. Wang, C.M., et al., *Update on the Mechanism and Treatment of Sevoflurane-Induced Postoperative Cognitive Dysfunction*. *Front Aging Neurosci*, 2021. 13: p. 702231.
77. Xiao, Y.Y., et al., *Delayed preconditioning by sevoflurane elicits changes in the mitochondrial proteome in ischemia-reperfused rat hearts*. *Anesth Analg*, 2011. 113(2): p. 224-32.
78. Ramos Ramos, V., et al., *Neuroprotective effect of sevoflurane in general anaesthesia*. *Medicina Clínica (English Edition)*, 2017. 148(4): p. 158-160.
79. Chen, Y., et al., *Sevoflurane preconditioning-induced neuroprotection is associated with Akt activation via carboxy-terminal modulator protein inhibition*. *Br J Anaesth*, 2015. 114(2): p. 327-35.
80. N P Franks, W.R.L., *Temperature dependence of the potency of volatile general anesthetics implications for in vitro experiments*. *Anesthesiology*, 1996. 84(3): p. 716-20.
81. Haseneder, R., et al., *Isoflurane and sevoflurane dose-dependently impair hippocampal long-term potentiation*. *Eur J Pharmacol*, 2009. 623(1-3): p. 47-51.
82. Micheva, K.D., R.J. Weinberg, and S.J. Smith, *A synapse census for the ages*. *Science*, 2020. 369(6501): p. 253-254.
83. Tang, Y., et al., *Total regional and global number of synapses in the human brain neocortex*. *Synapse*, 2001. 41(3): p. 258-73.
84. Magee, J.C. and C. Grienberger, *Synaptic Plasticity Forms and Functions*. *Annu Rev Neurosci*, 2020. 43: p. 95-117.
85. C F Stevens, J.S., *Synaptic plasticity*. *Curr Biology*, 1998. 8(5): p. R151-3.
86. Knierim, J.J., *The hippocampus*. *Curr Biol*, 2015. 25(23): p. R1116-21.
87. Peng, L., I. Bestard-Lorigados, and W. Song, *The synapse as a treatment avenue for Alzheimer's Disease*. *Mol Psychiatry*, 2022. 27(7): p. 2940-2949.
88. Arendt, T., *Synaptic degeneration in Alzheimer's disease*. *Acta Neuropathol*, 2009. 118(1): p. 167-79.
89. Gipson, C.D. and M.F. Olive, *Structural and functional plasticity of dendritic spines - root or result of behavior?* *Genes Brain Behav*, 2017. 16(1): p. 101-117.
90. Harris, K.M., *Structure, development, and plasticity of dendritic spines*. *Curr Opin Neurobiol*, 1999. 9(3): p. 343-8.
91. Zhou, Q., K.J. Homma, and M.M. Poo, *Shrinkage of dendritic spines associated with long-term depression of hippocampal synapses*. *Neuron*, 2004. 44(5): p. 749-57.
92. Harris KM and T.B. Jensen FE, *Three-dimensional structure of dendritic spines and synapses in rat hippocampus (CA1) at postnatal day 15 and adult ages: implications for the maturation of synaptic physiology and long-term potentiation*. *The Journal of neuroscience*, 1992. 12(7).
93. Runge, K., C. Cardoso, and A. de Chevigny, *Dendritic Spine Plasticity: Function and Mechanisms*. *Front Synaptic Neurosci*, 2020. 12: p. 36.
94. Smith, D.L., et al., *Reversal of long-term dendritic spine alterations in Alzheimer disease models*. *Proc Natl Acad Sci U S A*, 2009. 106(39): p. 16877-82.
95. Bourne, J. and K.M. Harris, *Do thin spines learn to be mushroom spines that remember?* *Curr Opin Neurobiol*, 2007. 17(3): p. 381-6.
96. Matias, I., J. Morgado, and F.C.A. Gomes, *Astrocyte Heterogeneity: Impact to Brain Aging and Disease*. *Front Aging Neurosci*, 2019. 11: p. 59.
97. Sofroniew, M.V. and H.V. Vinters, *Astrocytes: biology and pathology*. *Acta Neuropathol*, 2010. 119(1): p. 7-35.

98. Verkhratsky, A. and M. Nedergaard, *Physiology of Astroglia*. *Physiol Rev*, 2018. 98(1): p. 239-389.
99. Araque A, P.V., Sanzgiri RP, Haydon PG, *Tripartite synapses: glia, the unacknowledged partner*. *Trends Neurosci*, 1999. 22: p. 208-215.
100. Perea, G., M. Navarrete, and A. Araque, *Tripartite synapses: astrocytes process and control synaptic information*. *Trends Neurosci*, 2009. 32(8): p. 421-31.
101. Chung, W.S., N.J. Allen, and C. Eroglu, *Astrocytes Control Synapse Formation, Function, and Elimination*. *Cold Spring Harb Perspect Biol*, 2015. 7(9): p. a020370.
102. Attardo, A., J.E. Fitzgerald, and M.J. Schnitzer, *Impermanence of dendritic spines in live adult CA1 hippocampus*. *Nature*, 2015. 523(7562): p. 592-6.
103. Chung, W.S., et al., *Astrocytes mediate synapse elimination through MEGF10 and MERTK pathways*. *Nature*, 2013. 504(7480): p. 394-400.
104. Zhou, B., Y.X. Zuo, and R.T. Jiang, *Astrocyte morphology: Diversity, plasticity, and role in neurological diseases*. *CNS Neurosci Ther*, 2019. 25(6): p. 665-673.
105. Burda, J.E. and M.V. Sofroniew, *Reactive gliosis and the multicellular response to CNS damage and disease*. *Neuron*, 2014. 81(2): p. 229-48.
106. Tykhomyrov, A.A., A.S. Pavlova, and V.S. Nedzvetsky, *Glial Fibrillary Acidic Protein (GFAP): on the 45th Anniversary of Its Discovery*. *Neurophysiology*, 2016. 48(1): p. 54-71.
107. Hol, E.M. and M. Pekny, *Glial fibrillary acidic protein (GFAP) and the astrocyte intermediate filament system in diseases of the central nervous system*. *Curr Opin Cell Biol*, 2015. 32: p. 121-30.
108. Yang, Z. and K.K. Wang, *Glial fibrillary acidic protein: from intermediate filament assembly and gliosis to neurobiomarker*. *Trends Neurosci*, 2015. 38(6): p. 364-74.
109. Middeldorp, J. and E.M. Hol, *GFAP in health and disease*. *Prog Neurobiol*, 2011. 93(3): p. 421-43.
110. Messing, A. and M. Brenner, *GFAP at 50*. *ASN Neuro*, 2020. 12: p. 1759091420949680.
111. de la Gala, F., et al., *Postoperative pulmonary complications, pulmonary and systemic inflammatory responses after lung resection surgery with prolonged one-lung ventilation. Randomized controlled trial comparing intravenous and inhalational anaesthesia*. *Br J Anaesth*, 2017. 119(4): p. 655-663.
112. de Jong, R.H. and E.I. Eger, 2nd, *MAC expanded: AD50 and AD95 values of common inhalation anesthetics in man*. *Anesthesiology*, 1975. 42(4): p. 384-9.
113. Cesarovic, N., et al., *Isoflurane and sevoflurane provide equally effective anaesthesia in laboratory mice*. *Lab Anim*, 2010. 44(4): p. 329-36.
114. Pradhan, A.K., et al., *Quantification of astrocytic synaptic pruning in mouse hippocampal slices in response to ex vivo A β_{1-42} treatment via colocalization analysis with C1q*. *STAR Protoc*, 2022. 3(4): p. 101687.
115. Yang, Y. and J.J. Liu, *Structural LTP: Signal transduction, actin cytoskeleton reorganization, and membrane remodeling of dendritic spines*. *Curr Opin Neurobiol*, 2022. 74: p. 102534.
116. Xiao, H., et al., *Learning, memory and synaptic plasticity in hippocampus in rats exposed to sevoflurane*. *International Journal of Developmental Neuroscience*, 2016. 48(1): p. 38-49.
117. Briner, A., et al., *Volatile Anesthetics Rapidly Increase Dendritic Spine Density in the Rat Medial Prefrontal Cortex during Synaptogenesis*. *Anesthesiology*, 2010. 112(3): p. 546-556.

118. Hofmann, C., et al., *Inhalational Anesthetics Do Not Deteriorate Amyloid- β -Derived Pathophysiology in Alzheimer's Disease: Investigations on the Molecular, Neuronal, and Behavioral Level*. J Alzheimers Dis, 2021. 84(3): p. 1193-1218.
119. Xu, G., et al., *Effects of Dexmedetomidine on Postoperative Cognitive Dysfunction and Serum Levels of b-Amyloid and Neuronal Microtubule-Associated Protein in Orthotopic Liver Transplantation Patients*. Ann Transplant, 2016. 21: p. 508-15.
120. Sofroniew, M.V., *Astrogliosis*. Cold Spring Harb Perspect Biol, 2014. 7(2): p. a020420.
121. Liddelw, S.A., et al., *Neurotoxic reactive astrocytes are induced by activated microglia*. Nature, 2017. 541(7638): p. 481-487.
122. Kumar, A., I.C. Fontana, and A. Nordberg, *Reactive astrogliosis: A friend or foe in the pathogenesis of Alzheimer's disease*. J Neurochem, 2023. 164(3): p. 309-324.
123. Lin, N.H., et al., *Elevated GFAP isoform expression promotes protein aggregation and compromises astrocyte function*. Faseb j, 2021. 35(5): p. e21614.
124. Gomes, F.C., D. Paulin, and V. Moura Neto, *Glial fibrillary acidic protein (GFAP): modulation by growth factors and its implication in astrocyte differentiation*. Braz J Med Biol Res, 1999. 32(5): p. 619-31.
125. Culley, D.J., et al., *Isoflurane affects the cytoskeleton but not survival, proliferation, or synaptogenic properties of rat astrocytes in vitro*. Br J Anaesth, 2013. 110 Suppl 1(Suppl 1): p. i19-28.
126. Rammes, G., et al., *The NMDA receptor antagonist Radiprodil reverses the synaptotoxic effects of different amyloid-beta (A β) species on long-term potentiation (LTP)*. Neuropharmacology, 2018.
127. Wilcox, K.C., et al., *A β Oligomer-Induced Synapse Degeneration in Alzheimer's Disease*. Cell Mol Neurobiol, 2011. 31: p. 939-948
128. Cline, E.N., et al., *The Amyloid-beta Oligomer Hypothesis: Beginning of the Third Decade*. J Alzheimers Dis, 2018. 64(s1): p. S567-S610.
129. Shankar, G.M. and D.M. Walsh, *Alzheimer's disease: synaptic dysfunction and A β* . Mol Neurodegener, 2009. 4: p. 48.
130. Burge, M., et al., *The anaesthetic xenon partially restores an amyloid beta-induced impairment in murine hippocampal synaptic plasticity*. Neuropharmacology, 2019. 151: p. 21-32.
131. Stefanie Kaech, H.B., and Andrew Matus, *Volatile anesthetics block actin-based motility in dendritic spines*. Proc Natl Acad Sci U S A, 1999. 31(96(18)): p. 10433-7.
132. Platholi, J., et al., *Isoflurane reversibly destabilizes hippocampal dendritic spines by an actin-dependent mechanism*. PLoS One, 2014. 9(7): p. e102978.
133. Yang, G., et al., *Transient effects of anesthetics on dendritic spines and filopodia in the living mouse cortex*. Anesthesiology, 2011. 115(4): p. 718-26.
134. Hering, H. and M. Sheng, *Dendritic spines: structure, dynamics and regulation*. Nat Rev Neurosci, 2001. 2(12): p. 880-8.
135. Wang, X., et al., *Beta-Site Amyloid Precursor Protein-Cleaving Enzyme Inhibition Partly Restores Sevoflurane-Induced Deficits on Synaptic Plasticity and Spine Loss*. Int J Mol Sci, 2022. 23(12).
136. Johnson, S.C., et al., *Neurotoxicity of anesthetics: Mechanisms and meaning from mouse intervention studies*. Neurotoxicol Teratol, 2019. 71: p. 22-31.

137. Shi, D., et al., *The Anaesthetics Isoflurane and Xenon Reverse the Synaptotoxic Effects of Abeta(1-42) on Megf10-Dependent Astrocytic Synapse Elimination and Spine Density in Ex Vivo Hippocampal Brain Slices*. Int J Mol Sci, 2023. 24(2).
138. Lee, J.H., et al., *Astrocytes phagocytose adult hippocampal synapses for circuit homeostasis*. Nature, 2021. 590(7847): p. 612-617.
139. Yeh, C.Y., et al., *Early astrocytic atrophy in the entorhinal cortex of a triple transgenic animal model of Alzheimer's disease*. ASN Neuro, 2011. 3(5): p. 271-9.
140. Olabarria, M., et al., *Concomitant astroglial atrophy and astrogliosis in a triple transgenic animal model of Alzheimer's disease*. Glia, 2010. 58(7): p. 831-8.
141. Okonkwo, D.O., et al., *GFAP-BDP as an acute diagnostic marker in traumatic brain injury: results from the prospective transforming research and clinical knowledge in traumatic brain injury study*. J Neurotrauma, 2013. 30(17): p. 1490-7.
142. Halford, J., et al., *New astroglial injury-defined biomarkers for neurotrauma assessment*. J Cereb Blood Flow Metab, 2017. 37(10): p. 3278-3299.
143. Xu, Z., et al., *The potential dual effects of anesthetic isoflurane on A β -induced apoptosis*. Curr Alzheimer Res, 2011. 8(7): p. 741-52.